Geosynthetic Stabilization of Unpaved Roads on Soft Ground : a Field Evaluation

by

Oddur Sigurdsson

B.Sc., The Technical College of Iceland, 1991

A THESIS SUBMITTED IN PARTIAL FULFILLMENT OF
THE REQUIREMENTS FOR THE DEGREE OF
MASTER OF APPLIED SCIENCE

in

THE FACULTY OF GRADUATE STUDIES
(DEPARTMENT OF CIVIL ENGINEERING)

We accept this thesis as conforming
to the required standard

THE UNIVERSITY OF BRITISH COLUMBIA

October 1993

In presenting this thesis in partial fulfilment of the requirements for an advanced degree at the University of British Columbia, I agree that the Library shall make it freely available for reference and study. I further agree that permission for extensive copying of this thesis for scholarly purposes may be granted by the head of my department or by his or her representatives. It is understood that copying or publication of this thesis for financial gain shall not be allowed without my written permission.

(signature) _____

Department of Civil Engineering

The University of British Columbia
Vancouver, Canada

Date Okt. 15th 1993

Abstract

A full scale field trial was carried out to investigate the performance of different geosynthetics in unpaved road construction over soft ground. The test site comprises five 16 m long, by 4.5 m wide test sections, built on a subgrade of undrained shear strength approximately 40 kPa. One is unreinforced and serves as a control section in the study, three sections include a geotextile, and one includes a geogrid. Each test section incorporated a variable thickness of sandy gravel base course material, between 25 and 50 cm thick. They were trafficked in sequence by a vehicle of standard axle load. An important governing parameter for interpretation of behavior is the influence of base course thickness on the relationship between number of passes and rut depth. Performance of the test sections was evaluated from measurements of rut depth, base course thickness, base course deformations, geosynthetic strain, and deformed profile of the geosynthetic, with increasing number of vehicle passes. Vehicle trafficking was continued to a rut depth of about 20 cm, which constitutes a serviceability failure.

Results from the full scale field trial show a better performance in the reinforced sections than the unreinforced section. The performance of the unreinforced section shows good agreement with other well-documented field data at large rut depths, between 10 and 15 cm, but not at small ruts. Although the four geosynthetics exhibited a broad range of stiffness and material properties, the general performance of the four reinforced sections was similar on the thicker base course layers. This is attributed to a reinforced mechanism governed by stiffness and separation, and all materials appear adequately stiff for the site condition and vehicle loading. On the thinner subgrades, a tensioned-membrane effect is mobilized, and a significant difference is observed between the geosynthetics.

Table of Contents

Table of Contents (cont.)

Table of Contents (cont.)

List of Tables

List of Figures

List of Figures (cont.)

List of Figures (cont.)

List of Figures (cont.)

Acknowledgments

I wish to thank my supervisor, Dr. R.J. Fannin, for his invaluable support, encouragement, patience, and discussion throughout the research. My thanks are also extended to Dr. P.M. Byrne for his additional review of the thesis.

The project was supported by the Natural Sciences and Engineering Research Council of Canada (NSERC), through the Collaborative Research and Development (CRD) Grant program. The industrial partners were Polyfelt Inc., Texel Inc., and Tensar Earth Technologies Inc. Additional support from the Public Road Administration of Iceland is acknowledged. The test site and the loading vehicle were provided by the Geotechnical and Material Engineering section of B.C. Ministry of Transportation and Highways, and their in-kind contribution is gratefully acknowledged. I would also like to thank my friends and fellow students in the geotechnical research group and the Department of Civil Engineering for their friendship and cooperation during my graduate studies.

On a more personal note, I would like to thank my wife Nanna, my son Siggi, and my parents Hrefna and Sigurður, who encouraged me to undertake this endeavour and supported me throughout.

Chapter 1

Introduction

1.1 INTRODUCTION TO GEOSYNTHETICS

Geosynthetics is a relatively new term in the engineering practice, used for a range of synthetic materials which have become increasingly important in a wide variety of engineering applications. As the name indicates, geosynthetics are artificial materials, the vast majority of which are made from polymers. Polymeric materials are composed of many small parts, called monomers, in which homopolymers are the most common type of monomer used in the manufacture of geosynthetics. Polymers are also made of the so called copolymer and terpolymer which describe two and three repeating units in a chain, respectively. The synthetic materials made from polymers are non-biodegradable and are collectively called geosynthetics. They are further broken into the following categories: geotextiles; geogrids; geomembranes; geonets; and geocomposites; which are described in some detail in the next section.

1.1.1 Geotextiles

Geotextiles are the oldest type of geosynthetics. The main polymeric materials used in the manufacture of geotextiles are polypropylene and polyester which are thermoplastic materials, though polyamide and polyethylene are also used (Koerner, 1990). The manufacture of geotextiles begins with the production of fiber filaments by extruding melted polymers through a spinneret. The monofilament fibers are then obtained by hardening the fiber filaments and stretching them in order to reduce the diameter and improve the strength of the fiber. There are other types of fibers used in manufacturing of geotextiles, the multifilament which is produced by combining the monofilament, and staple fibers which are obtained by cutting filaments into a short lengths of 2 to 10 cm. These staples can then be twisted into staple yarns. Slit films which are typically 1 to 3 mm wide are another fiber type used in the construction of geotextiles. The slit films are produced by slitting an extruded plastic film with blades. Slit film yarn is then made by combining the slit film fibers.

In the geotextile manufacturing process, these fibers are converted into a planar permeable structure called a fabric. The types of fabrics most often used for geotextiles are wovens and nonwovens. Knitted fabrics are also available, but are rarely used in the geotextile industry.

The woven geotextiles are made of two perpendicular sets of parallel filaments or strands of yarn systematically interlaced using regular textile weaving machinery to form the planar structure. There are a wide variety of fabric weaves for use as geotextiles, but they are kept relatively simple for the conventional industrial fabrics.

The manufacture of nonwoven geotextiles is different from that of wovens, and more complicated. Nonwoven geotextiles are formed by arranging the fibers in an oriented or random pattern to form a continuous loose web. The fabric mat is then

bonded together by using one or a combination of the following processes: thermal or melt-bonding, where heat causes partial melting of filaments or fibers at their crossover points; chemical or resin-bonding, where an acrylic resin is either sprayed on the loose web or used to impregnate the filaments and fibers; mechanical bonding or needle-punching process, where barbed needles are punched through the loose web in order to entangle the fibers.

1.1.2 Geogrids

Geogrids are more recent than geotextiles in the field of engineering and are made of high-modulus polymer materials. The polymeric materials used in the manufacturing of geogrids are high-density polyethylene and high coherence and toughness polyester or polypropylene. Extruded sheets are either drawn or rolled, under controlled strain rates and temperature, in one or two perpendicular directions depending on which style is preferred. In the drawing or rolling process, the small regular pattern perforations become large quasi-rectangular openings. Geogrids are available in both uniaxial and biaxial styles which is dependent on how the heavy gauge polymer sheets are drawn after being perforated.

1.1.3 Geomembranes

Geomembranes form the second largest group of geosynthetic materials and are mostly made of semicrystalline thermoplastic resins such as polyethylene, polyvinyl chloride and chlorosulfonated polyethylene. The manufacturing of the three basic geomembrane types begins with production of the raw materials, which includes the polymer resin together with various additives used to obtain the final very low permeability thin plastic or rubber sheet product.

A single-layer, unreinforced geomembrane is the simplest production type, where the raw materials are compounded before the extrusion process. In the extrusion process the extruder melts down the raw materials, under a partial vacuum in order to eliminate air bubbles, into a homogeneous fluid mass that forms the final sheet. The extruder produces a sheet approximately 0.1 to 5 mm in thickness and up to about 10 m wide.

Multi-layer, unreinforced or reinforced geomembranes are somewhat different and more complicated to manufacture. As the name indicates, this type of geomembrane consists of two or more laminated plastic sheet layers that can be reinforced by placing a fabric scrim between the plastic layers.

Spread coating is the third and most recent production method for geomembranes. This technique uses geotextiles in combination with the molten polymer. Usually a needle-punched nonwoven geotextile is used as a substratum upon which the molten raw materials are placed and spread into its final thickness.

1.1.4 Geonets

Geonets are the smallest and the most recent segment of the geosynthetic production range. Geonets have a netlike configuration similar to that of geogrids, but serve a different function, and are typically made of polyethylene only. The manufacture of geonets begins with blending of the raw materials, which are fed into an extruder where the polymeric material is melted. It then passes into a counter rotating former which produces ribs at acute angles to one another; pressure is used to push the extrudate forward over a steel spreading mandrel which opens the ribs in a relatively large diamond-shaped apertures, typically 12 mm long by 8 mm wide, and 5 to 7 mm thick.

1.1.5 Geocomposites

Geocomposites are, as the name suggests, a combination of several geosynthetics. The concept is to use the best features of the other geosynthetics and, by combining the different attributes for two or more materials, achieve an improved performance for specific applications.

1.2 FUNCTIONS AND APPLICATIONS OF GEOSYNTHETICS

Since the early 1950's when the first geotextiles were introduced (van Zanten, 1986), the use of geosynthetics has been playing an increasingly important role in various engineering applications. There are numerous applications where geosynthetics are used, and their main functions can be divided into five categories:

- separation;
- reinforcement;
- filtration;
- drainage; and
- low permeability barrier.

These functions will be discussed subsequently, with emphasis placed on the use of geotextiles and geogrids in unpaved road construction.

1.2.1 Separation

Geosynthetics are commonly used to satisfy more than one function. When a geosynthetic is used as a separator, it must prevent the intermixing of particles from two soil layers with different properties, for example between a course base aggregate, or ballast, and a softer subgrade soil.

Unpaved roads fall within this application. The prime function of geosynthetics in unpaved road construction is often considered to be separation, the secondary functions being reinforcement and filtration. However, this situation is very dependent on the local conditions and might be true for some cases but over all, the reinforcement function is the primary function that geosynthetics serve today.

When designing for separation there are various material properties that must be taken into account to determine quantitatively which geosynthetic is suitable for a specific application, such as tensile strength, and resistance to tear, burst and impact.

There is a common misunderstanding between separation and filtration, and these two different but related functions are very often confused or considered as being the same. Separation might at first sight appear synonymous with filtration but the main difference is that unlike filtration the separation role is performed independently of the presence of water. Numerous applications can be found but only a few of them will be discussed and described herein. The products in the geosynthetic group do not all perform this function, which is generally referred to as the first identified function of geotextiles even though it is often underrated.

1.2.2 Reinforcement

Synthetic reinforcement is increasingly used for temporary and permanent earth structures. There are three main areas of application: slopes and embankments; foundations; and retaining walls. While specific applications are numerous, only one of them will be discussed in some detail, which is the reinforcement application in unpaved road construction.

The reinforcing function of geosynthetics, laid between the subgrade soil and the base course aggregate can be categorized by: subgrade and base course restraint; lateral restraint of base course; and tensioned membrane effect.

- *Subgrade and base course restraint*

When traffic load is applied to a base course layer tension forces are developed at the base and the cohesionless material tends to move apart, allowing intrusion of the subgrade and mixing of the two materials. Geosynthetics provide a tensile reinforcement, and when placed at the subgrade-base course interface, base course aggregate movement is restrained. The bearing capacity of the subgrade layer is also greatly reduced by outward acting shear stresses at the subgrade surface. The presence of a geosynthetic prevents these stresses from being transmitted to the subgrade, allowing the full bearing capacity of the subgrade to be mobilized. The presence of the geosynthetic has been found to prevent local shear failure in a soft subgrade soil and increase the bearing capacity towards a general shear failure.

- *Lateral restraint*

The lateral restraint provided by the presence of the geosynthetic increases the load distribution effectiveness of the base course layer resulting in decreasing compressive stresses on the subgrade.

- *Membrane effect*

The tensioned membrane effect is mobilized when the subgrade is deformed by rutting and as the subgrade deforms the geosynthetic stretches and tensile stresses are developed. The vertical component of the tension in the geosynthetic acts to reduce the load transmitted to the subgrade.

1.2.3 Filtration

Filtration is defined as the promotion of a natural filter in the adjacent soil: water or liquid can pass through the plane of the fabric while the soil is retained. The use of geotextile filters can be subdivided into three categories (John, 1987), based on the flow conditions. These are listed below in ascending order of severity:

- fairly steady unidirectional flow;
- reversing flow with a moderate cycle time; and
- reversing flow with a very short cycle time.

Examples of applications corresponding to these three flow conditions are respectively:

- land drainage filters;
- river and coastal defense filters; and
- anti-pumping filters beneath ballast under railroads.

Other applications include filtration beneath stone base for unpaved roads and airfields, around a perforated under-drain pipe, as a silt fence and/or curtain, and as a filter beneath stone rip-rap. Three main factors that must be taken into account in order to properly design a filter are; adequate permeability, soil retention, and long term compatibility.

The permeability criterion is one of the main factors in selecting an appropriate filter. However, the coefficient of permeability is difficult to determine accurately for a geotextile. Thick geotextiles are compressible, hence changes in applied stress causes changes in permeability. For these reasons the thickness is taken into account and a new term, permittivity, is defined.

The requirements of a high permeability and good soil retention are contradictory since the cross-plane water flow would be least restricted if the openings were large, whereas small openings would be most effective for a good soil retention. Consequently an upper and lower bound value of characteristic opening size is often specified in design.

Soil to fabric compatibility is one of the questions that have to be answered. A unidirectional flow promotes the formation of a graded filter in the adjacent soil when the pore size openings of a geotextile are compatible with the distribution of the soil particle sizes. However, if the geotextile openings are too large then piping will occur, either as an internal erosion or as soil suffusion (John, 1987), depending on the soil particle size grading.

In contrast, if the pores are small a graded filter may not form since insufficient initial wash-through of fine soil particles occurs. Blocking is likely to occur if the pores of the geotextile are too small, or even blinding, which is a special form of severe blocking. When soil particles sizes are very close to that of geotextile pore openings some of the soil particles are likely to enter the pores and cause clogging.

These factors are all important when designing for filtration and have only been briefly described. Filter design for various applications, soil conditions, fabric types, and flow regime is not an easy task since there are few good experimental and field data to support relationships for flow conditions other than unidirectional.

1.2.4 Drainage

Drainage or fluid transmission is the fourth basic function of geosynthetics. The term drainage refers to the flow of water or liquid within the plane of the geosynthetic. Geotextiles, geonets and geocomposites are materials frequently used to provide a relatively high flow capacity path within a soil structure along which water can flow

preserving good soil retention and a long term soil-to-geosynthetic compatibility. Some selected applications are listed below:

- chimney drain and drainage gallery in earth dams;
- wick drains;
- drainage behind a retaining wall;
- pore water dissipation in earth fills;
- leachate drainage of landfill side slopes and above landfill liners;
- drainage of frost susceptible soils;
- drainage beneath a surcharge fill and building foundations; and
- pavement edge drain.

When designing with geosynthetics the two general flow capacity categories (Koerner, 1990), are gravity flow and pressure flow. Gravity flow is governed by the slope while pressure flow is independent of orientation but occurs generally from higher pressure to locations of lower pressure.

Physical properties such as thickness, mechanical properties such as tensile compressive and shear strength, hydraulic properties, endurance properties and environmental properties all have to be considered in drainage design, where some of them are not as critical as others depending on the application.

1.2.4 Low Permeability Barrier

A low permeability barrier is used to prevent or minimize liquid movement from one point to another. Formerly this was done by using clay or other poorly draining soils, which dates back many centuries. Asphalt and various cements have been used since early this century, and more recently concrete and synthetic membranes have been developed.

Geomembranes have a very low permeability to both gases and fluids, and are used extensively as low permeability barriers. The potential applications of geomembranes are: sealing against fluid percolation; and as buffers against pollutants. The function of the geomembrane in case of the former application is to form a barrier between water or other liquid and the surroundings, and to keep liquid flow through the membrane to a minimum. The second function involves attenuation of contaminants during migration. Geomembrane properties and laboratory tests for geomembrane characterization according to the Canadian Foundation Engineering Manual are as follows:

- *identification properties;* such as:
  - thickness;
  - density;
  - mass per unit area;
  - melt index
  - hardness;
  - carbon black content; and
  - carbon dispersion;

- *performance tests*; e.g.:
  - tear;
  - tensile properties;
  - bursting;
  - puncture;
  - friction;
  - creep;
  - water and vapor permeability;

- *performance tests on joints*; e.g.:
  - shear;
  - peal; and
  - non destructive tests;

- *Durability*; e.g.:
  - chemical resistance;
  - biological resistance;
  - stress cracking;
  - abrasion;
  - thermal aging; and
  - light exposure.

1.3 SCOPE OF RESEARCH

While significant work has examined the mechanisms of reinforcement and stabilization at model scale in the laboratory, few well-controlled field tests have been performed and rigorously evaluated. This research project involves construction of an 80 m long unpaved road that was loaded using a special pavement test vehicle with a standard axle load. The project is unusual because the test road is not part of an existing highway and the only traffic loading is the pavement test vehicle. A consortium of three manufacturers of geosynthetics, and the B.C. Ministry of Transportation and Highways, are supporting the construction and trafficking test. Four sections of the road include a geosynthetic, and one is unreinforced. Simulated traffic loading is intended to evaluate the benefits of using geosynthetics in unpaved road construction.

1.4 RESEARCH OBJECTIVES

The main objectives of this study are to:

- quantify the improvement of a geosynthetic reinforced sections over an unreinforced section based on measurements of rut depths versus number of passes, base course and subgrade deformation profiles, and geosynthetic strain measurements;
- compare relative performance of different geosynthetics;
- identify the relative importance of the basic functions:
  - separation;
  - reinforcement; and
  - filtration;
- critically evaluate design methods

1.5 OUTLINE OF THESIS

This chapter has provided an introduction to the fundamentals of geosynthetics. In chapter two, the literature related to this research project is reviewed, with special emphasis placed on bearing capacity, model studies, analytical studies and other field studies. Design procedures are also reviewed. The test site is described in the third

chapter. A short geological history of the Lower Mainland is given as well as surficial geology of Lulu Island. The location and description of the test site are described and subgrade soil properties reported. Chapter four deals with material properties of the base course and the properties of the four different geosynthetics used in the test sections. It also describes the five test sections, with reference to construction design and instrumentation. A short description is given of the loading vehicle used in the trial and the trafficking schedule.

A comprehensive summary of the field measurements is given in chapter five. Since huge amount of data was collected during the tests, there is no possibility of including all this "raw" data in the thesis. Chapter six contains an analysis and interpretation of the results. A comparison is made between the test sections and the results are compared to design methods and other available field trials. The last chapter contains recommendations and the conclusions from this research.

Chapter 2

Literature Review

2.1 INTRODUCTION

Geotextiles and geogrids have been used successfully in unpaved road construction over soft ground for many years. The geotextiles often fulfill more than one of the basic functions of separation, reinforcement, filtration and drainage in their applications in unpaved roads. Geogrids, however, serve mainly as reinforcement and in some cases as separators.

Over the past two decades a considerable amount of research on geosynthetic reinforcement of layered soil systems has been carried out internationally. These studies have been in the form of field, model and analytical studies, and have supported the development of design procedures for unpaved road construction over soft ground. Although most of the design procedures are similar in their approach, different assumptions are made with respect to vehicle traffic, bearing capacity formulation, the

effect of anchorage, and the mechanism of stabilization, particularly the relative importance of a tensioned-membrane effect.

2.2 FUNDAMENTALS OF DESIGN APPROACHES

Although geosynthetics have been used in road construction for over two decades, the design is based largely on empirical rules. Theoretical work has, however, grown to make a significant contribution based on interpretation of field observations, small and large scale laboratory models, analytical work and sophisticated finite element studies. The current understanding of geosynthetic-soil interaction and the procedures used in design are described below.

2.2.1 Bearing Capacity

The ultimate load that a soil body can support is termed its bearing capacity, and is dependent not only on the mechanical properties of the soil but also on the shape, size and the location of the loaded area.

The first rational approach to estimate the bearing capacity of soil was provided by Terzaghi (Terzaghi, 1943), who reasoned that if the weight of the soil, the effects of the surcharge, and the strength parameters of the soil could be assessed on the basis of a conservative mechanism, then the sum of these factors would in turn provide a conservative estimate. In his bearing capacity formulation he differentiates between general shear failure, characterized by recognizable failure planes extending from the edge of the loaded area, and local shear failure, where plastic flow causes large settlement under the footing without noticeable bulging at the surface. He also distinguished between smooth and rough footings.

The conditions for general shear failure of a shallow continuous footing, see Fig. 2.1, show the zones assumed for a smooth and rough footing. The shearing resistance of the soil located above the level of the base of the footing can be neglected if the condition of a shallow footing is satisfied, that is D_f is less than B, for which soil can be replaced by a surcharge q_o equal to $D_f\gamma$ per unit of area, where γ is the unit weight of the soil and D_f is the distance between the surface of the ground and the base of the footing.

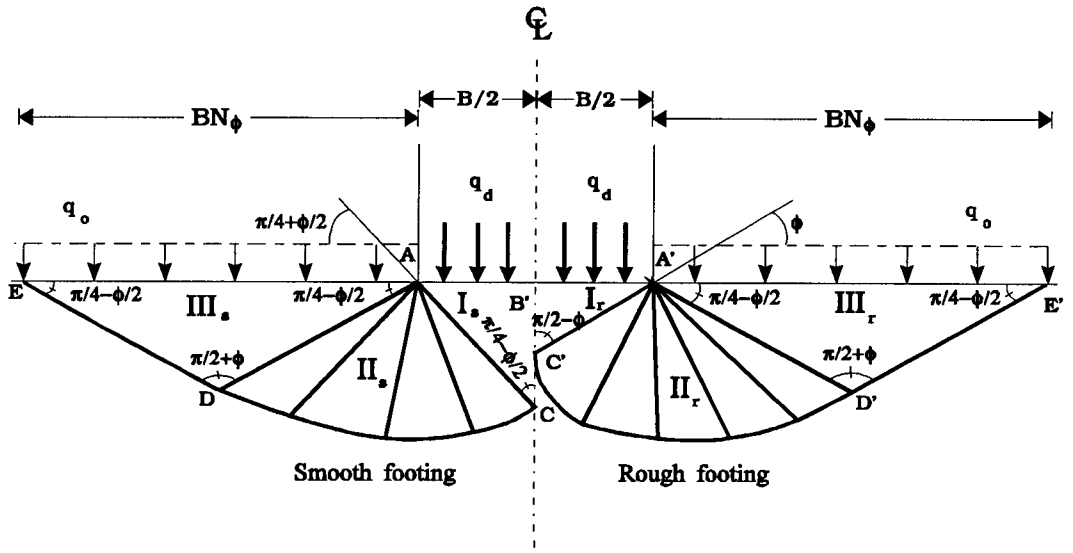

Figure 2.1 Failure of soil beneath continuous smooth and rough footing.

The zone of plastic equilibrium for the smooth footing is defined by the area ACDE, and by the area A'C'D'E' for the rough footing. The difference is the assumed boundary between the elastic zone I and the zones of radial shear II: for the smooth footing it is inclined at an angle of $\pi/4+\phi/2$, whereas for the rough footing it is inclined at an angle ϕ. Zone I for both cases is assumed to remain in the elastic state because of friction and adhesion between the soil and the base of the footing, and acts as a part of

the displaced footing. This downward movement produces outward lateral forces on both sides of the wedge and a passive Rankine state is developed in zones III_r and III_s.

Terzaghi's classical bearing capacity formula is based on earlier solutions by Prandtl and Reissner, and the approximate value of the ultimate bearing capacity is given by the equation

$$q_u = cN_c + \gamma D_f N_q + \tfrac{1}{2}\gamma B N_\gamma \tag{2.1}$$

in which N_c, N_q and N_γ are dimensionless bearing capacity factors related to the cohesion (c), surcharge and weight of the soil, respectively, and only dependent on the angle of internal friction. The values of N_c and N_q are determined by the following equations derived by Terzaghi (Terzaghi, 1943) from those published by Prandtl and by Reissner for continuous footings with a rough base:

$$N_c = \cot\phi\left[\frac{a_\theta^2}{2\cos^2(45°+\phi/2)} - 1\right] \tag{2.2}$$

$$N_q = \frac{a_\theta^2}{2\cos^2(45°+\phi/2)} \tag{2.3}$$

where

$$a_\theta = e^{(3/4\pi-\phi/2)\tan\phi} \tag{2.4}$$

giving

$$N_c = \cot\phi\left(N_q - 1\right) \tag{2.5}$$

Currently the most widely used values for the factor N_γ are those obtained by Hansen and Meyerhof (Craig, 1992), represented by the following approximations:

$$N_\gamma = 1.80\left(N_q - 1\right)\tan\phi \quad \text{(Hansen)} \tag{2.6}$$

$$N_\gamma = \left(N_q - 1\right)\tan(1.4\phi) \quad \text{(Meyerhof)} \tag{2.7}$$

The boundaries that CD and C'D' define (Fig. 2.1) are generally log spirals. If however $\phi = 0°$ the spirals become arcs of circles and the corresponding values of the dimensionless bearing capacity factors N_c, N_q and N_γ become:

$$N_c = \tfrac{3}{2}\pi + 1 = 5.7, \quad N_q = 1, \quad \text{and} \quad N_\gamma = 0$$

Hence, for a rough footing at the ground surface the value of the bearing capacity per unit area is:

$$q_u = \left(\tfrac{3}{2}\pi + 1\right)c = 5.7c \tag{2.8}$$

The equations above refer to footings with a rough base where the boundary between zones I_r and II_r is inclined at an angle ϕ, see Fig. 2.1. If the frictional resistance of the footing reduces, the angle between I and II increases. Assuming an angle β for the case of a footing having less resistance to sliding than the rough footing, but not perfectly frictionless, where $\phi < \beta < 45° + \phi/2$, the equations become:

$$N_c = \tan\beta + \frac{\cos(\beta - \phi)}{\sin\phi\cos\beta}\left[a_\theta^2(1 + \sin\phi) - 1\right] \tag{2.9}$$

and

$$N_q = \frac{\cos(\beta - \phi)}{\cos\beta} a_\theta^2 \tan\left(45° + \tfrac{\phi}{2}\right) \tag{2.10}$$

where

$$a_\theta = e^{\left(\frac{3}{4}\pi + \phi/2 - \beta\right)\tan\phi} \tag{2.11}$$

Assuming a perfectly frictionless base, i.e. $\beta = 45° + \phi/2$:

$$N_c = \cot\phi\left[a_\theta^2 \tan^2\left(45° + \tfrac{\phi}{2}\right) - 1\right] \tag{2.12}$$

and

$$N_q = a_\theta^2 \tan^2\left(45° + \tfrac{\phi}{2}\right) \tag{2.13}$$

where

$$a_\theta = e^{\frac{1}{2}\pi\tan\phi} \tag{2.14}$$

If the footing is assumed perfectly smooth and if $\phi = 0°$ the bearing capacity factors N_c, N_q and N_γ become:

$$N_c = \pi + 2 = 5.14, \quad N_q = 1, \quad \text{and} \quad N_\gamma = 0$$

Hence, for a smooth footing at the ground surface the value of the bearing capacity per unit area is:

$$q_u = (\pi + 2)c = 5.14c \tag{2.15}$$

The above procedure is for the case of general shear failure. For the case of local shear failure the values of c and ϕ must be replaced by c' and ϕ' in the equations above in order to calculate the corresponding values N'_c, N'_q and N'_γ. This is done by using (Terzaghi, 1943)

$$c' = \tfrac{2}{3}c \tag{2.16}$$

and

$$\tan\phi' = \tfrac{2}{3}\tan\phi \tag{2.17}$$

in the above equations, and the bearing capacity is then given by:

$$q'_u = \tfrac{2}{3}cN'_c + \gamma D_f N'_q + \tfrac{1}{2}\gamma B N'_\gamma \tag{2.18}$$

Hence, for a smooth footing at the ground surface the value of the bearing capacity in the case of local shear failure is:

$$q'_u = \tfrac{2}{3}cN'_c = \tfrac{2}{3}q_u = \tfrac{2}{3}(\pi + 2)c = 3.43c \tag{2.19}$$

It should be noted that Terzaghi's bearing capacity derivation above is based upon limit equilibrium conditions and therefore the resultant bearing capacities are a

measure of the ultimate failure pressure that can be applied to a footing. Furthermore, the preceding discussion refers only to continuous footings, and for shapes other than strip footing the bearing capacity equation has to be modified. Based on experimental results, the following semi-empirical equations are used (Terzaghi and Peck, 1967) for a circular footing of radius R:

$$q_{uR} = 1.2cN_c + \gamma D_f N_q + 0.6\gamma R N_\gamma \tag{2.20}$$

and a square footing, B×B:

$$q_{uC} = 1.2cN_c + \gamma D_f N_q + 0.4\gamma B N_\gamma \tag{2.21}$$

Hence, the bearing capacity of a footing at the ground surface, for $\phi = 0$, is given by:

$$q_{uR} = q_{uC} = 1.2(\pi+2)c = 6.17c \tag{2.22}$$

To account for the geometric-loading and depth-influence factors, Skempton proposed the following expression for values of $D_f/B \leq 2.5$ in the case of a rectangular footing of length L:

$$q_u = (\pi+2)\left[\left(1+0.2\frac{D_f}{B}\right)\left(1+0.2\frac{B}{L}\right)\right]c \tag{2.23}$$

A width to length ratio of unity gives the same value of bearing capacity as eqn. (2.22).

For two layer systems, several methods have been developed for calculation of the ultimate bearing capacity. Purushothamaraj et al.(1973) used Prandtl-Terzaghi's mechanism for a rough shallow footing, assuming that both soil layers are homogeneous and isotropic. By applying the kinematics consideration of the Drucker-Prager (1952) second theorem, they developed a theoretical procedure to estimate the bearing capacity factors. Meyerhof (1974) presented analyses of different modes of soil failure for a dense sand overlying a clay, and compared the results to model tests

and field observations. He showed that the influence of the sand layer thickness beneath the footing was governed primarily by the bearing capacity ratio of the two layers, the friction angle of the sand, and the shape and location of the footing.

In the case of reinforced unpaved roads several variations of the bearing capacity equation have been proposed, where the placement of a geosynthetic on the soft subgrade is believed (Bakker, 1977; Barenberg et al., 1978; Giroud and Noiray, 1981; Sellmejer et al., 1982) to promote a general shear failure where otherwise a local failure would occur. Although there is some difference of opinion on the relative importance of the physical actions of the geosynthetic, the increase in bearing capacity seems to be well accepted.

2.2.2 Membrane Effect

The concept of a tensioned membrane effect due to the geosynthetic which develops as the road undergoes deformations, is illustrated schematically in Fig. 2.2.. In order to develop any benefit from a membrane action, the geosynthetic must be anchored effectively outside the loaded area and significant vertical deformations must occur.

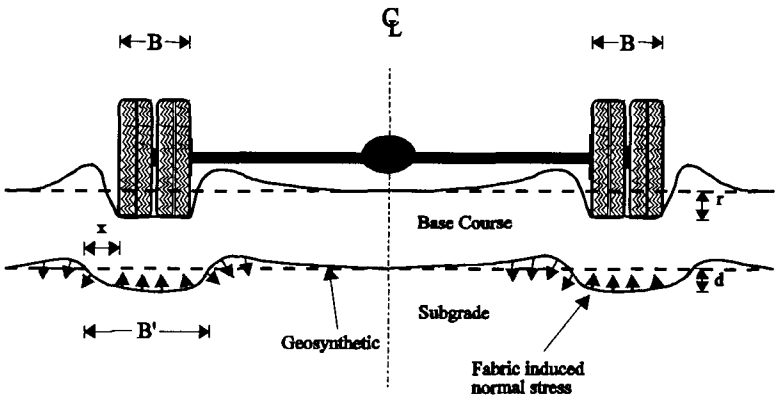

Figure 2.2 Membrane action of geosynthetic in unpaved road.

Stress-strain characteristics of the geosynthetic are also important when considering the membrane action. The higher the modulus of the geosynthetic, the less vertical deformation is required to develop the equivalent support from an inclusion of lower modulus.

The membrane effect is attributed to the in-plane tensile stress in the geosynthetic inducing stresses perpendicular to the plane of the geosynthetic: the imposed stresses on the subgrade in the concave up-section of the membrane beneath the wheels is reduced and the stress in the adjacent concave-down section outside the wheel path is increased.

Several tension membrane models are available in the literature (Barenberg, 1980; Giroud and Noiray, 1981; Raumann, 1982; and Sellmeijer et al., 1982). They vary in complexity, but result in a similar contribution to the predicted bearing capacity. In order to clarify some of the assumptions which are made, a simple model developed by Gourc et al. (1982) will be described briefly, see Fig. 2.3.

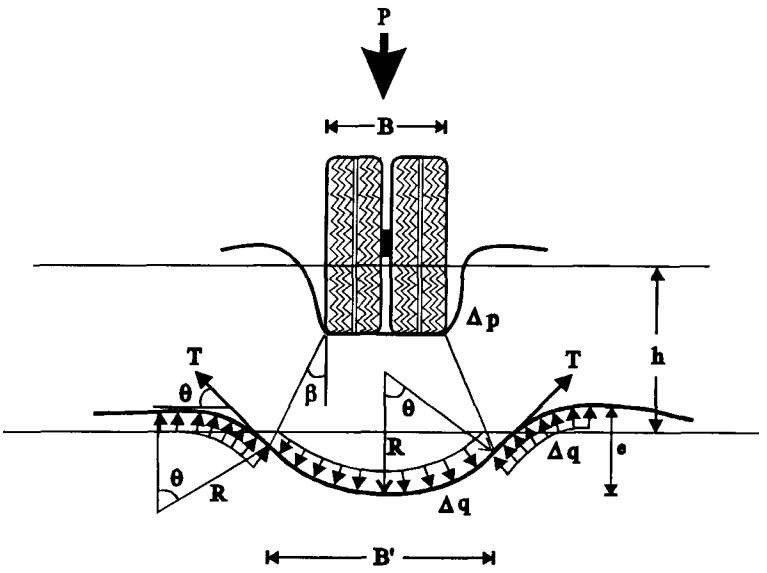

Figure 2.3 Membrane effect in unpaved roads with geosynthetics - basic parameters.

The deformed shape of the geosynthetic was approximated by three circular arc segments of equal radius, for which

$$\tfrac{1}{2}e = R - \cos\theta \Rightarrow e = 2R(1-\cos\theta) \tag{2.24}$$

and

$$B' = 2R\sin\theta \tag{2.25}$$

The geometric relationship between the deflection of the geosynthetic (e) and the settlement through diameter B', is therefore (Fig. 2.3):

$$\frac{e}{B'} = \frac{1-\cos\theta}{\sin\theta} \tag{2.26}$$

The strain (ε) in the geotextile assuming perfect anchorage and a constant tension over the width of the membrane is equal to the elongation due to the deformation over the initial length B', is given by:

$$\varepsilon = \frac{\Delta l}{l_i} = \frac{l_2 - l_1}{l_1} = \frac{2\theta R - 2R\sin\theta}{2R\sin\theta} = \frac{\theta - \sin\theta}{\sin\theta} \tag{2.27}$$

The tensile force per unit width in the geosynthetic, assuming a linear stress-strain relationship, is therefore:

$$T = E\varepsilon = E\frac{\theta - \sin\theta}{\sin\theta} \tag{2.28}$$

The component of this tension which acts vertically upward, reducing the imposed stress on the subgrade in the concave-up section of the membrane underneath the vehicle wheel, is:

$$\Delta qB' = 2T\sin\theta = 2E(\theta - \sin\theta) \tag{2.29}$$

The reduction of applied stress is therefore strictly dependent on the rut depth and the modulus of the geosynthetic. It should be noted that the above procedure is only one of several methods which all are approximations to what really takes place in situ. Some shortcomings in the assumptions which have been established from testing are an underestimation of lateral slippage between the geosynthetic and the subgrade soil and a different tensile stress distribution in the deformed geosynthetic (Jarrett, 1986).

2.2.3 Effect of Anchorage

Many design methods consider the role of the tensioned membrane effect important to the increased bearing capacity of reinforced unpaved roads, and place emphasis on the need for anchorage of the geosynthetic outside the loaded area to mobilize it. Several papers have been published which discuss geosynthetic-soil interaction and anchorage (Holtz, 1977; Myles, 1982; Jarrett and Bathurst, 1985; Douglas and Kelly, 1986; Bourdeau and Holtz, 1988; and Dembicki, 1991. Unanchored and anchored tests conducted by Douglas et al.(1985) and Douglas and Kelly (1986) indicated no significant variation with different anchorage details for the geosynthetic used in their laboratory study. Similar conclusions were also reported by de Garbled and Javor (1986). Douglas and Kelly (1986) also observed from their tests that the overall stiffness of the model road did not seem to change significantly with a different tensile modulus of geosynthetic, for the range examined in their study. Dembicki (1992), who conducted model tests to examine the friction of geotextiles and the effect of anchorage on the bearing capacity of the subgrade, concluded the length of anchorage section is of a great importance

A difference in stiffness for unreinforced and reinforced tests with single and dual footing was observed in a small scale model test conducted by Love et al.(1987).

Where for the single footing no significant difference was observed between the unreinforced and the reinforced case, whereas when the load was applied by using dual footing a considerable difference was observed as well as increase in stiffness between the two loading patterns, affirming that the loading pattern is of importance when comparing the performance of reinforced and unreinforced unpaved roads.

The observations of Douglas and Kelly (1986) did not meet with universal agreement and an interesting debate on this matter has ensued, see Douglas and Kelly (1986), Bourdeau and Holtz (1988), Douglas (1990), and Bourdeau and Holtz (1992). The main conflict arises from their interpretation of the results, since they show a difference in behavior which is less that might be expected for a geosynthetic-soil system.

In summary, the mechanism of geosynthetic-soil interaction in unpaved roads appears to be complex and is not fully understood. The effect of anchorage, and consequently the contribution of a tensioned membrane effect, is not well-defined. Since the basic function that a geosynthetic serves in an unpaved road varies with the type of vehicle loading, subgrade strength and base course material properties, it would seem inappropriate to consider only one conceptual model when interpreting results of studies.

An interesting approach to the design of unpaved road using geosynthetics, which might explain some of the contrariety existing in the literature, has been developed, Milligan et. al (1989). Their method which is based on extensive research program consisting of model test under monotonic loading (Love, 1984), under cyclic loading (Fannin, 1987), and finite element analysis (Burd, 1986), disregards the membrane effect and therefore the effect of anchorage as well for small deformations.

Instead it is postulated that the outward acting shear stresses are picked up by the geosynthetic and only vertical stresses are transmitted to the subgrade below. Their procedure will be described in some detail in section 2.4.

2.3 UNPAVED ROAD CONSTRUCTION

Over the past fifteen years a number of methods for designing with geosynthetics in unpaved roads have been published. The design approaches are typically based on field studies, model studies or analytical studies, or in some cases a combination of the three.

2.3.1 Field Studies

Few well-controlled field trials have been performed to examine the influence of geosynthetics in unpaved roads. Early work, to which much reference made in more recent design methods, is that of the U.S. Army Waterways Experiment Station (Webster and Watkins, 1977; Webster and Alford, 1978). Webster and Watkins (1977) report details of a field trial involving seven test sections: one was reinforced with a nonwoven spun-bonded needle punched polyester geotextile, one with a neoprene-coated one-ply woven nylon membrane, and one was left unreinforced to act as a control section. The remaining sections were reinforced with materials other than geosynthetics. The test sections were 9.1 m long, and 3.7 m wide; They comprised a 35 cm thick crushed stone base course placed on a 61 cm thick clay subgrade of undrained shear strength 21 - 30 kPa in the upper 25 cm and 30 - 69 kPa below. Vehicle loading was applied using a 44.5 kN tandem axle dump truck, but analyzed in terms of an equivalent 80.1 kN single axle, dual wheel load. The performance of the

sections was evaluated from visual observations, photographs, and deformations of cross-sections recorded at intervals throughout the trafficking period. The sections were trafficked up to an average rut depth of 28 cm, which can be considered as failure. Results showed the performance of the reinforced sections was significantly better than the unreinforced section. The unreinforced section accepted 200 passes, the non-woven geotextile section 2500 passes, and the woven membrane 37000 passes.

This investigation was probably the first clear affirmation that using geosynthetics in construction of unpaved roads on soft ground leads to a significant improvement in traffickability.

Other field trials are reported (Potter and Currer, 1981; Sowers et al., 1982; Ramalho-Ortiago and Palmeira, 1982; Ruddock et al., 1982; Delmas et al., 1986; de Gardiel and Javor, 1986; Itoh et al., 1990; Austin and Coleman, 1993) which vary in their construction procedure, base course and subgrade soil properties, and imposed trafficking. Yet they all have one thing in common: the reinforced sections perform significantly better than unreinforced sections.

Besides reduced surface deformation due to the presence of the geotextile at the base course-subgrade interface, Potter and Currer (1981) also observed a considerable reduction in transient horizontal strains in the subgrade. The presence of the fabric did however not influence the amount of vertical stress and strains, and similar observations were reported by Ruddock et al. (1982). Sowers et al. (1982) reported their results for both light and heavy loads. They observed in the case of a light load that the presence of the geotextile helped to maintain a load spreading action in the base course by preventing intrusion of the subgrade into the base course material as well as providing restraining effects of the base course layer. For heavier loads, and increased rut depths, a tensioned-membrane effect was observed; when the subgrade was re-graded by filling in the ruts after the fabric had developed substantial

deformations, a further significant improvement in traffickability was observed that was attributed to the tensioned-membrane effects.

The most interesting observation in the field test described by Ramalho-Outrage and Palmeira (1982) is the effect of different anchorage details on the performance of an unpaved road. However, it must be noted that the base course was not a typical recommended base course material for unpaved roads, it consisted of a residual clayey soil and the thickness of the base course was therefore approximately 1 m instead of 30 cm thick if a good material would have been used. Field measurements showed 10 to 24% volumetric savings of the fill material when geotextiles where used where the difference in savings is attributed to the different anchorage details.

Delmas et al. (1986) performed a full scale test using four different geotextiles, two nonwoven and two woven geotextiles, of different tensile stiffness. The results showed a considerable difference in rut development with number of passes for the different fabrics, with the stiffer woven materials giving the best performance. They also observed a better performance for a given fabric if the anchorage length outside the wheel path was longer. De Garbled and Javor (1986) also observed a better performance from reinforced sections in their field test, using three different geotextiles of tensile strength in the range 35 kN/m (non-woven) to 480 kN/m (woven). However, they did not detect any significant difference in rut development between the three different geotextiles; this might be due to heterogeneity in the subgrade soil. Similar observations were reported by Austin and Coleman (1993).

From these full scale field trials it is evident that the inclusion of a geosynthetic does improve the performance of an unpaved road over soft ground. It is, however, not clear what the main function of the geosynthetic is, and further well-documented field trials are very important to the provision of good quality data for calibration of approaches used in design.

2.3.2 Model Studies

Numerous model tests, both at large and small scale, have been performed to analyze the bearing capacity and deformation behavior of a base course layer over a soft subgrade, with a geosynthetic inclusion, e.g.,(Jessberger, 1977; Sørlie, 1977; Jarrett et al., 1977; Bell et al., 1977; Barvashov et al., 1977; Andersson, 1977; Robnett et al., 1980; Barksdale et al., 1982; Robnett and Lai, 1982; Gourc et al.,1982; Kinney, 1982; Raumann, 1982; Milligan and Love, 1985; Jarrett and Bathurst, 1985; Laier and Bräu, 1986; Douglas and Kelly, 1986; Bauer and Preissner, 1986; De Garidel and Javor, 1986; Resl and Werner, 1986; Jarrett, 1986; Milligan et al., 1986; Love et al., 1987; Fannin, 1987; Floss et al., 1990; Houlsby and Jewell, 1990; Burd and Brocklehurst, 1990; Guido et al., 1991; Alenowicz and Dembicki, 1991; Dembicki, 1991; Douglas and Valsangkar, 1992). The review of the literature is however quite confusing since conflicting observations are reported in some of these studies and indicate everything from inferior to superior performance of unpaved road incorporating geosynthetics compared to roads without any reinforcement.

Due to the amount of available reported model studies a review herein would be to comprehensive and difficult to choose between reported studies in order to condense the review.

2.3.3 Analytical Studies

The tensioned membrane effect which is mobilized by deformations of the geosynthetic in an unpaved road over soft subgrade is considered as being of great importance in most of the available design methods. Some of the published methods for calculating the membrane effect are summarized briefly below.

The first attempt at describing the behavior of the tensioned membrane was made by Nieuwenhuis (1977) and Bakker (1977), who both observed the important

interaction between development of deformations in the subgrade and the tensile forces in the fabric. Nieuwenhuis (1977) assumed a linear elastic behavior of the membrane, and described the stress-strain characteristics of the subgrade by employing a coefficient of subgrade reaction or a spring constant; vertical equilibrium was addressed using Boussinesq theory for calculation of the load transferred through the base course layer. Bakker (1977) considered the ultimate bearing capacity of the subgrade, which was modified for the case with a geotextile by assuming a bilinear deformed shape of the geotextile under the loaded area, and a linear elastic behavior in the membrane.

Giroud and Noiray (1981) followed a similar approach, but assumed the deformed shape as parabolic. Sowers et al. (1982) also assumed a parabolic deformed shape for the geotextile, but instead of assuming a linear stress-strain relationship as others had done, they employed a strain-dependent tension in the fabric; strains were calculated from an empirical formula, and the tension established from approximate stress-strain curves.

Bourdeau et al. (1982) followed a similar approach to that of Nieuwenhuis (1977) but instead of using a Boussinesq solution for the semi-infinite half space for computing the load distribution through the base course layer, Bourdeau et al. (1982) used a probabilistic concept for the vertical stress diffusion in a particulate media. Assuming the subgrade deformation characteristics as a Winkler media the governing differential equation for vertical equilibrium is solved.

Sellmeijer et al. (1982) developed a method for calculating the tensioned membrane effect from a theoretical consideration that satisfies both subgrade and geotextile equilibrium. The equilibrium equations are then solved simultaneously assuming a bilinear elastoplastic behavior in the subgrade, and adequate anchorage of the geotextile. Sellmejer et al. (1982) will be discussed in more detail subsequently.

2.4 REVIEW OF DESIGN PROCEDURES

Several design methods for unpaved roads incorporating geosynthetics have been published over the last two decades. Many have been developed for specific commercial products, but others are intended to be generic. They may be grouped into three broad classes: the first is empirical; the second is classified as semi-theoretical, where field experience and experimental data are used in association with available theory; the third approach is purely analytical, and includes the finite element method.

2.4.1 Empirical Design Approaches

Few empirical design methods are available in the literature, and only one that can be classified as being strictly empirical was found in the literature review. This method, described by Jaecklin (1986), was developed using a sophisticated regression analysis on a large data base of case histories, and a survey of European. It takes into account traffic, rut depth, subgrade strength, base course aggregate properties and thickness, and a geotextile factor which is dependent on the mobilized strain in the fabric. These design factors are defined as follows:

V - factor : Traffic or vehicle load

V = 0.5	*very light vehicles and cars*	
V = 1	*light vehicles*	maximum 10 trucks per day.
V = 2	*medium*	10 - 50 trucks per day
V - 2.5	*heavy*	50 - 100 trucks per day
V = 3	*very heavy*	more than 100 trucks per day

Cars and light vehicles are considered to weigh less than 3500 kg (34.3 kN) and truck has a total weight of 36 tons (353.2 kN) on 4 axles or 9 tons (88.3 kN) per axle.

R - factor : Rut depth

R = 3-4 rut depth up to 3 cm

R = 5 rut depth up to 5 cm

R = 10 rut depth up to 10 cm

R = 15 rut depth up to 15 cm

K - factor : Base course aggregate

K = 0.5 *crushed rock*

K = 1 *clean gravel*

K = 2 *silty gravel*

U - factor : Subgrade strength

U = 1 *(firm)* CBR of 5-10 %, or S_u = 150-300 kPa

U = 2 *(soft)* CBR of 2-5 %, or S_u = 60-150 kPa

U = 3 *(very soft)* CBR of 1-2 %, or S_u = 10-60 kPa

D - factor : Base course thickness

The D factor is related to the traffic and subgrade strength which determines the minimum required base course thickness.

Traffic type	Minimum base course thickness (cm)		
	U = 1	U = 2	U = 3
V = 1	30	35	40
V = 2	35	40	45
V = 3	40	45	50

The D factor is then determined based on the minimum base course thickness requirements: D = 3, 4 and 5 for base course thickness of 30 - 40 cm, 40 - 50 cm and 50 - 80 cm, respectively.

The minimum failure force, F_{min} in kN/m, is then calculated according to the empirical formula shown below:

$$F_{\min} = G\left[5+2.1\times(V+0.8)^{0.8}\times\frac{4}{3R^{0.8}}\times 0.9U^{1.2}\times\frac{3.6}{D}\times\sqrt[4]{1+\left(1/K-1\right)^2}\right] \qquad (2.30)$$

Where G is assumed to be 1 if failure strain is higher than required minimum strain and if the failure force is larger than the required minimum too. Otherwise, if failure strain is not as high as determined the G - value is calculated as follows

$$G = \frac{\varepsilon_r^{required}}{\varepsilon_r^{effective}} \qquad (2.31)$$

The empirical equation for calculating the required minimum strain in the geotextile at failure is:

$$\varepsilon_f = \frac{1.4\times\log R\times\left(U^{1.5}+10+10\times\log D\right)}{V^{0.1}\times K^{0.1}} \qquad (2.32)$$

The actual failure strain is then determined by:

$$\varepsilon_r = 7.95\times e^{0.2457P} \qquad (2.33)$$

where

$$P = \ln\left(\frac{\varepsilon_f}{6.913}\right)^{\frac{1}{0.2457}} - 1 \qquad (2.34)$$

The above formulas can then be used to produce various design charts, such as failure strain and failure force versus base course thickness for various traffic loading, rut depths, base course types and subgrade or a more common chart with required base course thickness versus subgrade strength for different rut depths, loading and failure force.

2.4.2 Semi-Theoretical Design Methods

The most rational basis for a design method is indisputably a combination of field experience, experimental data, and theory. There are many design methods that are semi-theoretical, but they differ in how they combine theory and experience and to what extend different design factors are considered and the results interpreted.

Barenberg et al. (1975) and Bender and Barenberg (1978) developed a simple design procedure based on a laboratory testing program using large scale three dimensional and small scale two dimensional model systems of a nonwoven geotextile reinforced aggregate-subgrade system. Based on their results they concluded that failure in the unreinforced system occurred when the ratio of applied stress to the undrained shear strength of the subgrade was about 3.3 in the unreinforced system and about 6 in the reinforced system. These conclusions compare well to Terzaghi's bearing capacity factors for general and local shear failure, respectively. For determining the base course thickness when a geotextile is used in construction, the vertical stress is calculated using Boussinesq theory, where the allowable stress on the subgrade is not to exceed six times the undrained shear strength of the subgrade. In the unreinforced system, the same procedure is used but a bearing capacity factor of 3.3 rather than 6 is used. It should be noted that in the research program only one type of geotextile was used, Mirafi 140, and therefore caution should be used when applying the results to other fabrics.

Stewart et al. (1977), modified the recommendations of Barenberg after completing a full scale field trial where seven different geotextiles where used for reinforcement in an unpaved road over a soft subgrade. It was concluded that deep rutting, which was defined as being about 10 cm, would occur at stress levels of $3.3c_u$ without a fabric and at $6.0c_u$ with fabric. The values are the same as those reported by Barenberg earlier, but Stewart et al. (1977) also established that very little rutting (less

than 5 cm) would occur if stress levels in the subgrade did not exceed $2.8c_u$ in the unreinforced system at high traffic volume and $5.0c_u$ in the reinforced case.

Based on the tensioned membrane model developed by Kinney and Barenberg (1978,1982), Barenberg (1980) modified his original design approach in order to include the tensioned membrane effects. The applied stress on the subgrade is calculated according to Boussinesq theory and the base course thickness (h) then calculated by setting the applied stress equal to the sum of the permissible stress and the differential normal stress across the fabric. The vertical stress underneath the center line of the applied load is calculated assuming circular contact area using the following equation.

$$\sigma_z = \frac{P}{a^2\pi}\left[1 - \frac{h^3}{\left(a^2+h^2\right)^{3/2}}\right] \tag{2.35}$$

where P is the wheel load in kN and a is the radius of the loaded area in meters and

$$a = \sqrt{\frac{P}{\pi p}} \tag{2.36}$$

where p is the average contact pressure which is assumed to be equal to the tire inflation pressure in kPa for a single wheel or 0.7 to 0.8 times the air pressure of dual tires.

The permissible subgrade stress, which is expressed as a function of the undrained shear strength of the subgrade, is calculated using the following equation :

$$\sigma_{per} = A\pi c_u \tag{2.37}$$

where A is a dimensionless coefficient varying between 1.9 and 2.0 governed by the lateral restraint provided by the geotextile.

Vertical support from the geotextile is described by a differential stress across the fabric, assuming a circular deformed shape of the geotextile-subgrade interface shown in Fig. 2.4.

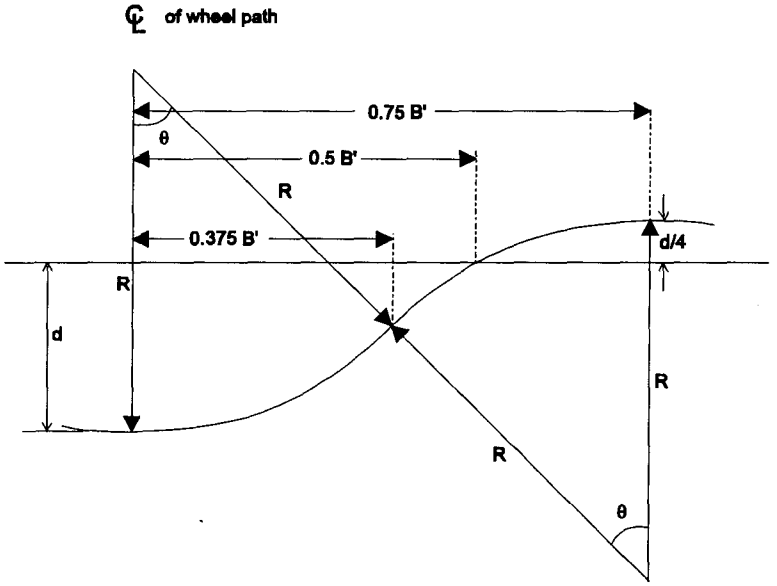

Figure 2.4 Assumed deformed shape of base course-subgrade interface (Kinney and Barenberg, 1982)

The differential normal stress in kPa across the geotextile is

$$\Delta\sigma_{z-g} = \frac{t_g}{R} \tag{2.38}$$

where t_g is the tension in the geotextile

$$t_g = \varepsilon_g E_g (kPa) \tag{2.39}$$

and ε_g and E_g are the geotextile strain (%) and geotextile modulus (kN/m/% strain), respectively.

The average strain in the geotextile is determined from the assumed deformed circular shape according to the following equation:

$$\varepsilon_g = \frac{4\pi R\theta}{135B'} - 2 \tag{2.40}$$

where $$R = \frac{\frac{3}{8}B'}{\sin\theta} \tag{2.41}$$

and $$\theta = 2\arctan\left(\frac{5d}{3B'}\right) \tag{2.42}$$

Design charts can then be produced based on the above procedure, where the applied stress on the subgrade surface is set equal to the permissible stress plus the differential normal stress in the geotextile

$$\sigma_z = \sigma_{per} + \Delta\sigma_{z-g} \tag{2.43}$$

and the expression solved for various values of the subgrade undrained shear strength.

Giroud and Noiray (1981) developed a design procedure based on theoretical considerations and data from field trials. Their approach has become the basis for many design methods, and is described in detail below. It includes a tensioned membrane effect and incorporates, for the reinforced system, a bearing capacity failure in the subgrade that is one of general shear failure, rather than a local shear failure.

Essentially, failure is anticipated if the sum of the surcharge pressure on the subgrade below the loaded area, minus the pressure reduction due to the tensioned membrane effect, exceeds the ultimate bearing capacity of the subgrade, that is

$$q_u = (\pi + 2)c_u + \gamma h = p - p_g \tag{2.44}$$

where q_u is the ultimate bearing capacity of the subgrade, p is the surcharge pressure on the subgrade and p_g is the reduction of pressure due to the tensioned-membrane effect.

The failure of the unpaved road can occur in the subgrade or the geotextile. The base course material is assumed to have sufficient friction to ensure mechanical stability of the layer and to prevent sliding over the geotextile. A pyramidal load distribution is

assumed (Fig. 2.5). For a base course thickness of h_0 without a geotextile, the pressure at the base of the base course layer is given by:

$$p_0 = \frac{2LBp_{ec}}{2(B+2h_0\tan\alpha_0)(L+2h_0\tan\alpha_0)} + \gamma h_0 \qquad (2.45)$$

A base course thickness of h in the reinforced case, yields a stress on the subgrade of:

$$p = \frac{2LBp_{ec}}{2(B+2h\tan\alpha)(L+2h\tan\alpha)} + \gamma h \qquad (2.46)$$

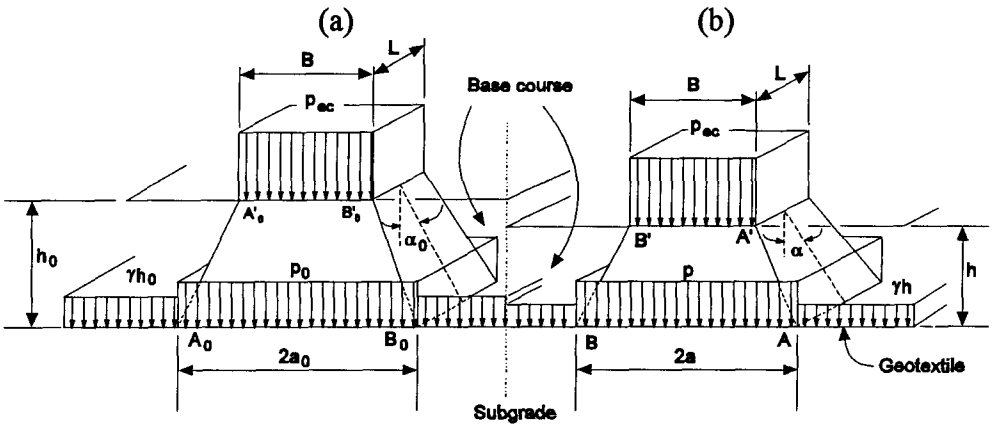

Figure 2.5 Load distribution by base course layer: (a) Case without geotextile; and (b) Case with geotextile (Giroud and Noiray, 1981)

The axle load, P, is evenly distributed between the two wheel sets and assuming dual wheels:

$$P = 4A_c p_c \qquad (2.47)$$

where A_c is the contact area (m^2) and p_c is the tire inflation pressure (kPa).

In the method each dual wheel contact area $2A_c$ is replaced by a rectangle of a larger area of B times L according to following relationship:

$$LB = 2A_c\sqrt{2} \qquad (2.48)$$

Two different cases are examined, on-highway trucks and off-highway trucks. For a tire inflation pressure of p_c the following approximate relationship between L and B is introduced:

$$L = \frac{B}{\sqrt{2}} \quad \Rightarrow \quad B = \sqrt{\frac{P}{p_c}} \qquad \text{(on-highway trucks)} \qquad (2.49)$$

and

$$L = \frac{B}{2} \quad \Rightarrow \quad B = \sqrt{\frac{P\sqrt{2}}{p_c}} \qquad \text{(off-highway trucks)} \qquad (2.50)$$

The maximum subgrade pressure in the unreinforced case is equal to the elastic bearing capacity, which is the same as local shear failure value according to Terzaghi:

$$p_0 = \pi \cdot c_u + \gamma \cdot h_0 \qquad (2.51)$$

Using the above relationship and equations 2.49, 2.50 and 2.45, the base course aggregate thickness h_0 in the unreinforced case can be determined from the following equations:

$$c_u = \frac{P}{2\pi\left(\sqrt{\frac{P}{p_c}} + 2h_0 \tan\alpha_0\right)\left(\sqrt{\frac{P}{2p_c}} + 2h_0 \tan\alpha_0\right)} \qquad \text{(on-highway trucks)} \qquad (2.52)$$

$$c_u = \frac{P}{2\pi\left(\sqrt{\frac{P\sqrt{2}}{p_c}} + 2h_0 \tan\alpha_0\right)\left(\sqrt{\frac{P}{2p_c\sqrt{2}}} + 2h_0 \tan\alpha_0\right)} \qquad \text{(off-highway trucks)} \qquad (2.53)$$

The subgrade soil is assumed to be fully saturated, and therefore incompressible in the undrained state under traffic loading.

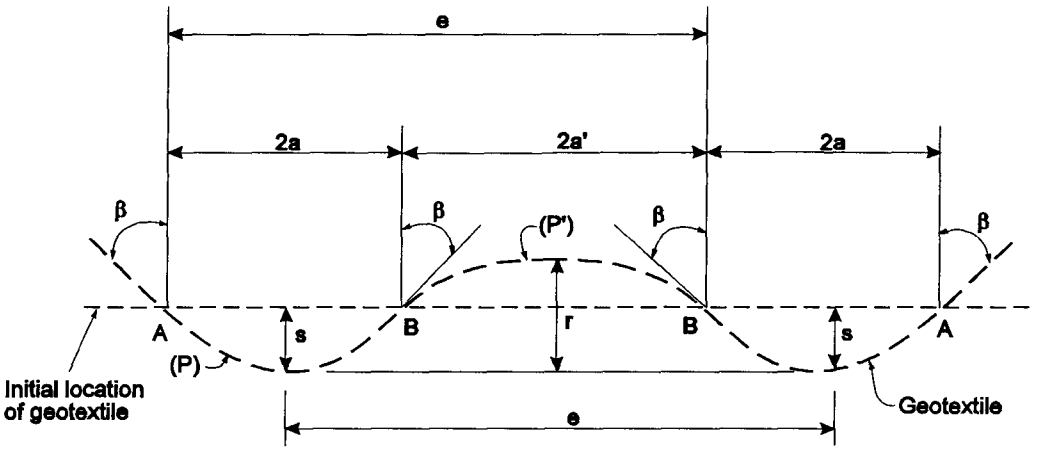

Figure 2.6 Assumed parabolic shape of deformed geotextile (Giroud and Noiray, 1981)

Strain in the geotextile is calculated, for an assumed parabolic deformed shape, from the following:

$$\varepsilon = \frac{b+b'}{a+a'} - 1 \qquad \text{for a' > a} \tag{2.54}$$

$$\varepsilon = \frac{b}{a} - 1 \qquad \text{for a > a'} \tag{2.55}$$

where b and b' are the half length of (P) and (P'), respectively, and the widths a and a' are obtained from Figs. 2.5 and 2.6:

$$2a = B + 2h\tan\alpha \tag{2.56}$$

$$2a' = e - B - 2h\tan\alpha \tag{2.57}$$

The chord lengths b and b' are calculated using the following relationship between the arc of a parabola and a chord:

$$\frac{b}{a}-1=\frac{1}{2}\left[\sqrt{1+\left(\frac{2s}{a}\right)^2}+\frac{a}{2s}\ln\left\{\frac{2s}{a}+\sqrt{1+\left(\frac{2s}{a}\right)^2}\right\}-2\right] \tag{2.58}$$

$$\frac{b'}{a'}-1=\frac{1}{2}\left[\sqrt{1+\left(\frac{2(r-s)}{a'}\right)^2}+\frac{a'}{2(r-s)}\ln\left\{\frac{2(r-s)}{a'}+\sqrt{1+\left(\frac{2(r-s)}{a'}\right)^2}\right\}-2\right] \tag{2.59}$$

The reduction in pressure due to the tensioned-membrane effect, p_g, is considered to be a uniformly distributed pressure on AB (Fig. 2.6) and is equal to the vertical component of the tension T in the geotextile at points A and B:

$$ap_g = T\cos\beta \tag{2.60}$$

Knowing the strain ε , and the geotextile elastic modulus E, the tension is given by:

$$T = E_g\varepsilon \tag{2.61}$$

and from the following property of a parabola:

$$\tan\beta=\frac{a}{2s} \tag{2.62}$$

then p_g is established from:

$$p_g = \frac{E_g\varepsilon}{a\sqrt{1+\left(\frac{a}{2s}\right)^2}} \tag{2.63}$$

The thickness of the base course layer in the reinforced case is then determined from equations 2.44, 2.46, and 2.63:

$$(\pi+2)c_u = \frac{P}{2(B+2h\tan\alpha)(L+2h\tan\alpha)} - \frac{E_g\varepsilon}{a\sqrt{1+\left(a/2s\right)^2}} \tag{2.64}$$

The reduction in the base course aggregate thickness due to the action of the geotextile is then given by:

$$\Delta h = h_0 - h \tag{2.65}$$

using equation 2.52 or 2.53 to establish h_0, and solving equation 2.64 for h. The value of reduction thickness, Δh, is assumed to be independent of the traffic volume.

In order to account for traffic loading Giroud and Noiray (1981) proposed a formula based on work by Webster and Alford (1978) to determine the required base course thickness of an unreinforced road:

$$h_0' = \frac{0.19 \log N_s}{CBR^{0.63}} \tag{2.66}$$

where N_S is the number of passes of a standard axle load, P_S = 80 kN. This equation is restricted to a standard axle load and to a rut depth of 0.075 m. It was suggested other axle loads be accommodated through the widely used power rule in unpaved road design:

$$\frac{N_s}{N_i} = \left(\frac{P_i}{P_s}\right)^{3.95} \tag{2.67}$$

where N_i is the number of passes of axle load P_i. Equation 2.67 was extended to rut depths other than 0.075 m using an expression, deduced from the Webster and Watkins (1977) test results, where log N_S was replaced by:

$$\log N_s - 2.34(r - 0.075) \tag{2.68}$$

The unreinforced base course thickness can now be determined for traffic loading by combining equations 2.66, 2.67 and 2.68, and substitution of:

$$c_u(kPa) = 30 \cdot (CBR) \tag{2.69}$$

giving:

$$h_0' = \frac{1.61935 \cdot \log N + 6.39642 \cdot \log P - 3.78927 \cdot r - 11.88877}{c_u^{0.63}} \quad (2.70)$$

This equation is not recommended for more than 10,000 vehicle passes.

Finally, the thickness of the base course in the case of a reinforced system, again considering the influence of trafficking, given by:

$$h' = h_0' - \Delta h \quad (2.71)$$

Use of these equations was simplified by creation of design charts. It should be noted that the rut depth, r, is defined as the vertical distance between the highest point of the road surface between the wheels and lowest point of the rut (Fig. 2.6).

Giroud et al. (1984), modified the above design approach for use of geogrids rather than geotextiles to take into account interlocking of the geogrid and base course material. Progressive deterioration of the subgrade shear strength is described by:

$$\lambda = \frac{c_{uN}}{c_u} = \frac{1}{\left[1 + (\log N)^{1.5} \frac{c_u}{1000}\right]} \quad (2.72)$$

Progressive deterioration of the base course layer is taken into account by decreasing the load distribution angle with increasing number of passes. The load distribution angle α_0 is determined by combining equations 2.46 and 2.49, 2.51, 2.66 and 2.72, resulting in the following equation:

$$\tan \alpha_0 = \frac{\sqrt{0.17157 \cdot \frac{P_s}{2p_c} + \frac{2P_s}{\lambda \pi c_u}} - (2.41421)\sqrt{\frac{P_s}{2p_c}}}{\frac{6.5 \cdot \log N}{c_u^{0.63}}} \quad (2.73)$$

The design is the performed according to the same procedure described by Giroud and Noiray (1981), with a recommendation that the tensioned-membrane effect be neglected or if the membrane effect is not negligible a lump reduction of 10% of the designed base course layer is recommended.

Sellmeijer et al. (1982) developed a design method based on the tensioned membrane theory. Different from other available design procedures, their method fulfills equilibrium conditions for both the membrane action of the geotextile and the subgrade soil. Therefore the deformed shape of the geotextile-subgrade interface is not defined arbitrarily which is contrast to other semi-empirical methods.

When a geotextile is subjected to a traffic load q_0 the geotextile starts to deform and goes into tension, hence developing the tensioned membrane action. The equilibrium equations are:

$$T = T_h\sqrt{\left(\frac{ds}{dx}\right)^2 + 1}$$

$$T_h\frac{d^2s}{dx^2} = -(q_0 - q_1) - \gamma h \tag{2.74}$$

where T is the tensile force in the geotextile, T_h is the horizontal component, s is the vertical displacement of the fabric and x is the horizontal distance from the truck axis. The subgrade soil is assumed to behave in a bi-linear elasto-plastic manner, where the linear elastic phase is described by using a subgrade reaction coefficient, C_c:

$$q = C_c \cdot s \tag{2.75}$$

In the rigid plastic phase the subgrade behavior is described based on Brinch Hansen bearing capacity formula:

$$q_1 = N_c\left(c + \tfrac{3}{4}W\gamma' \tan^2\phi\right) \tag{2.76}$$

where N_c is assumed to be 5.14 and ϕ is the internal friction angle of the subgrade.

This method is two dimensional and the distributed traffic load is assumed to be constant acting over the whole length of the road structure given by the following equation:

$$q_0 = \frac{P}{2(nB+2eh)(B+2eh)} \tag{2.77}$$

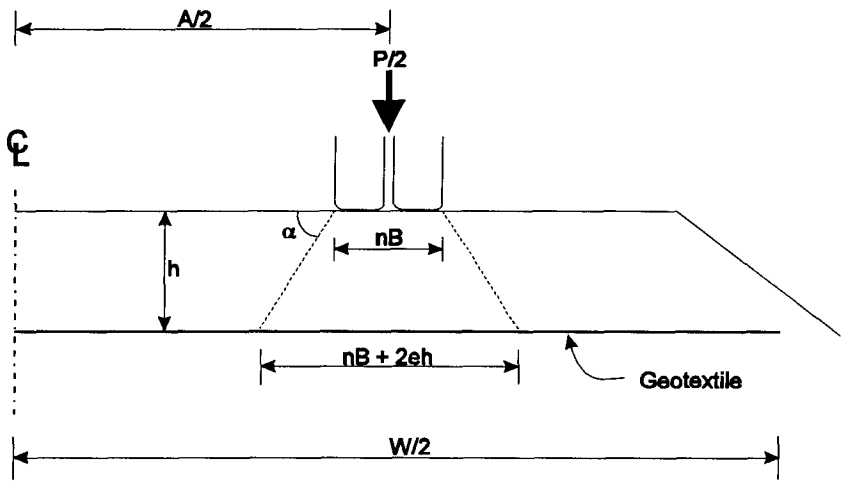

Figure 2.7 Road cross section showing pertinent factors

Solving equation 2.74 for the constant load distributed by the base course layer gives the following:

$$\frac{C_c s}{q_0} = \frac{2\cosh(\beta-\alpha)\cosh\xi\sinh\eta}{\sinh\beta} \tag{2.78}$$

$$\frac{C_c s}{q_0} = \frac{2\cosh(\beta-\alpha)\cosh\xi\sinh\eta}{\sinh\beta+1-\cosh(\xi-\alpha+\eta)} \tag{2.79}$$

$$\frac{C_c s}{q_0} = \frac{2\cosh\alpha\cosh(\xi-\beta)\sinh\eta}{\sinh\beta} \tag{2.80}$$

where:

$$\alpha = \tfrac{1}{2} A \cdot \sqrt{\frac{C_c}{T_h}} \qquad \beta = \tfrac{1}{2} W \cdot \sqrt{\frac{C_c}{T_h}}$$

$$\eta = \tfrac{1}{2}(nB + 2eh) \cdot \sqrt{\frac{C_c}{T_h}} \qquad \xi = x \cdot \sqrt{\frac{C_c}{T_h}}$$

Equation 2.78 is valid for $0 < \xi < \alpha-\eta$, equation 2.79 is valid for $\alpha-\eta < \xi < \alpha+\eta$, and equation 2.80 for $\alpha+\eta < \xi < \beta$.

The width of the plastic zone, b, is obtained from equilibrium considerations of the subgrade reaction to the sum of the wheel load and the base course layer aggregate weight:

$$bq_1 = \frac{P}{2(B+2eh)} + \gamma hb$$

or (2.81)

$$b = \frac{P}{2(q_1 - \gamma h)(B+2eh)}$$

The three possible locations of the plastic area of the soil stress are shown in Fig. 2.8, in which the occurrence of the first case is the most frequent one.

Equation 2.74 can now be solved together with equations 2.76 and 2.81 for each of the three cases. The horizontal tension force, T_h, is however still unknown but can be determined by the compatibility condition of the geotextile if its anchorage is considered being sufficient.

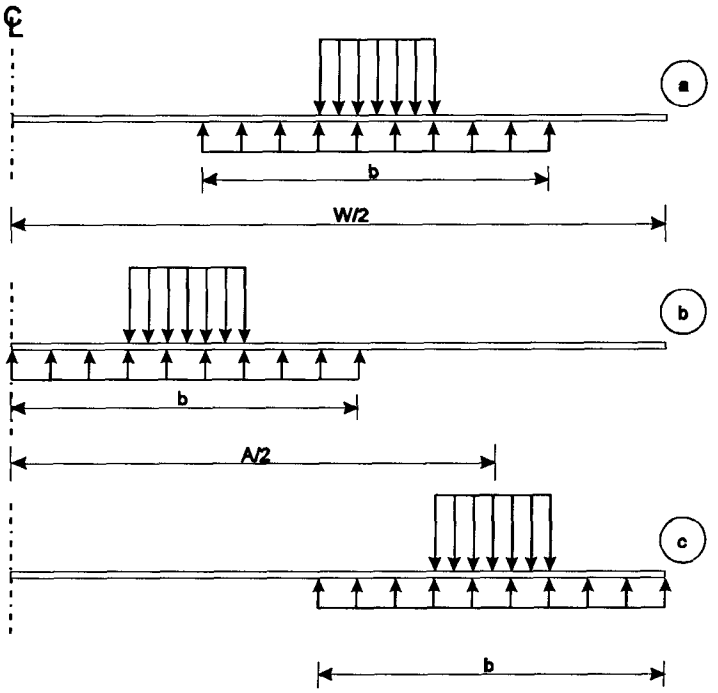

Figure 2.8 Location of the plastic zones

The ultimate solution of the membrane equation is given in the following way:

$$\Delta s = \tfrac{1}{4}\frac{(b - nB - 2eh \pm d)^2}{(b - nB - 2eh)\lambda} \tag{2.82}$$

$$\lambda = \left[\left(\frac{2E_g}{3(q_1 - \gamma h)W}\right)\frac{(b - nB - 2eh)^2 + 3d^2}{b^2}\right]^{\frac{1}{3}} \tag{2.83}$$

$$T_m = \tfrac{1}{2}(q_1 - \gamma h)b\sqrt{\left(\frac{b - nB - 2eh + d}{b^2}\right)^2 + \lambda^2} \tag{2.84}$$

In the above equations, Δs is the total rut depth, E_g is the geotextile Young's modulus and T_m is the maximum tensile stress in the geotextile.

The location of the plastic zone is defined by the plastic location parameter, d:

$d = 0$ if $b < A$ and $b < W - A$ (case a)

$d = W - A$ if $b > A$ and $b < W - A$ (case b)

$d = W - A - b$ if $b < A$ and $b > W - A$ (case c)

This design method does not take traffic into account, but based on the Moordrect test results, described by Sellmeijer and Kenter (1983), the following equation is suggested to calculate an equivalent axle load P_i for N passes of a real axle load P_s:

$$P_i = P_s^{6.2} \cdot \sqrt{2} \qquad (2.85)$$

Haliburton and Barron (1983) presented a design method based on a scale model laboratory tests and previous research by Haliburton et al. (1980) and Haliburton and Lawmaster (1981). The approach focuses on placement of the reinforcement at an optimum depth within the base course layer, given the width of the loaded area. Research showed that maximum restraint of the base course material occurred when the base course aggregate thickness was equal to 0.33B, where B is the width of the loaded area. This optimum depth was found to significantly increase the ultimate strength and deformation resistance of the base course material as well as showing a significant stress reduction at the subgrade interface of 50%, based on a Burmister layered system theory (Burmister 1943, 1944).

In design, knowing the axle load and the tire inflation pressure, the contact area is established, either as circular or rectangular. Then, by applying Boussinesq theory stresses are calculated at a depth of 0.5B tan ϕ, or alternatively at a depth of 0.33B, which are considered comparable. The predicted stress is then reduced by half to reflect stress reduction effects observed in the research. The reduced stress is

compared to the ultimate bearing capacity of the subgrade, and if it smaller the design is satisfactory.

Milligan et al. (1989) presented a design method for designing unreinforced and reinforced unpaved roads based on extensive tests on small and large scale models under monotonic and cyclic loading, and a large strain finite element analysis. Their method does not follow the conventional tensioned-membrane approach, but emphasizes the role of shear stresses at the subgrade surface. When load is applied to the base course layer it produces vertical and horizontal stresses in the subgrade layer. Some of the horizontal stress is resisted by the base course material outside the loaded area, and the remainder develops outward acting shear stresses on the subgrade surface. This action reduces the subgrade bearing capacity significantly. If a geosynthetic is installed at the subgrade surface, the outward acting shear stresses will be taken up by tension in the geosynthetic, promoting a vertical stress only to be transmitted to the subgrade soil.

The method, which is developed for use in design of unpaved roads at small rut depths, does not consider a tensioned-membrane effect and anchorage is considered to be less important than in other procedures. However, stiffness of the geosynthetic is important if small ruts are desirable. The authors recognize the importance of the tensioned-membrane effect, but only at considerable rut depth. The bearing capacity of a strip footing is predicted by using upper and lower bound theorems of plasticity theory (Fig. 2.9):

$$N_{ca} = 1 + \frac{\pi}{2} + \arccos\left(\frac{\tau_r}{s_u}\right) + \sqrt{1 - \left(\frac{\tau_r}{s_u}\right)^2} \qquad (2.86)$$

where $$N_{ca} = \frac{\sigma_{va} - \sigma_{vo}}{s_u}$$

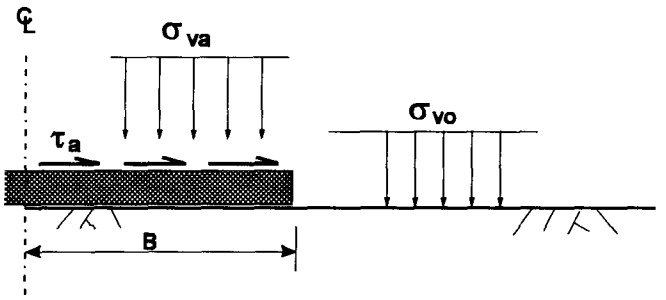

Figure 2.9 Bearing capacity of subgrade

The load spread angle β is used to estimate the vertical stress within the base course layer. It should be noted that B is taken as the half-width of the footing width (Fig. 2.10). The vertical stress p is applied to the footing of width 2B and resulting stress at depth z below the base course surface is given by:

$$\sigma_v' = \frac{pB}{B + z\tan\beta} + \gamma z \tag{2.87}$$

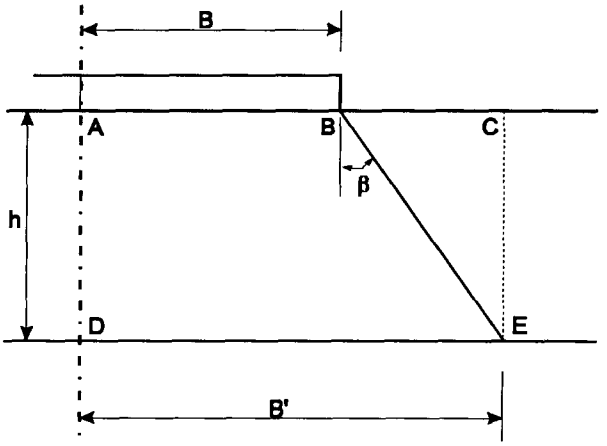

Figure 2.10 Load spread angle below plain strain footing

Underneath the footing the base course is pushed outwards, developing active pressures, and passive pressures are developed outside the influence zone of loading.

Taking into account the angle of friction δ on the base of the footing, the minimum average shear stress required on the subgrade surface for stability is determined by solving the horizontal equilibrium of the rectangular area shown in Fig. 2.11:

$$\tau_r = \tfrac{1}{2}\left(K_a - K_p\right)\left(\frac{1}{B'}\right)\gamma h^2 + \frac{K_a p}{\tan\beta}\left(\frac{B}{B'}\right)\cdot\log\left(\frac{B}{B'}\right) - p\left(\frac{B}{B'}\right)\tan\delta \qquad (2.88)$$

This equation gives the linear increase of the required shear stress with vertical load shown as the "required" line intercepting the available shear stress at point A in Fig. 2.12.

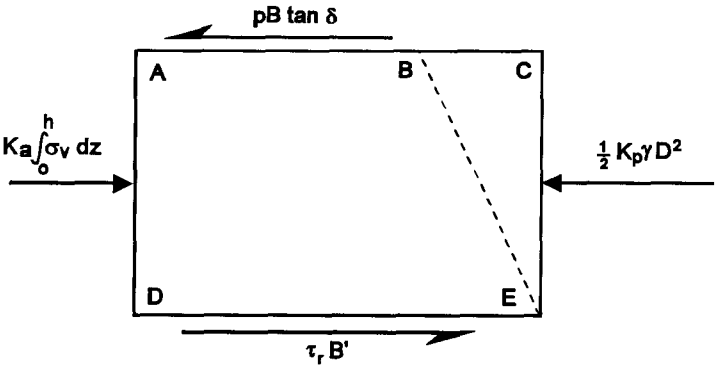

Figure 2.11 Soil block in equilibrium analysis

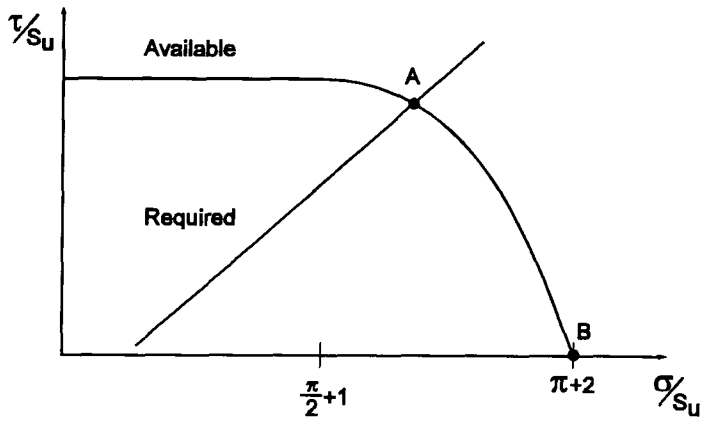

Figure 2.12 Normal and shear stress interaction at subgrade-base course interface

Limiting equilibrium is achieved when the required subgrade bearing capacity matches the available subgrade bearing capacity. The applied vertical stress can be calculated, once the mobilized bearing capacity is determined, using the following equation:

$$p = N_c c_u \left(1 + \frac{h}{B} \tan\beta\right) \tag{2.89}$$

Bearing capacity failure can also occur in the base course layer, and it is therefore necessary to check that the axle load is not limited by the bearing capacity of the base course.

Design using this method requires knowledge of the half-width of the loaded area, the base course thickness, value for the load spread angle, base course friction angle and unit weight, and the undrained shear strength of the subgrade. The interception point, A, is determined graphically or numerically. The applied vertical stress, p, is then calculated and the required reinforcement force in the geosynthetic determined knowing that $T = \tau_r B'$.

Interpretation of the results established that the greatest benefit of a reinforcement is obtained when using a poor base course material on very soft subgrades, a normal strength base course on relatively firm subgrades, and strong base course on strong subgrades.

Houlsby and Jewell (1990) extended the procedure in to cases of axisymmetric loading, though the modification complicates the calculations to an extent that may be unnecessary given the nature of the application.

Chapter 3

Test Site Description

3.1 GEOLOGICAL HISTORY

3.1.1 Geological History of the Lower Mainland

The test site is located on Lulu Island in the Fraser Delta of the Lower Mainland of British Columbia. The geological history of the Lower Mainland has been studied by Armstrong (1956, 1957, 1984), Blunden (1973, 1975) and Clague and Luternauer (1983), who reported that the bedrock geology of this area has evolved over millions of years and the unconsolidated Quaternary sediments over the last several thousand years. Since the bedrock at or within 10 m of the surface forms less than five percent of the Fraser Lowland, the main concern for shallow foundations is the Quaternary sediments.

The Fraser Lowland experienced at least three major advances and retreats of glaciers during the Ice Age, and the present surficial geology of the Vancouver area is

strongly influenced by these repeated Pleistocene glaciations. Each major glaciation in the lowland, which was accompanied by isostatic and eustatic adjustments, went through three main stages (Armstrong, 1984); an advance stage, a maximum stage when ice attained a thickness of 1800 m or more, and a retreat or deglaciation stage. As a consequence of the complex deposition environment, the sediment types range from glacial to deltaic and demonstrate considerable heterogeneity both laterally and vertically.

The Fraser Lowland, also known as the Whatcom Basin, is a triangular area of approximately 3500 km^2 that forms the southwest corner of the mainland British Columbia and the adjoining northwest corner of Washington State (Fig. 3.1). The Lowland is bounded on the west by the Straight of Georgia, on the north by the Coast Mountains and on the south-east by the Cascade and Chuckanut mountains. For the last 100 millions years the geology of the greater Vancouver area has been that of the infilling of this structural basin which originated during the Upper Cretaceous time.

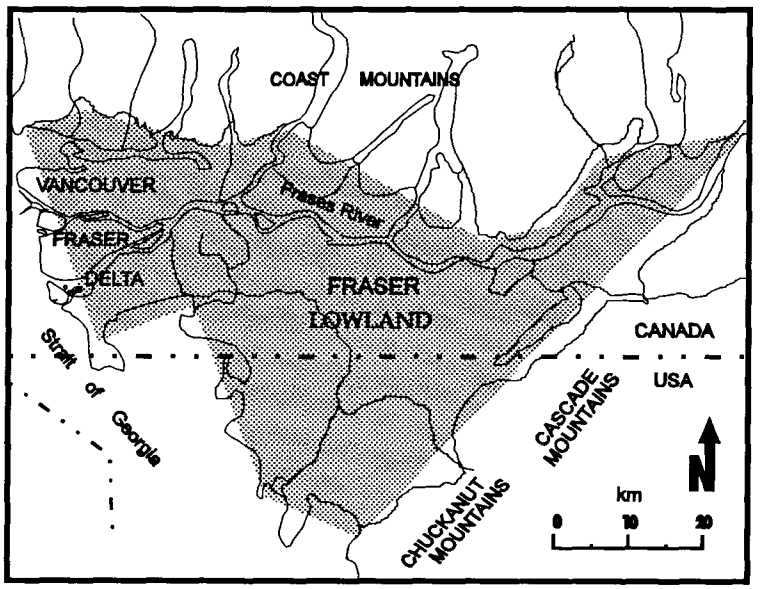

Figure 3.1 Index map showing location of Fraser Lowland.

Approximately 11,000 years ago, after the ice sheets of the Fraser Glaciation had retreated from most of the low lying areas of southwestern British Columbia the surface of the Lower Mainland, which had been depressed by the weight of the ice, rose 150 meters (Eisbacher, 1977). Following the complete withdrawal of the ice and the adjustment of the level of the land some 10,000 to 8,000 years ago the Fraser River, which is the most important agent for the deposition in the region began discharing into the Strait of Georgia. Currently it discharges approximately 18 million tonnes of sand, silt and clay each year (Armstrong, 1984), most of which is deposited in the Strait of Georgia to add to the growing delta.

Due to the large volume of sediments supplied to the river by the retreating ice sheet, the delta expanded very rapidly and attained its present position about 5,000 years ago. The advance of the delta continues to this day, causing the mouth of the river to move seaward at an average rate of 2 meters per year near the water surface. At a depth of 100 meters the advance of the delta front is as much as 9 meters per year.

3.1.2 Surficial Geology of Lulu Island

There are a wide variety of Quaternary deposits found in the Fraser Lowland. The three major sediment groups are: waterlain sediments; glacier ice sediments; and glaciomarine and glaciolacustrine sediments. In addition to these sediments occasional deposits of windblown material are found. Peat bogs and organic sediments are very common in flat lowland areas.

Lulu Island and adjacent Sea Island, see Fig. 3.2, are only a few thousand years old and both owe their existence to the growth of the Fraser Delta complex. They likely originated as sand bars at what was then the mouth of the Fraser River, some 8,000 years ago. Approximately 1000 years later the area had become a mud flat and salt marsh, and the Fraser River had developed what are now termed the North and

South Arms. Lulu Island grew to its present size 4,000 years ago, at which time extensive peat bogs had formed upon the earlier salt marshes. These peat bogs now cover about 14 km^2. The top layer of the peat bog is referred to as unhumified peat, which is a dead sphagnum moss that is only slightly decompressed.

The current surficial deposits of Lulu Island comprises a thin discontinuous layers of clays, silts and peats, which have been laid down in fluviatile, interdistributary swamps, and salt marsh environments. They overlie a thick sequence of sands and silts. The bedrock is of Tertiary age and is found at depths of between 200 and 270 meters.

3.2 DESCRIPTION AND LOCATION OF TEST SITE

The research site is located on the eastern part of Lulu Island, see Fig. 3.2. It is on ground which is owned by the Province of British Columbia Ministry of Transportation and Highways, being on a right-of-way parallel to and southeast of Highway 91/91A, some 30 km from UBC.

The site is bounded to the north and west by Highway 91/91A, and to the south and southwest by a main drainage ditch that runs due north, see Fig. 3.3. The south side, between the site and Hamilton Road, is an agricultural land. The site area is approximately 100 m long and 10 m wide, and located about 350 m east of the Hamilton Interchange. It forms part of a future highway development area, but is undeveloped, being covered by grass overlying a 30 to 60 cm thick sand layer that was the edge of the preload for existing highway.

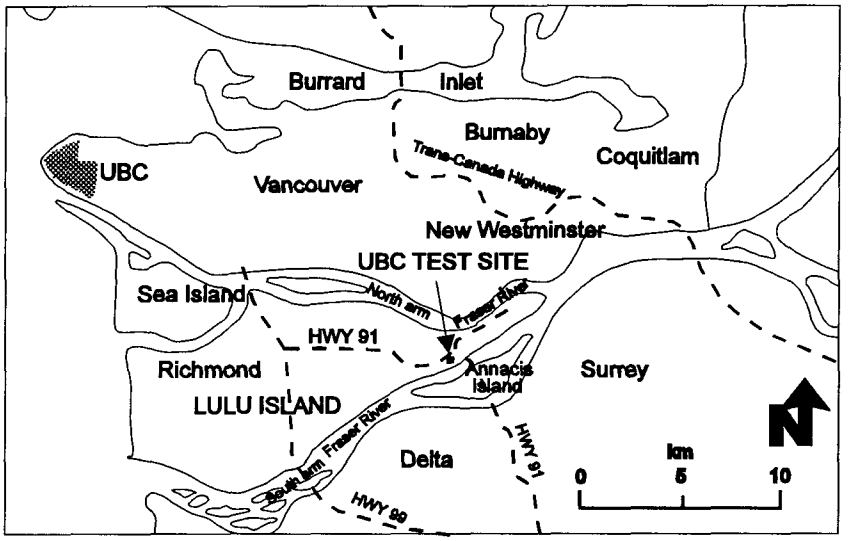

Figure 3.2 Location of the research site.

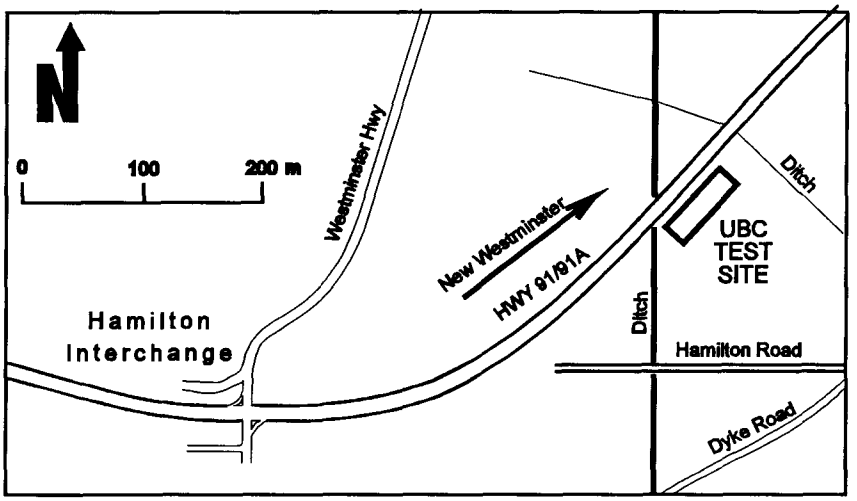

Figure 3.3 General research site details.

The ground surface elevation at the site is about + 1.0 m with respect to the average sea water table. The thickness of the surficial soils, which generally comprise layers of peat, organic silts, and clays, silts, and sandy silts, is about 15 m; these soils are underlain by a fairly dense sand or silty-sand . The depth of peat formation in this

part of Lulu Island varies greatly from 0 m to 6.1 m (Kern and Buchanan, 1984). The elevation of the groundwater table as determined from the ditchwater levels varies between + 0.0 to + 0.5 m.

3.3 SUBGRADE SOIL PROPERTIES

The final location of the test site was selected to give a reasonably uniform near surface stratigraphy along the unpaved road test section, which was 80 m long and 6 m wide. Following a review of borehole logs in the general area, a detailed site investigation was conducted, that included test pits, laboratory tests and field vane tests. The site investigation was done to establish the uniformity of soil stratigraphy and to determine the variation in physical properties of the subgrade soil both spatially and with depth. Locations of the test pits and sampling points at the final location are illustrated in Fig. 3.4. A total of 9 test pits were dug that varied in depth from 0.5 m to 2.0 m, and 10 field vane tests were performed. Details of the site stratigraphy, soil properties and variation of shear strength with depth are given below.

3.3.1 Site Stratigraphy

The description of site stratigraphy is based on examination of the nine test pits, six of which were relatively shallow and used to determine the depth to the soft subgrade and to locate the groundwater table. The other three are deeper and provide more detailed information.

The characteristic sequence of soil layers is illustrated in Fig. 3.5. The sequence is an average of the three deep test pits and the elevation shown is based on the local elevation system in the City of Richmond. The vegetated topsoil overlies a slightly

silty sand and a yellowish-brown sandy, very clayey silt, both of which showed some variation in thickness across the site.

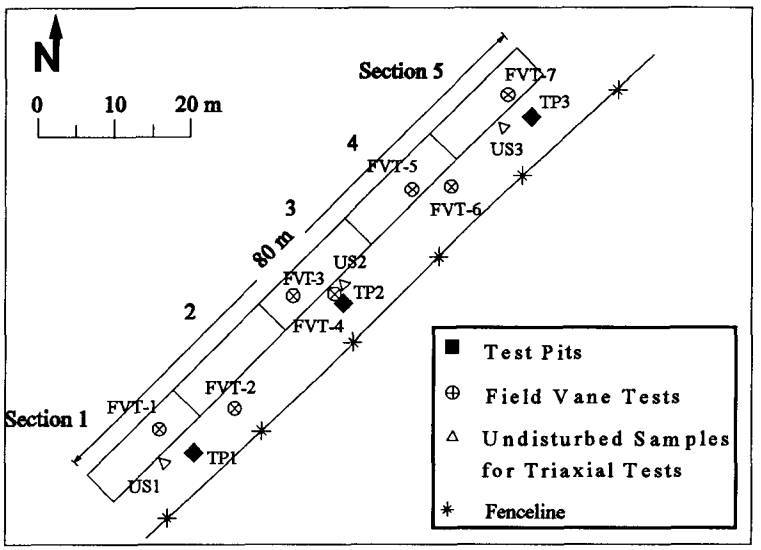

Figure 3.4 Location of tests

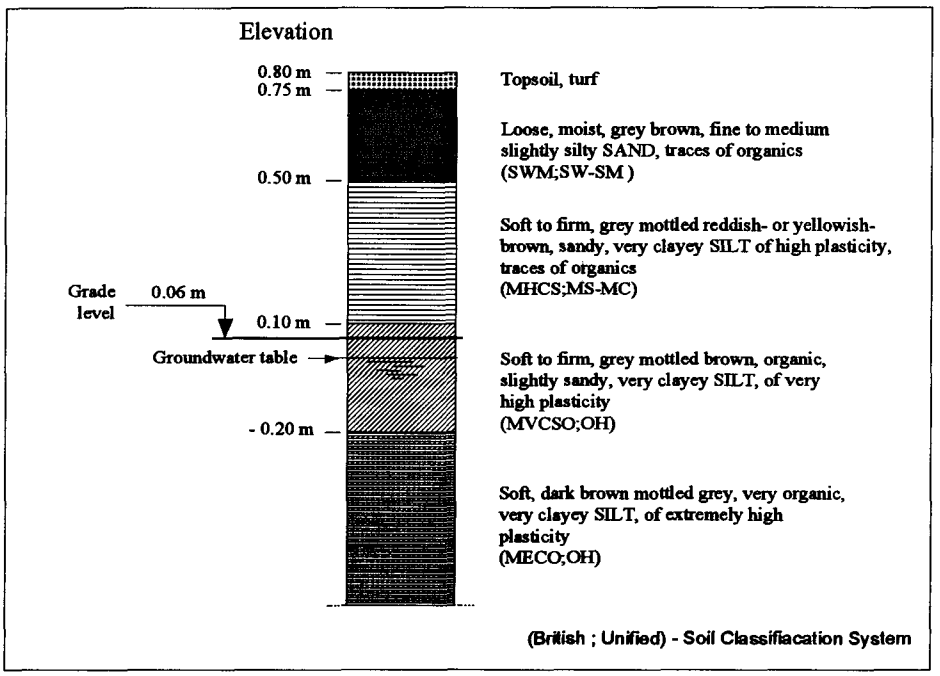

Figure 3.5 Typical test pit results

Below this was an organic very clayey silt, the upper part of which was slightly sandy. Uniform thickness of the upper soil layers, which varied in thickness from 0.0 up to about 0.6 m and was interbedded in some places with 5 - 20 cm thick sand lenses.

Prior to construction of the test sections, these upper soil layers were excavated to the grade level (see Fig 3.5) to promote a uniformity of soil stratigraphy along the length of the trial.

3.3.2 Soil Properties

Properties of the subgrade soil were established from grain size analysis and Atterberg Limit tests. Samples were taken at 0.2 m intervals below grade from the three deeper test pits, the locations of which are shown relative to the road trial in Fig. 3.4.

Specific gravity values were obtained from two different depths from each test pit, at 0.1 m and at 0.9 m depth. Since soil in the field composed of only one type of soil or clay mineral is rarely found, but more often the soil is composed of various percentages of sand, silt and clay, the specific gravity value of the solids obtained by the specific gravity test procedure is actually an average of all the types of minerals occurring in the soil being tested. Results from the specific gravity test performed are shown in Table 3.1.

Table 3.1 Specific Gravity Results

TP1 G_s	**TP2** G_s	**TP3** G_s	Average Value
2.656	2.573	2.690	2.640

The grain size distribution for the subgrade soil was determined from the above mentioned test pits at 0.2 m interval using the average specific gravity values from Table 3.1. A hydrometer method, which depends on Stokes' equation for the terminal velocity of falling sphere, was used for this purpose. A total of 24 hydrometer analysis were performed to establish the grain size distributions, see Fig 3.6. The shaded area is the result from all the test performed for the two subgrade soil layers, where the lower bound of the shaded area represents the slightly sandy material, MVCSO, and the upper bound represents the MECO material which starts at depth of 0.26 m, see Fig. 3.7 for more details.

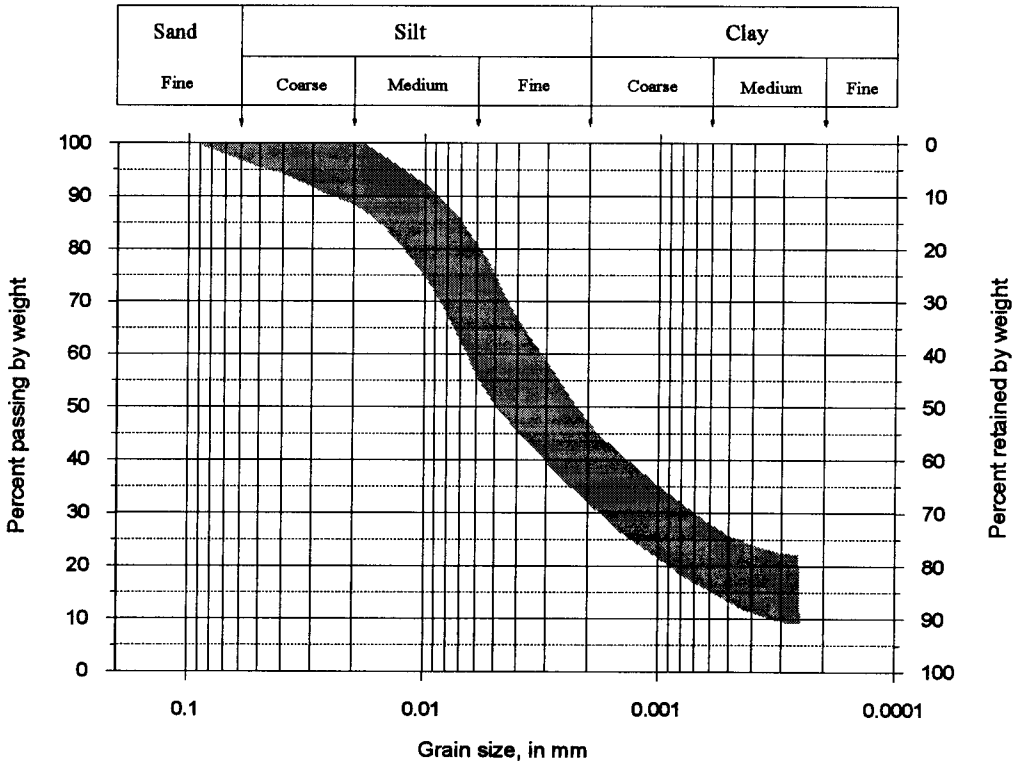

Figure 3.6 Particle size distribution curve - Hydrometer analysis

A knowledge of the range of moisture content over which soil will exhibit a certain consistency is often beneficial because the behavior of fine grained soils is often

related to the amount of water contained in the pore spaces. After a cohesive soil has been remolded, its consistency can be changed by increasing or decreasing the water content, and the water contents that correspond to the boundaries between the states of consistency are called the Atterberg limits.

The variation of plastic and liquid limit, and the natural water content of the soil, with depth below grade are reported in Fig. 3.7. The values were determined at 0.2 m interval, and represent average values from the three deeper test pits. The values of all three indices increases uniformly to a nearly constant value at a depth of 1 m.

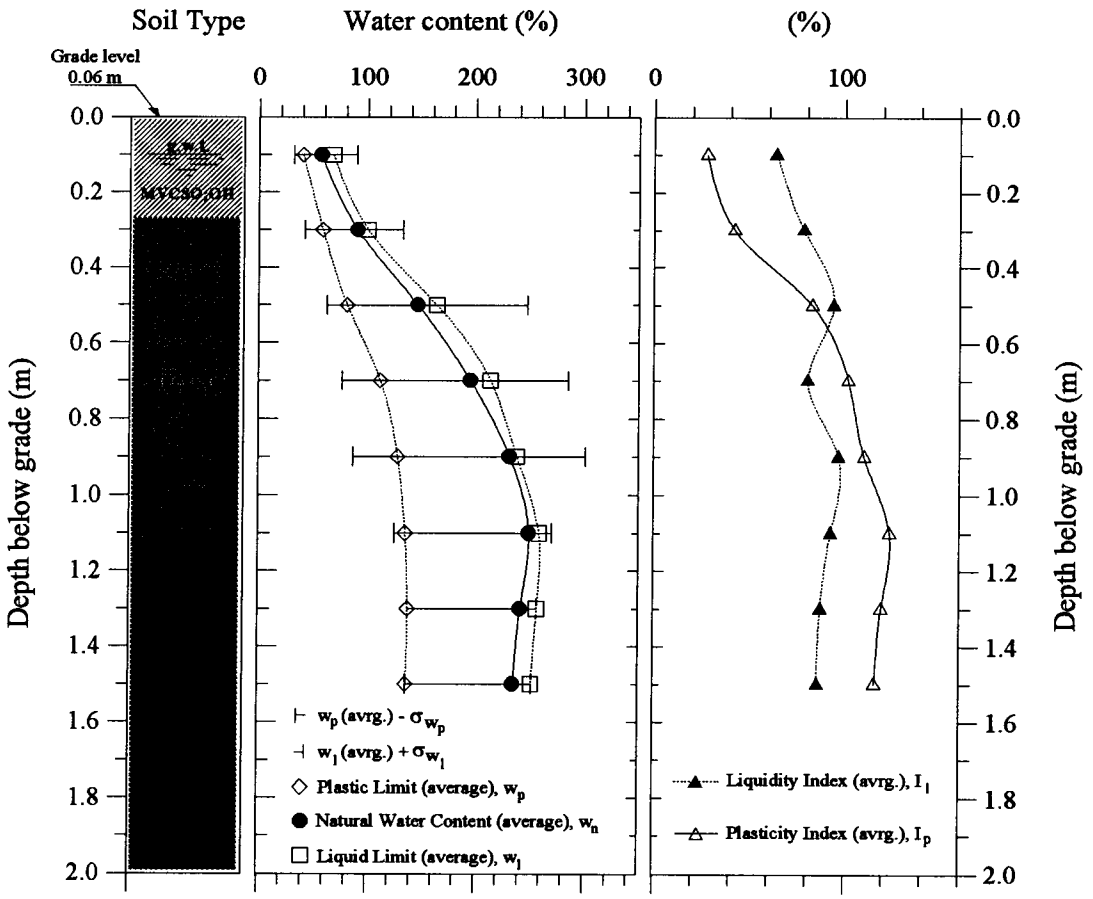

Figure 3.7 Atterberg limits and indices - Test Results

The results indicate the subgrade material is highly plastic (LL > 50%). The water content is very close to the liquid limit throughout the profile, but does not exceed it. A water content in the lower subgrade layer greater than 100 % suggests that the subgrade is very organic.

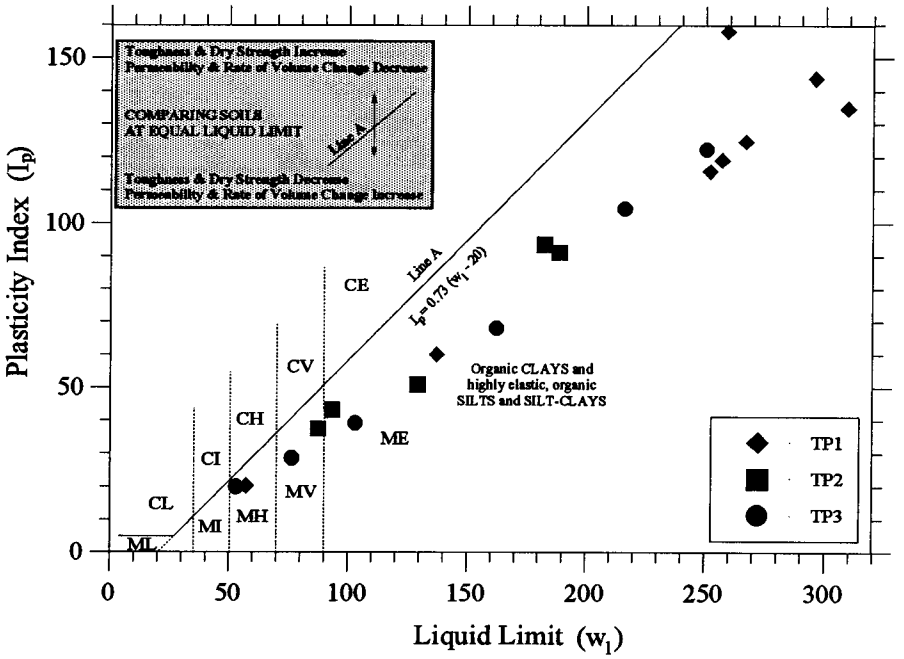

Figure 3.8 Relationship between liquid limit and plasticity index for the subgrade soil

The same data are illustrated on a plasticity chart in Fig. 3.8. The plasticity chart is based on the British Soil Classification System (BS 5930:1981) and is devided into five ranges of liquid limit where the four highest ranges (I, H, V and E) can be combined as the upper plasticity range or the high plasticity range for the Unified Soil Classification system. The A-line on the plasticity chart is used to differentiate between clay (C) and silt (M), where silt plots below the A-line and clay above, which means that silts exhibit plastic properties over a lower range of water content than clays having the same liquid limit. If fine grained soils contain a significant amount of

organic material they usually have high to extremely high liquid limits and plot below the A-line as organic silts. A peat typically exhibits water content greater than 350%. The liquid limits for most of the samples taken from the subgrade soil have extremely high liquid limits. Those with a liquid limit between 50% and 90% are samples taken from the upper subgrade layer shown in Fig. 3.7, between 0 and 0.26 m depth, and those with a liquid limit close to 300% were taken at a depth of 1.1 m. This interpretation of the tests indicates the subgrade soil to be an organic clayey silt, which is in a good agreement with the grain size analyses.

3.3.3 Shear Strength Characteristics

The undrained shear strength of the subgrade material was determined using a field vane: locations of the seven profiles within the test section area are shown in Fig. 3.4. For comparison purposes, unconsolidated undrained triaxial tests were also performed, and the locations of the undisturbed sampling for these UU-tests are also shown in Fig. 3.4.

The field vane is a widely used in-situ test for evaluating the undrained shear strength of fine-grained soils. Originally used in Sweden in late 1920s, it has been employed extensively worldwide since the late 1940s. Even though the field vane has been used for over 70 years there are still numerous questions that still remain unanswered about the interpretation of the test. Among the various factors that affect the interpretation of the test, it is recognized that shear stress distribution around the vane, rest period following vane insertion, fabric disturbance, pore-pressure buildup, strain rate effects, progressive failure and shear strength anisotropy have major influence on the measured strength (e.g.: Chandler, 1988; Roy and Leblanc, 1988; Becker et al., 1988; Silvestri and Aubertin, 1988).

The field vane tests were performed at 0.5 m interval for the first 4.2 m depth and thereafter at 1 m intervals. The equipment used was a Swedish Vane Borer like that developed at Chalmers University of Technology in Sweden, manufactured by Nilcon. The main advantage of the Swedish vane is that it needs no protective casing around the vane and the rods, which makes the operation much faster. Also, in soft ground, no pre-bored hole is required. A disadvantage of the vane is that there is no guarantee that the rods will advance into the ground without bending. The vanes used were 13 cm high and 6.5 cm in diameter and 17.2 cm high and 8 cm in diameter.

The vane borer consists of an instrument for applying torque, supported by a portable frame. The 20 mm diameter rods pass through the torque recorder and are connected through a slip-coupling to a vane. The vane is advanced into the ground by a system of hand cranking and as the vane advances into the ground the slip coupling allows the vane to rotate in a clockwise direction through approximately an angle of 15° in order to measure the soil-rod friction. A torque is then is applied at the rate of 0.2°/s at the top of the rod (2 handle rotations/s in low gear), and recorded with respect to angular rotation on a sheet of waxed paper in the torque recorder. The results are used to calculate the shear strength of the soil, knowing the difference between torque required to turn the rods plus vane, and torque required to turn the rods alone. All field vane undrained strengths were calculated using the conventional expression (Greig et al., 1988):

$$c_u = \frac{6M}{7\pi D^3} \tag{3.1}$$

where

c_u = undrained shear strength,

M = applied torque, and

D = diameter of the vane.

It has been noted that the waiting period following vane insertion has a very significant effect on the shear strength and in order to minimize the influence of this time lag between intrusion of the vane and shearing a delay time of less than 1 min was retained throughout all the tests.

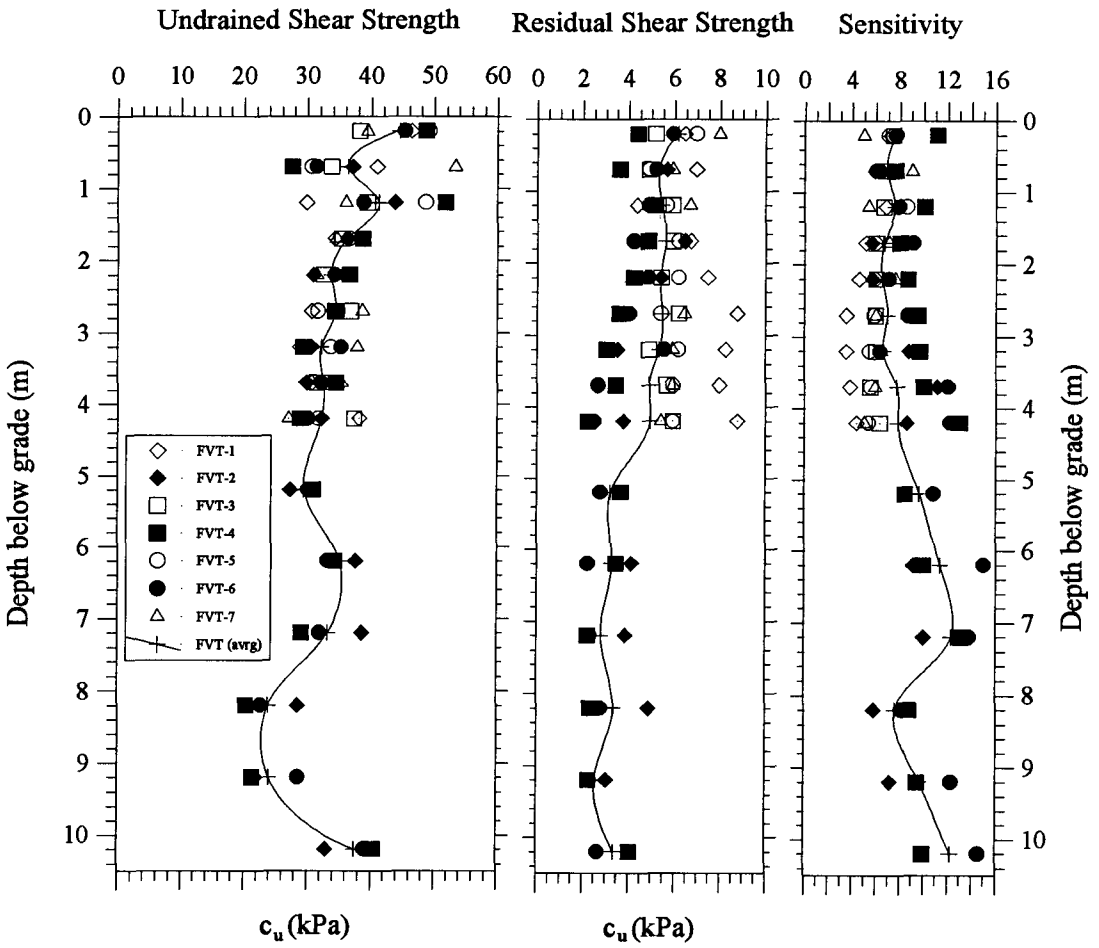

Figure 3.9 Field vane shear test results

Results of the vane tests are shown in Fig. 3.9. The solid line on the figures represents the average value from all of the tests. The profile of strength with depth is nearly uniform, and between 30 and 40 kPa. There is a slight increase in strength near

grade level which is attributed to the lower water content of the soil in this zone. Apart from this zone, below 0.5 m the consistency of the subgrade according to British classification is soft, that is a undrained shear strength between 20-40 kPa.

The sensitivity of the subgrade soil, which is defined as the ratio of the undrained strength in the undisturbed state to the undrained strength at the same water content in the remolded state, is fairly uniform through the first 4 m in depth. The average sensitivity is about 6. Clays with sensitivity between 4 and 8 are described as sensitive, and those with sensitivities between 8 and 16 are described as extra sensitive.

Field vane corrections and correction factors have been developed through comparison of field vane strength and the strength back calculated from actual failures, and from laboratory tests. However, most engineers use eqn. 3.1 when calculating the shear strength, even though it results in some conservatism. No correction factors were applied to the vane data reported in Fig. 3.9, and it is felt the data may slightly underestimate the shear strength.

Results from the unconsolidated undrained triaxial tests were in good agreement with the field vane tests. Undisturbed samples for the UU-tests were taken at about 10 - 25 cm below grade level at the locations shown in Fig. 3.4. A total of nine UU-tests were performed, three from each hole, giving an average undrained shear strength value of 41 kPa.

Chapter 4

Description of Test Sections

4.1 TEST SECTION LAYOUT

The test site comprises five test sections. One is unreinforced, three sections include a geotextile and one includes a geogrid. Each was trafficked in sequence by a vehicle of known axle loading. Design methods proposed by Steward, Williamson and Mohney (1977), Bender and Barenberg (1978), Giroud and Noiray (1981), and Haliburton and Barron (1983), were used to estimate the required thickness of the base course layer. The basic design criterion, apart from the subgrade properties, was the number of passes to be applied by the vehicle: the sections were intended to have a lifetime of a minimum of 100 passes and a maximum lifetime less than 1000 passes.

Lifetime is defined with respect to a serviceability type of failure, and taken to be a rut depth at which the vehicle can no longer traffic the structure. An important governing parameter for each geosynthetic is the influence of base course thickness on

the relationship between number of passes and rut depth. Therefore each section incorporated a variable thickness of base course aggregate.

The arrangement, construction and instrumentation of the test sections are described in detail below. Material properties of the base course aggregate and geosynthetics are reported in Sections 4.2 and 4.3, respectively.

4.1.1 Arrangement of the Test Sections

The five test sections were arranged in sequence, see Fig. 4.1, to facilitate traffic loading. The arrangement was selected to accommodate constraints of the site and promote ease of construction. Each test section is 4.5 m wide and 16 m long. The first section is the unreinforced section and serves as a control section in the study. The next section is reinforced with a geotextile, Texel Geo 9 and the section thereafter which also includes a geotextile, is the Polyfelt TS 700. The fourth section includes a geogrid, Tensar BX 1100, and the last test section is has a geotextile, Polyfelt TS 600.

Details of the base course layer are shown in Fig. 4.2. The thickness varies in each test section between a minimum value of 25 cm and a maximum value of 50 cm. The 25 cm layer is 3 m long, and increases in thickness to 50 cm over a length of 5 m, giving a slope gradient of 5 %. This longitudinal geometry was based on the area at disposal, specifically the total length, the length of the loading vehicle, and a desire to assess the repeatability with regard to the layer thickness within each section. Therefore, instead of only taking measurements during traffic loading at one base course thickness in each test section, it allowed two measurements, which greatly improves the quality of the data by allowing the repeatability and uniformity of an individual section to be quantified.

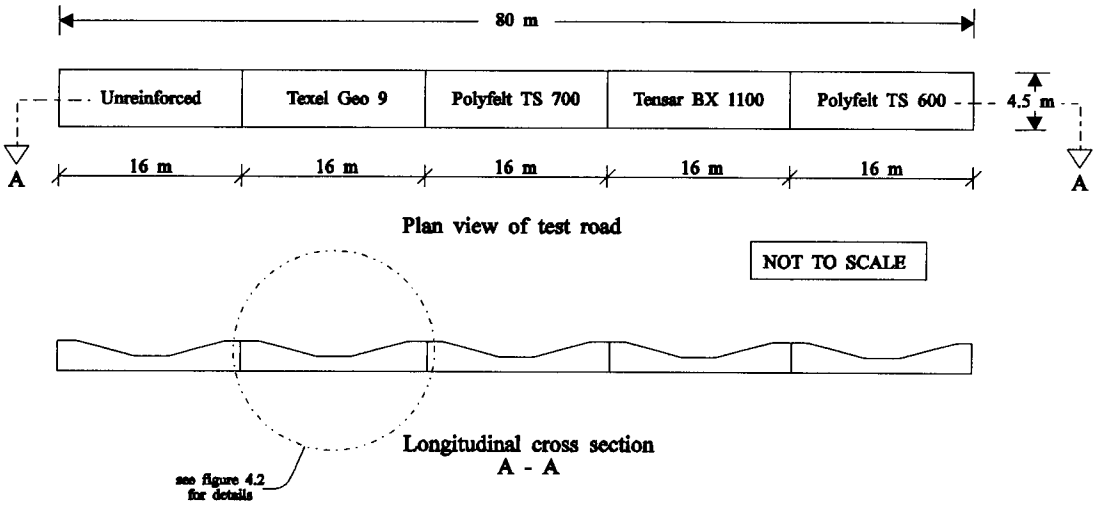

Figure 4.1 Test section layout

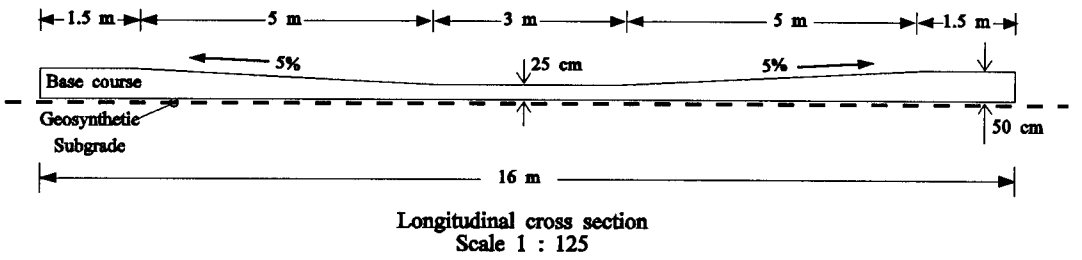

Figure 4.2 Test section geometry

4.1.2 Instrumentation and Measurements

Performance of the test sections was evaluated from measurements of:

- rut depth;
- base course thickness;
- base course deformations;
- geosynthetic strain; and
- deformed profile of the geosynthetic,

with increasing number of vehicle passes.

Rut depth measurements were taken across ten different stations, see Fig. 4.3, defined by the two locations in each test section where the base course thickness was 50, 40, 35, 30 and 25 cm.

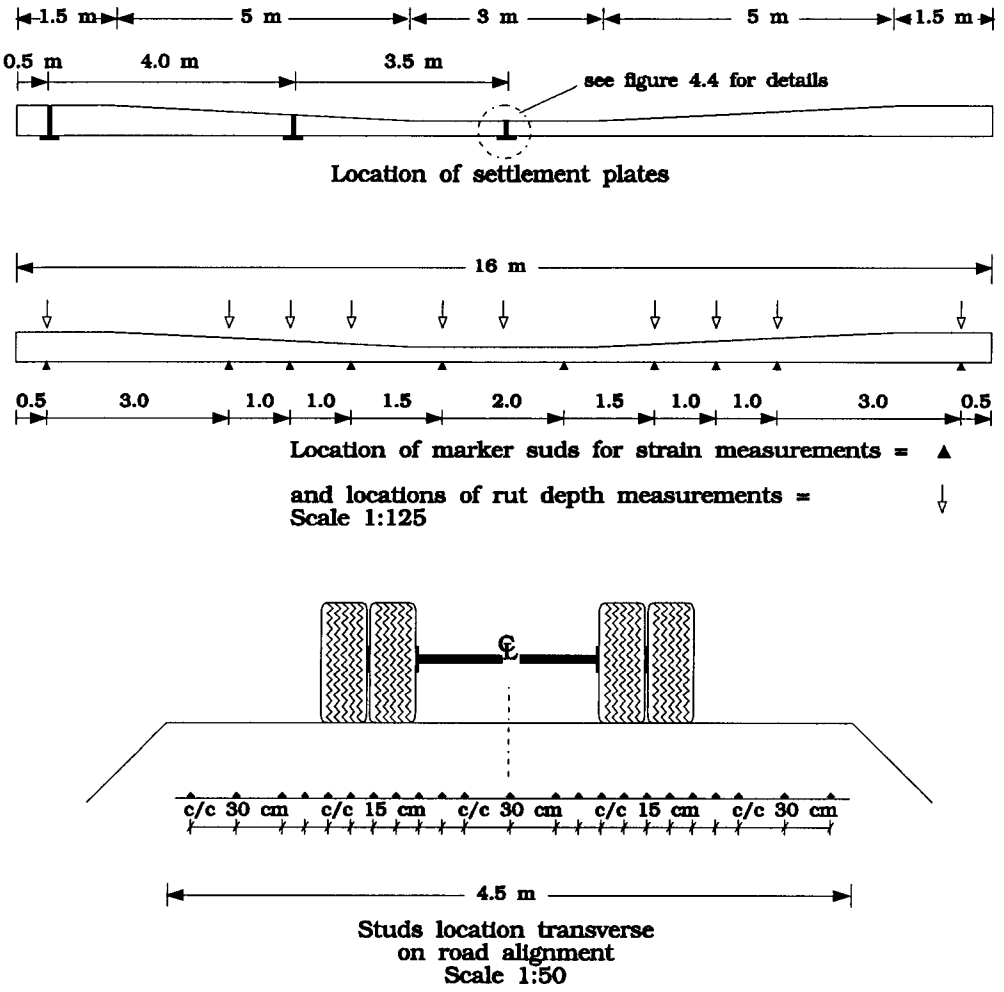

Figure 4.3 Instrumentation details

A sophisticated survey network was established to expedite the recording of these values, together with the development of surface rutting with cumulative vehicle passes. At every measurement station, wooden pegs were driven into the ground on

both sides of the test road. The tops of the each pair of pegs at every station were placed at the same elevation, using a nearby bench mark and the local elevation system. To measure the rut depth at every station a string was stretched between the pegs and, knowing the elevation of the pegs, a measuring tape was used to measure the distance from the datum elevation to the base course surface. The same datum was used to establish the deformed profile of the geosynthetics after trenching down to expose them at selected locations. The elevations of the pegs were checked periodically to ensure they were not disturbed by the vehicle passes. Figure 4.3 shows the locations of the rut measurements, which is at the same locations as the strain measurements, except in the middle where the rut measurement is above the settlement plate in the 25 cm thickness section.

The thickness of the base course was established from measurements using settlement plates incorporating a special tube that passes up through the base course layer. They were installed at three different locations within each test section, at base course thicknesses of 50, 35, and 25 cm to measure both the settlement of the subgrade surface and the thickness change directly in the channelized wheel path. Features of the settlements plates are illustrated in Fig. 4.4. To measure the thickness the top cap was removed and a measuring tape used to measure the depth to the bottom of the settlement plate. These measurements were taken at certain intervals during trafficking and, knowing the initial elevation of the top cap and depth to the subgrade surface, settlement of the subgrade was calculated.

Measurement of elongations in the geosynthetics during trafficking is important in order to examine the influence of the base course layer thickness on mobilized strain in the geosynthetic. An array of fifteen marker studs was used to measure the elongation in the geotextiles. They were fixed transverse to the road alignment at ten different locations, see Fig. 4.3. The spacing between the studs is 15 cm underneath

the influence zone of the tire load, and 30 cm in the middle of the sections and in the outside anchorage zones. The exact initial spacing between the markers was measured before placing the base course aggregate and the elongation was measured at certain interval by trenching down to the geotextiles. A similar approach was used in the case of the geogrid, but instead of attaching studs the initial length between every fourth rib junction was measured prior to installation.

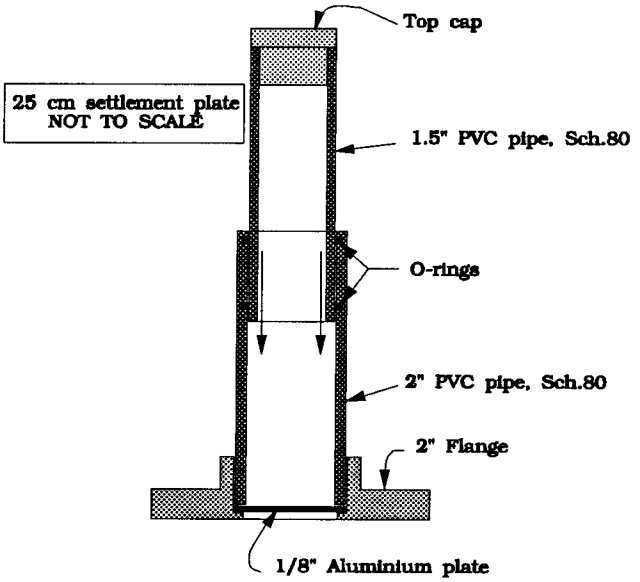

Figure 4.4 Settlement plate - Details

4.1.3 Construction of the Test Section

Construction of the test sections started with removal of the topsoil vegetated cover and excavation to the 0.06 m grade level referred in Section 3.4. The construction equipment was not permitted to traffic the road subgrade during construction, therefore all excavation and grading was done from the sides of the trial section. The surface of the clayey silt subgrade was leveled to a elevation of 0.06 m +/- 1.5 cm.

The geosynthetics for the reinforced sections were placed directly on the prepared subgrade surface. Each geosynthetic was placed to overlap the adjacent test sections by 50 cm in the direction of anticipated fill placement. The geotextiles were 4.5 m wide, and overlapping in the transverse direction therefore not needed. The geogrid, which was 4 m wide, was overlapped in transverse direction of about 1 m by placing a additional 1.8 m wide strip along the length of the test section.

The base course aggregate was also placed from the sides of the test sections in several lifts. The first base course layer was placed to a 15 cm loose thickness and compacted using a small vibrating plate to a finished thickness of approximately 12.5 cm. A small vibrating plate was used in all compaction work in order to minimize subgrade disturbance. After the compaction of the first lift, the second lift was placed raising the finished thickness up to 25 cm, which is the minimum thickness in each test section. Compaction measurements were taken to ensure the uniformity and the amount of compaction using a nuclear densometer. The specification was a minimum value of 90% of Standard Proctor. The 5% slope gradients were achieved by placing and compacting a wedge of gravel in two layers. The final surface was then leveled to the target elevation after compaction to 96 % of Standard Proctor with a standard deviation of 0.67 %. The final surface was measured using regular builders level and graded to the target elevation +/- 5 mm using manual labor.

The final stage of the construction was digging a small drainage ditch on both sides of the test road. Since the elevation of the subgrade of the test area was lower than the surrounding environment, due to the excavation to grade level, ditches were necessary to prevent water from draining into the test section from the surrounding soil.

4.2 BASE COURSE MATERIAL PROPERTIES

The base coarse material used in the road construction is defined as being well-graded, angular gravel with sand/sand with gravel, with coefficient of uniformity, $C_u = 48$, and the coefficient of curvature, $C_Z = 0.6$. The grain size characteristic of the aggregate is shown in Fig. 4.5.

The compaction characteristics of the base course aggregate were measured employing a standard Proctor test, according to ASTM D698, method C. The GRAVEL/SAND has a standard Proctor maximum dry unit weight of 21.5 kN/m^3 at an optimum moisture content of 7.1 %. After placement and final compaction in-situ, the water content was measured using the nuclear densometer. At the in-situ dry unit weight of 20.7 kN/m^3 the water content was 6.7 % with standard deviation of 1.15 %.

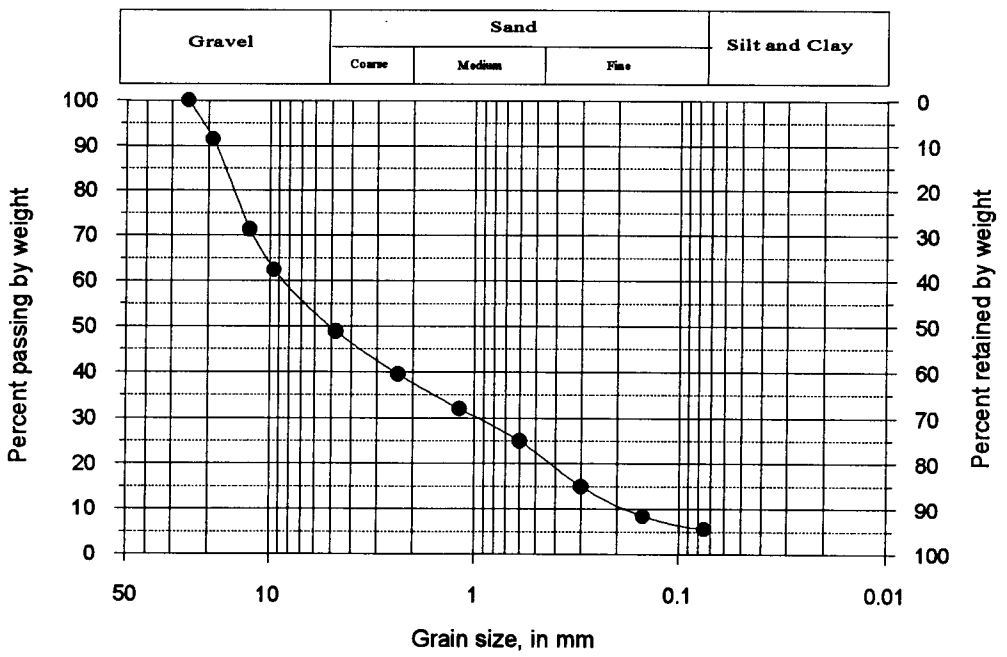

Figure 4.5 Base course aggregate grain size distribution

4.3 GEOSYNTHETIC PROPERTIES

Properties of the geotextiles used in the field trial are shown in Table 4.1. These values are based on manufacturers minimum average roll value data. Unfortunately there is no standardization of how properties of geosynthetics are reported and can therefore be difficult to compare properties of geosynthetics from different manufacturers.

Table 4.1 Properties of the geotextiles

		Polyfelt TS 600	Polyfelt TS 700	Texel Geo 9
Property	Units	Value	Value	Value
Structure		Non-wowen	Non-woven	Non-woven
Polymer Type		Polypropylen	Polypropylen	Polypropylen
Thickness	mm	1.8	2.3	1.8
Mass Per Unit Area	g/m2	204	268	310
Apparent Opening Size	mm	0.25	0.21	0.10
Permittivity	1/sec	1.8	1.3	0.7
Puncture	kN	0.355	0.445	N/A
Mullen Burst	kN/m2	1517	2207	2400
Trapezoid Tear	kN	0.311	0.38	N/A
Grab Tensile/Elongation	kN (%)	0.711 (50)	0.933 (50)	N/A
Wide Width Strength/Elongation				
MD	kN/m (%)	12.3 (95)	15.8 (95)	7.0 (10)
XD	kN/m (%)	10.5 (50)	14.0 (50)	7.0 (10)

MD = machine (or roll) direction; XD = cross machine direction

N/A = not available

It should be noted that the Texel Geo 9 is a reinforced non-woven geotextile, where a woven geotextile (Texpro 120) is used to reinforce a non-woven (Texel 7609). Test data from several wide width tests on the Texel Geo 9, indicated an ultimate load of 14 kN/m at about 21% strain.

The properties of the Tensar BX 1100 geogrid are shown in Table 4.2. The tensile strength of the geogrid is reported as a minimum specified value. Values of wide width ultimate strength, based on manufacturers Q/A testing, show between 10 to 70% higher values than reported, depending on the direction, where strength in the cross machine direction is considerably higher. Strains at failure are typically 9 to 12%.

Table 4.2 Properties of the geogrid

		Tensar BX 1100
Property	Unit	Value
Tensile		
- modulus @ 2% strain	kN/m	204.0
- ultimate strength	kN/m	12.4
Dimensional Stability		
- junction strength	kN/m	11.2
- junction efficiency	%	90.0
Geometry		
- aperture MD	mm	25.0
- aperture XD	mm	33.0
- rib thickness	mm	0.76
- junction thickness	mm	2.80
- open area	%	70.0
Material		
- Polypropylen	%	98.0
- Carbon Black	%	0.5

4.4 LOADING VEHICLE

The load vehicle used to traffic the test sections was a single axle, dual tire truck, with a standard axle load (80.3 kN) and a tire inflation pressure of 620 kPa. A layout of the wheel spacing and axle load of the test vehicle is shown in Fig. 4.6.

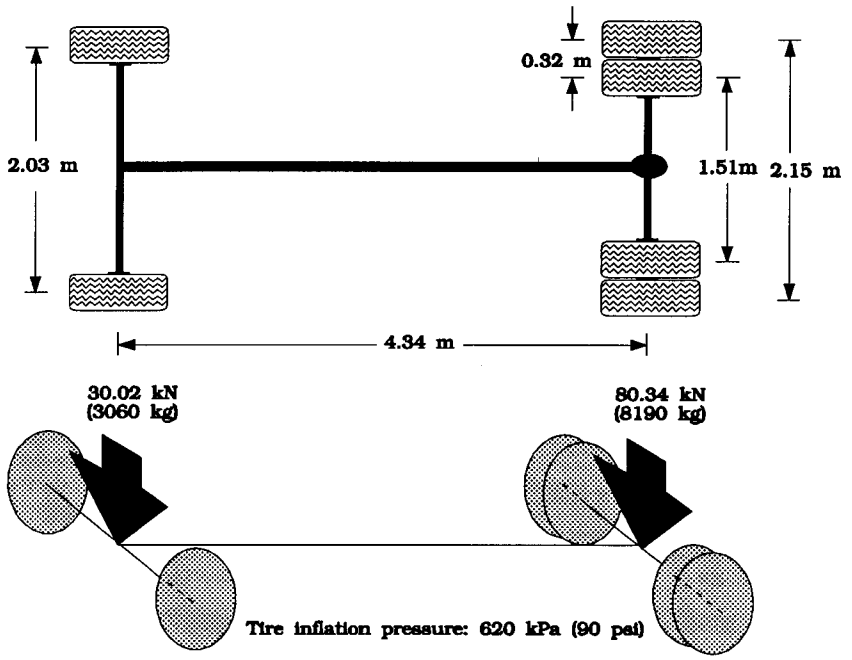

Figure 4.6 Configuration of the loading vehicle

The truck was driven in forward and then in reverse over the entire length of the test section at an average speed of 7 km/hour. Traffic was recorded in terms of number of passes of a standard axle load. The front single-axle, single wheels of the test vehicle has negligible effects on the road performance and was therefore discarded when reporting the number of passes of the load vehicle.

Chapter 5

Field Data

5.1 INTRODUCTION

Field testing took place between mid-December 1992 and late June 1993. A total of 500 passes were made with the loading vehicle during this time. In the early stage of traffic loading only a few passes were made each day, and measurements were taken frequently in order to get a better feel for the behavior of the reinforced soil-aggregate system and to determine the initial trend of base course and subgrade deformations. After eight passes, on the second day of traffic loading, the field trial was postponed until the second week in February due to inclement weather conditions. Considerable effort was put in to keeping the general condition of the site and road as unchanged throughout the period of field trafficking. This was done by regular site inspection and observations of the groundwater table in the drainage ditch parallel to

the test road, and covering the road surface with plastic sheets between the days of trafficking.

Measurements in each test section, where "test section" refers to one of the five different sections in the test road, are taken at pre-defined cross-sections in that test section. Each test section is numbered in sequence from 1 to 5, with the unreinforced being No.1 and the Polyfelt TS 600 No.5, as shown in Fig. 4.1.

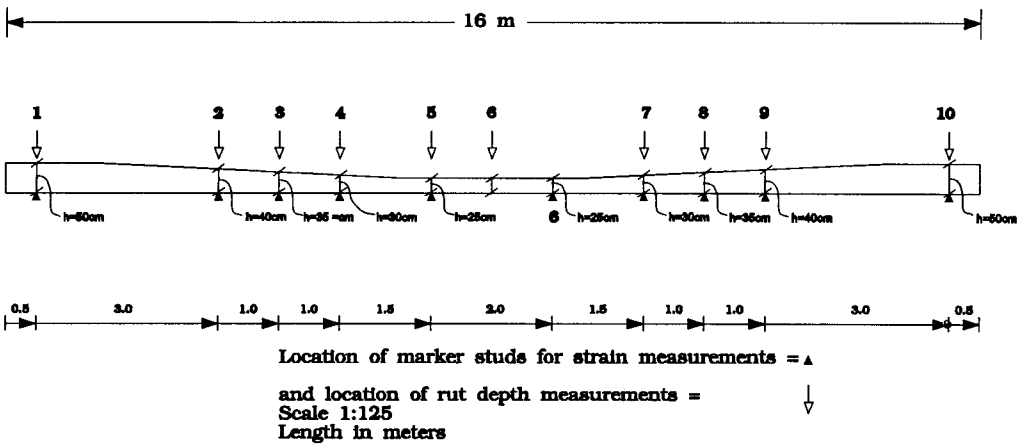

Figure 5.1 Cross-section numbers in each test section

A total of ten cross-sections were monitored in every test section, see Fig. 5.1. Consequently, the test section number and cross-section number are combined and used as a reference system in the reporting of results: the first number refers to the test section and second to the cross-section, hence location 2.3 is on Texel Geo 9, cross- section 3, where the base course thickness is 35 cm. Where "left" or "right" is used in describing the field observations, the definition of left assumes the observer is looking east from the unreinforced section (No.1) towards the reinforced sections (Nos.2 to 5).

5.2 FIELD DATA

Measurements of surface profiles, ruts, subgrade profiles and settlements, and strains in the geosynthetics were taken during vehicle trafficking. The data are presented and described below.

5.2.1 Surface Profiles

Measurements of surface deformations across the width of the road were taken frequently during the first 40 vehicle passes. The profile measurements were taken at every cross-section in all test sections, giving a total of 50 measurements each time. Figures 5.2a, b and c show the development of surface deformation with increasing passes at a base course thickness of 25, 35 and 50 cm, respectively. The three cross-section locations are 5, 3, and 1 respectively; they are selected for presentation because they also include the settlement plates. In the figures, elevation refers to the surface of the base course and offset refers to the distance from the survey peg on the left side of the road. The interception of the offset axis with the elevation is fixed at the mean subgrade elevation of 0.06 m. A vertical:horizontal scale of 1.7:1 is used to clarify the nature of the deformations.

The field observations of surface deformation, Fig. 5.2, indicate a clear symmetry between the dual wheels for each base course thickness and with increasing rut depth. Heave is localized between the wheels, and no significant vertical displacement occurred at the longitudinal centerline. All profiles show a small difference in deformation between the inner and outer wheel path for each of the dual wheels, with the outer wheel developing a slightly greater rut. It is felt this might be caused to some extent by the alignment of the front wheel of the vehicle with the outside wheel of the rear assembly: however it is also recognized that the front axle

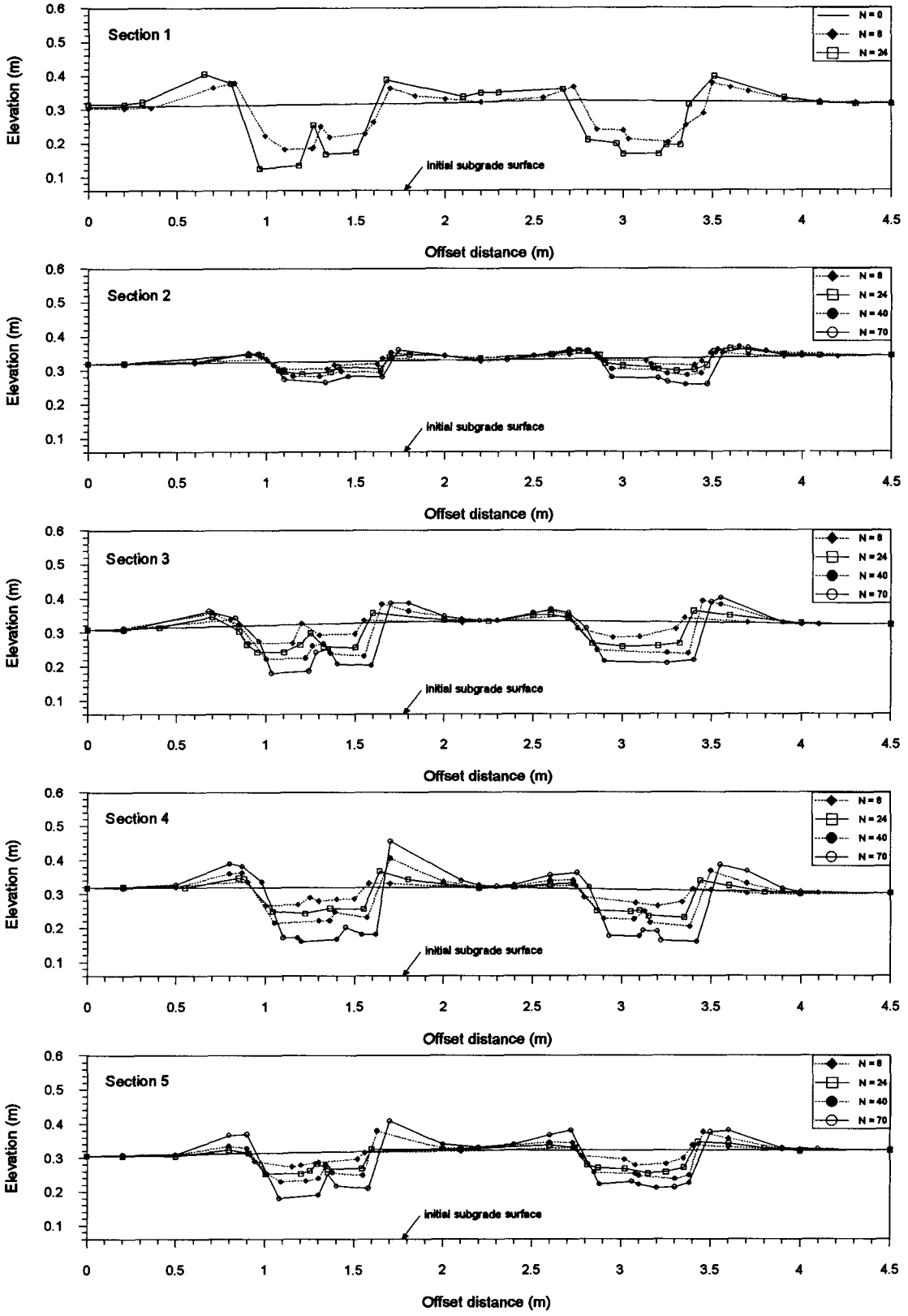

Figure 5.2a Surface profiles at cross-sections 5, h = 25 cm, tests sections 1 to 5

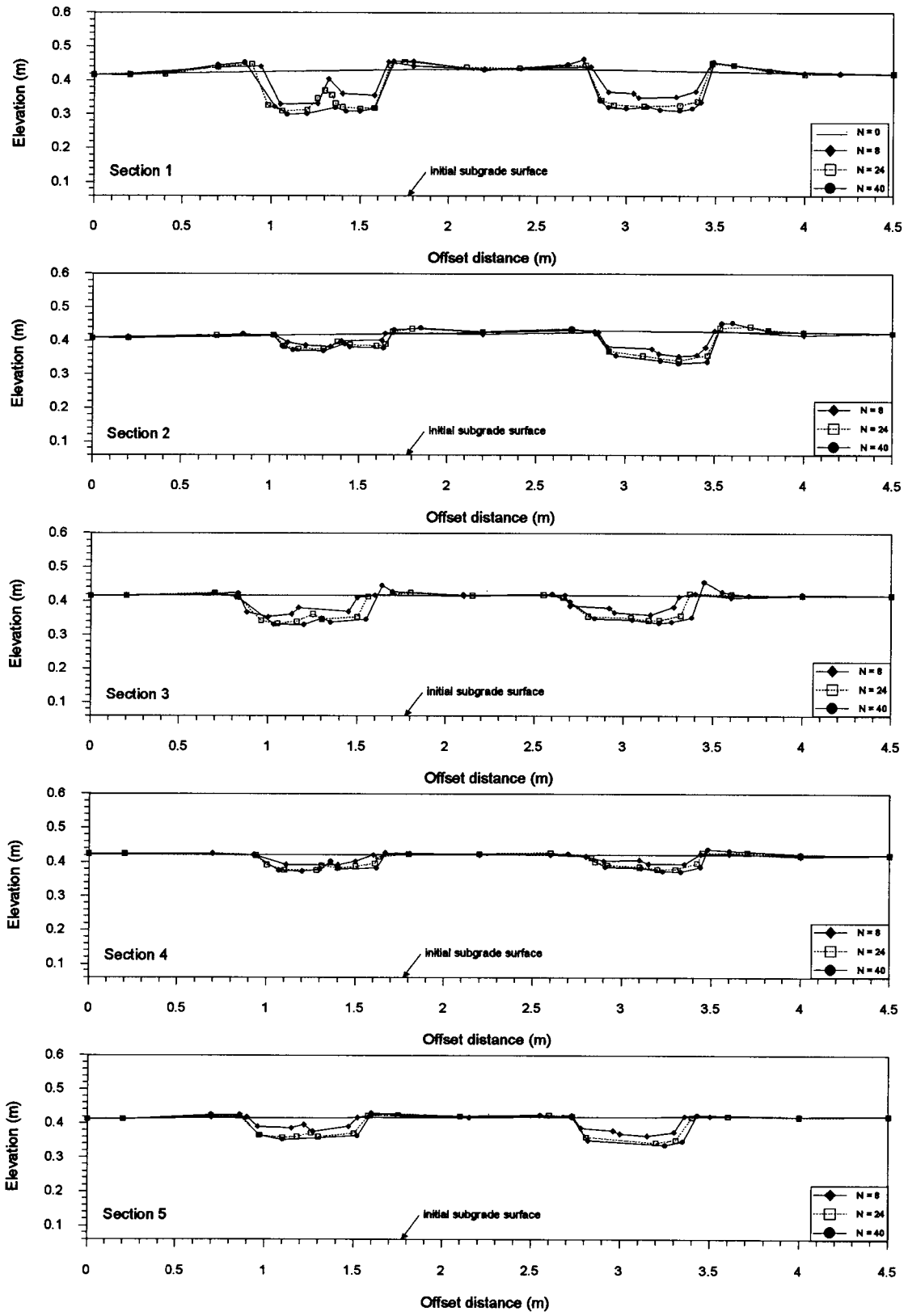

Figure 5.2b Surface profiles at cross-sections 3, h = 35 cm, tests sections 1 to 5

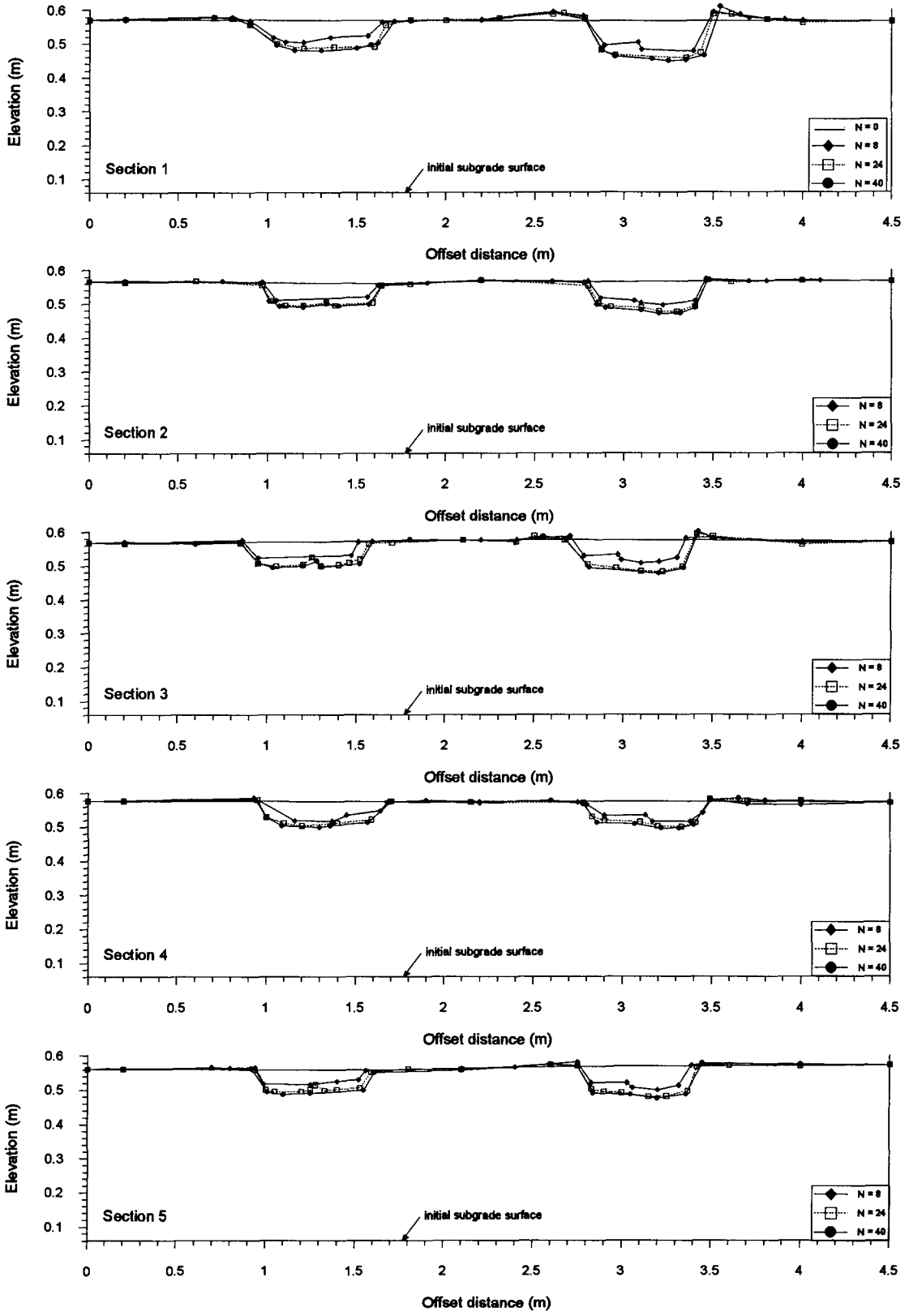

Figure 5.2c Surface profiles at, cross-sections 1, h = 50 cm, tests sections 1 to 5

load is very small in comparison with the rear axle load.

The 25 cm thick sections, Fig. 5.2a, show substantial heave on either side of the dual wheels. The heave is greatest on the outside of the dual wheels in most cases, which is in agreement with the larger rut in the outer wheel path. The behavior is attributed to interaction between the wheels, rather than an action of the geosynthetic, since this same trend is also apparent in the unreinforced section. The cross-sectional area of heave in these 25 cm thick sections appear to be less than the cross-sectional area of the ruts in all five sections: the response is attributed to compressibility of the base course material in the early stage of trafficking, since the difference seems to diminish with increasing number of passes.

The 35 cm thick sections, Fig. 5.2b, do not show any significant heave in the reinforced sections and a much smaller vertical displacement is observed in the unreinforced sections than in the 25 cm thick sections. The heave that did occur seems to develop in the first few passes. The development of ruts without any significant heave, as in the case of the thicker base course reinforced and unreinforced sections, is attributed to some localized compaction of the base course. This same behavior is observed in the 50 cm thick sections, Fig. 5.2c, where there is little heave in the unreinforced section and almost none in the reinforced sections.

5.2.2 Rut Development

Rut measurements were conducted after every vehicle pass at cross-sections 1, 3 and 6 (Fig. 5.1) in all test sections for the first 24 passes, and after every second pass in other cross-sections. Then measurements were taken after approximately every 10 passes in all cross-sections up to 130 passes, every 20 passes up to 300 passes, and every 50 passes thereafter.

Rut depth is defined as the difference between the initial average base course elevation, before trafficking, and the elevation measured in the developed rut. When determining the rut depth, four measurements were taken at a cross-section, two on each dual wheel path, one in the inner wheel path and another in the outer wheel path. The measurements were taken at the lowest point in each wheel path. Since the test sections have two cross-sections of the same base course thickness, eight values were recorded in total.

The resolution of measurement is about ± 2 mm, which accounts for the elevation of the datum pegs which the reference string is attached, and the measurement from the string down to the base course surface.

The development of rut depth with number of passes for the five test sections is shown in Figs. 5.3 to 5.7. The upper figure for each section shows the relationship between ruts and number of passes, for both the minimum base course thickness (25cm) and the maximum thickness (50cm). They illustrate the nature of the raw data: the data points collected from the two cross-sections of equal thickness in each test section. Variations in the data are attributed to the two different locations of rut measurements for each base course thickness, and the slight difference in rut between the outer and inner wheel path for the dual wheel assembly (see Fig. 5.2). The repeatability of measurements is considered excellent, therefore the average value of rut depth for each base course thickness is reported in the lower figure.

Curves for the unreinforced section, Fig. 5.3, show two distinct general shapes. One defines a rapid development of rut at low passes followed by a nearly constant, but slightly increasing value with further trafficking. The other defines the same initial trend of rapid development of rut at low passes, but is followed by continued rutting to a value of approximately 20 cm, which is considered a serviceability failure.

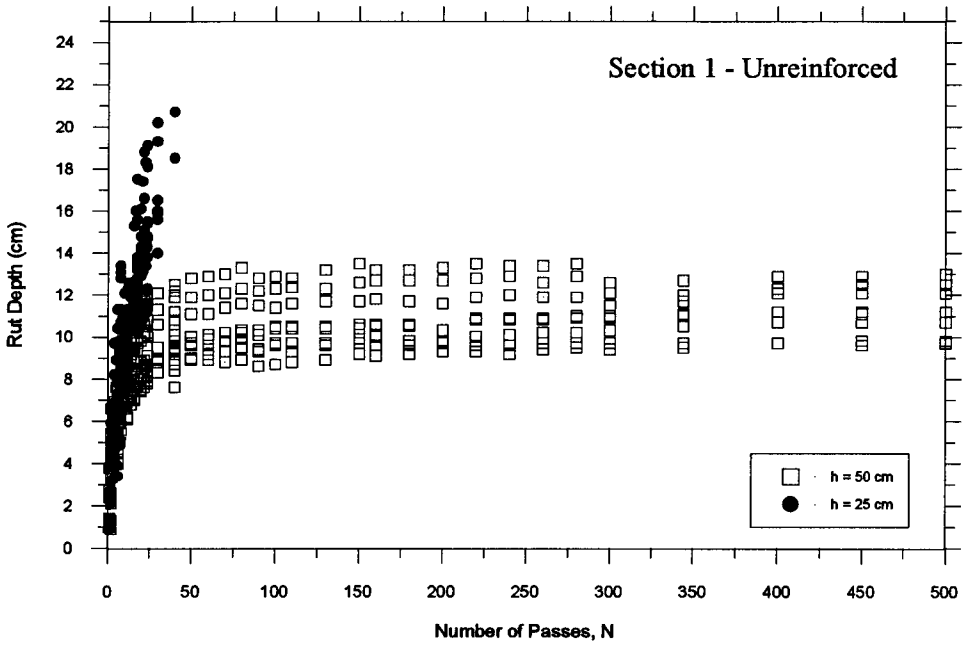

Figure 5.3a Rut depth versus number of passes - Section 1 raw data

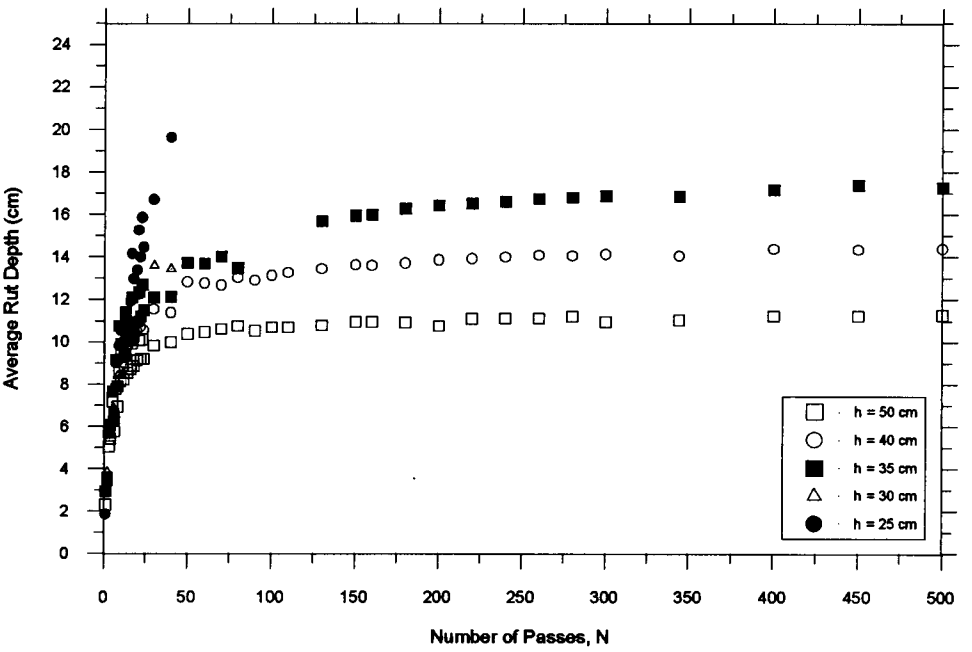

Figure 5.3b Average rut depth versus number of passes - Unreinforced data

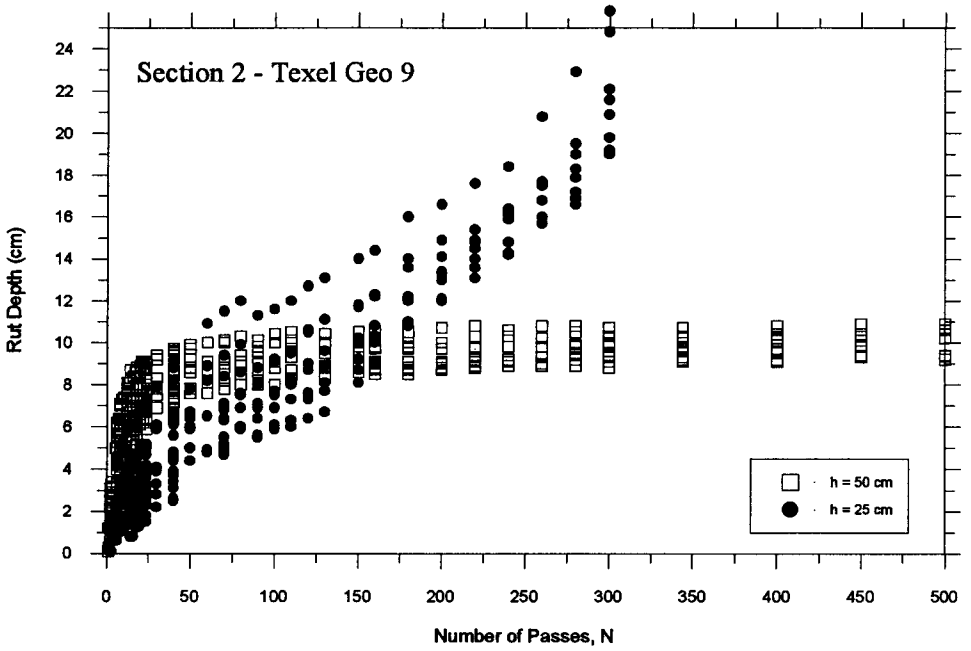

Figure 5.4a Rut depth versus number of passes - Section 2 raw data

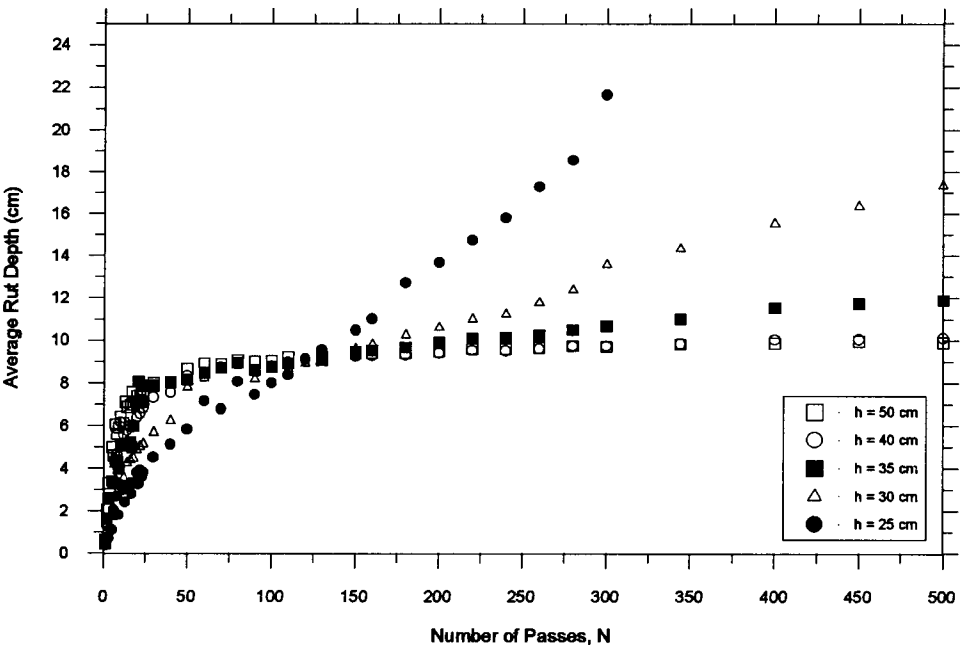

Figure 5.4b Average rut depth versus number of passes - Texel Ego 9 data

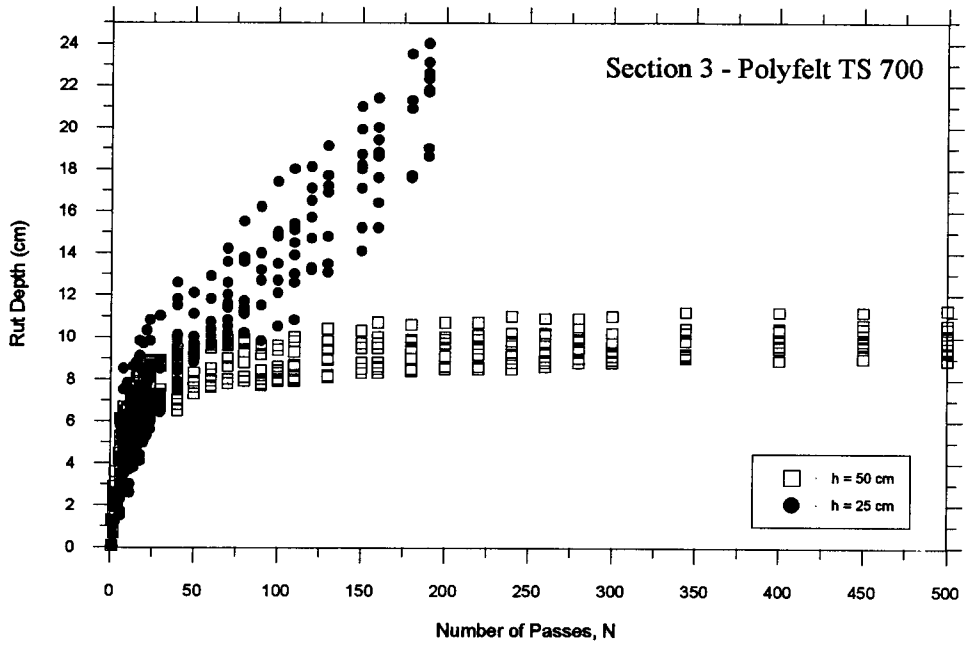

Figure 5.5a Rut depth versus number of passes - Section 3 raw data

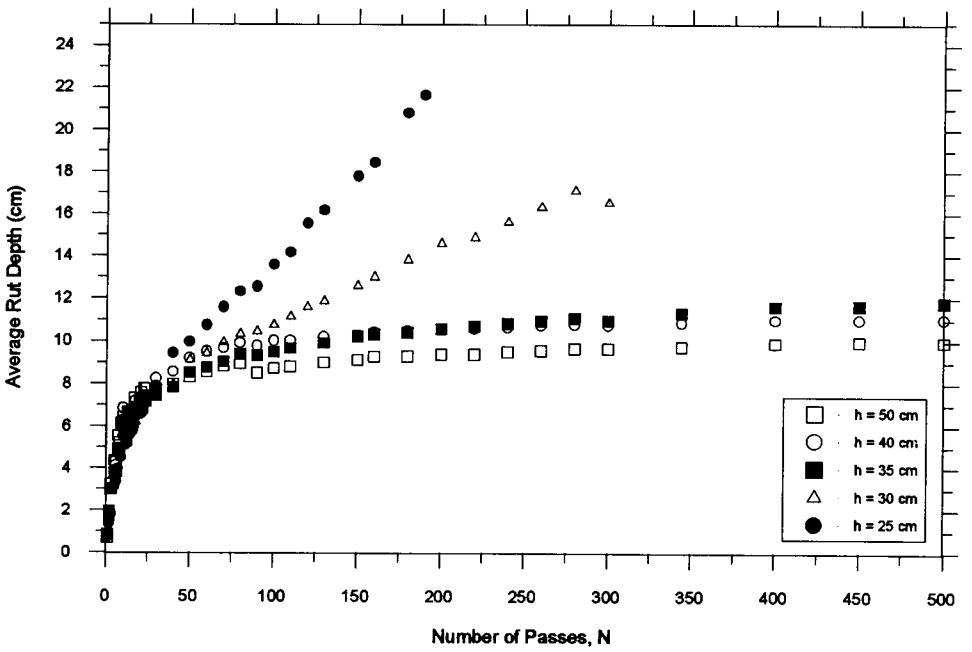

Figure 5.5b Average rut depth versus number of passes - Polyfelt TS 700 data

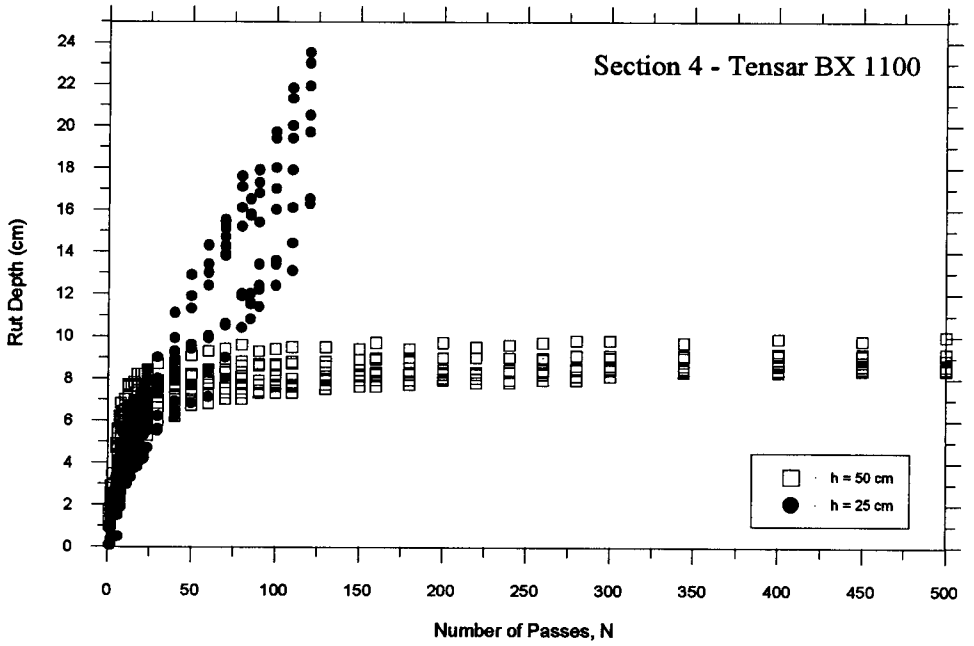

Figure 5.6a Rut depth versus number of passes - Section 4 raw data

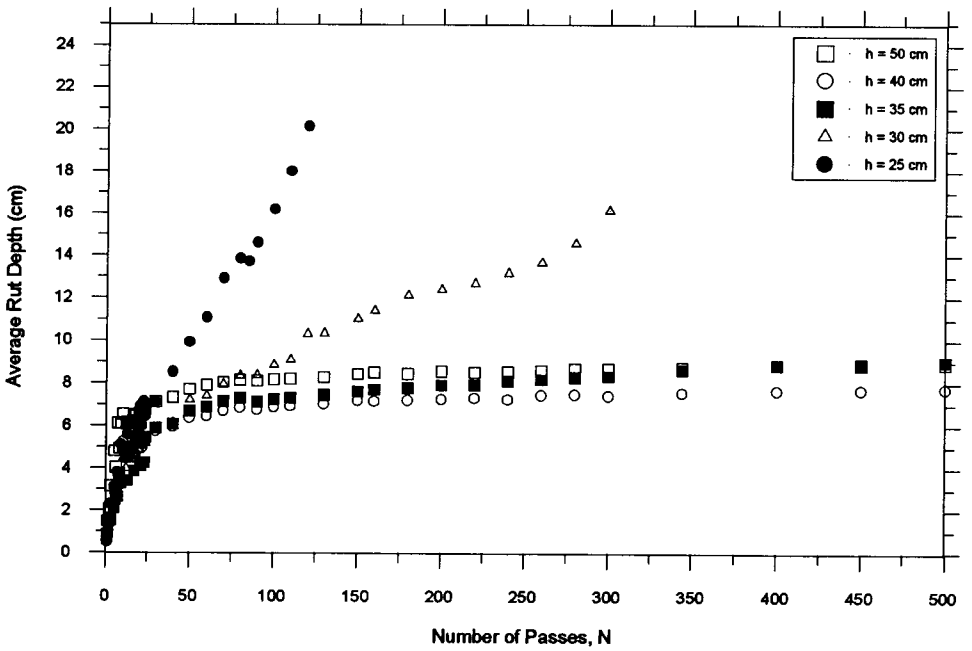

Figure 5.6b Average rut depth versus number of passes - Tensar BX 1100 data

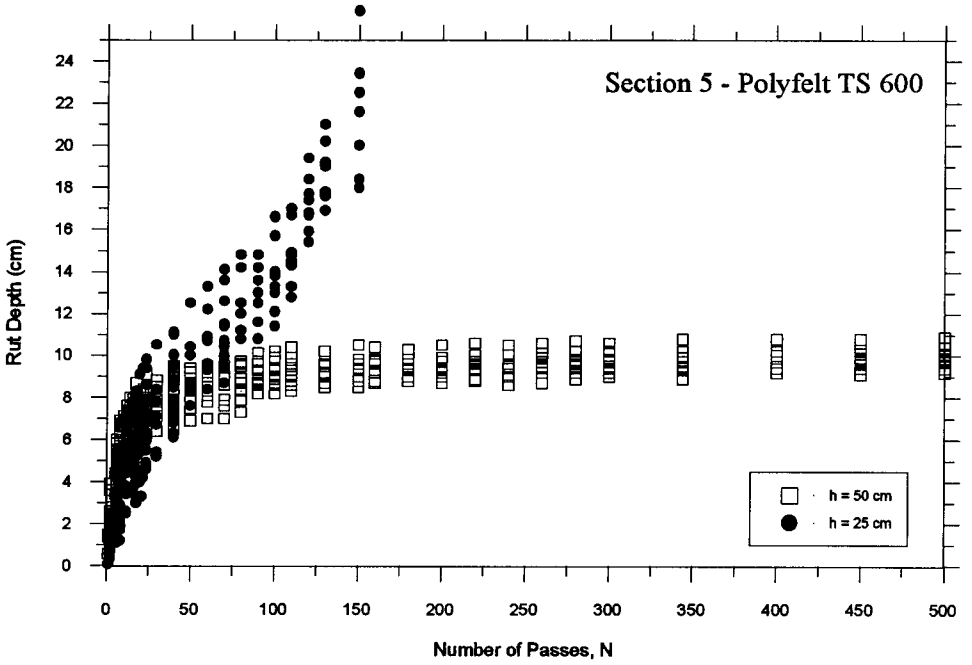

Figure 5.7a Rut depth versus number of passes - Section 5 raw data

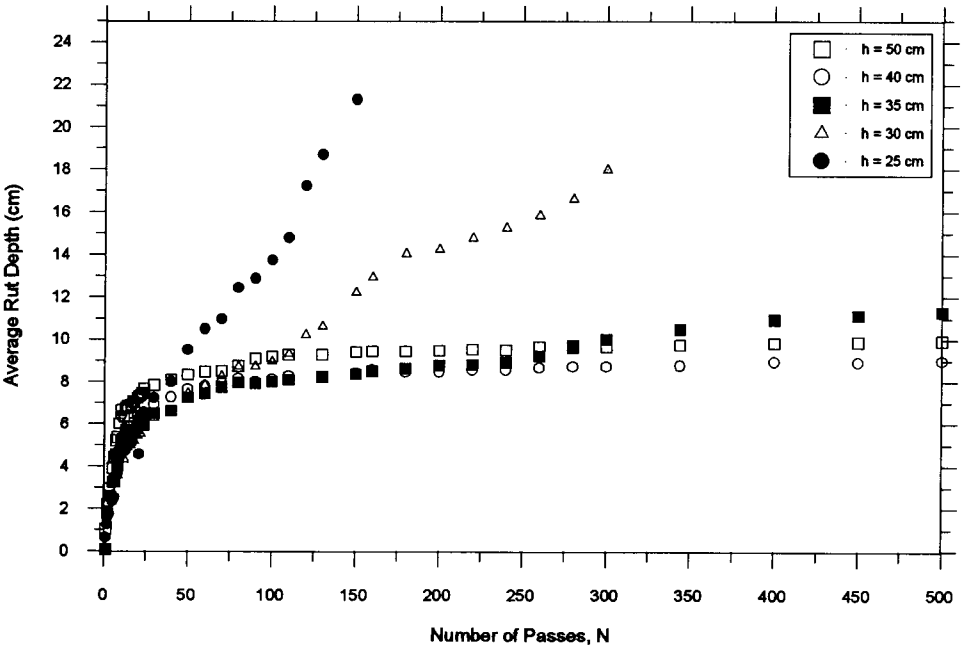

Figure 5.7b Average rut depth versus number of passes - Polyfelt TS 600 data

A relationship is apparent between rut depth, number of passes and base course thickness: smaller ruts are observed with increasing base course thickness for the same number of passes. The rut development in the unreinforced 25 cm thick section was very rapid and trafficking was stopped after 40 passes at an average rut depth of 19.6 cm. Trafficking of the 30 cm thick cross-sections on either side of the 25 cm thick section was also discontinued, even though the average rut was only 13.6 cm: this was due to the need for repair of the 25 cm thick unreinforced cross-section (which was the first to fail). The repairing procedure was modified for later repairs in order to keep the 30 cm thick cross-sections in the data base until a serviceability failure was achieved. An estimation, based on the data obtained for the first 40 passes of the 30 cm thick unreinforced section, suggests a serviceability failure would have been achieved within the first 100 passes.

Although the 35, 40 and 50 cm thick unreinforced sections did not reach serviceability failure, and show a very similar response, there is a noticeable difference in rut development. The final average rut depth after 500 vehicle passes for the 35, 40 and 50 cm sections were 17.3, 14.4 and 11.3 cm, respectively.

The five different test sections, unreinforced and reinforced, all show the same two general shapes of curves which characterize a response to trafficking which is termed either unstable or stable. Although there is a definite relationship between rut, number of passes and base course thickness for the reinforced sections, with less rutting in the thicker subbase layers, it is not as consistent as that in the unreinforced section. The exceptions are in sections 4 and 5, see figure 5.6b and 5.7b, where the 40 cm thick sections show less average rutting than the 50 cm thick cross-section after 500 passes. This is attributed to compressibility of the base course material, and may change with increasing number of passes in accordance with the observations for section 3 between the 35 and 40 cm thick sections (Fig. 5.5b).

All of the 25 cm thick reinforced sections were loaded to a serviceability failure. Although there is a considerable difference in rut development between the reinforced sections, they all demonstrate a significant improvement in behavior over the equivalent unreinforced section: test sections 2, 3, 4 and 5 failed at average rut depths of 21.6, 21.6, 21.3 and 20.1 cm, after 300, 190, 140 and 150 passes, respectively.

The 30 cm thick sections tended toward an unstable response, but did not reach the condition of a serviceability failure after 500 passes. The curves show some periodic variations in the relationship between average rut depth and the number of passes, see for example the 30 cm thick section in Fig. 5.7b. The behavior is attributed to the sequence of trafficking. It is felt some dissipation of excess pore pressure generated by vehicle loads took place during waiting periods between trafficking days. This would lead to an increase in undrained shear strength, and therefore a slightly greater resistance to the onset of the next loads. This behavior was observed when the elapsed time between trafficking periods exceeded two weeks.

The remaining reinforced test sections between 35 and 50 cm thick all show a stable response, and an average rut depth at the end of the field trial that is less than the equivalent unreinforced section. A comparison of the reinforced section shows the magnitude of the rut depth is very similar for the 35, 40 and 50 cm thick sections, although there is some indication of slightly less rutting in the geogrid section. It would appear that the performance of these thicker sections, at 500 passes, is essentially independent of the type of geosynthetic. There is a difference in rut depth between the reinforced sections and the unreinforced section that is less significant for the thicker sections: behavior of the 50 cm thick layers is almost identical for all of the test sections.

5.2.3 Subgrade Profiles and Settlements

Deformations of the subgrade surface were measured at certain stages throughout the trial by trenching down to the surface of the geosynthetics and recording vertical displacement with respect to a horizontal datum. Most of the trenches extended over half the width of the road to minimize any disturbance of the system. They were about 30 cm wide, and after taking the measurements they were backfilled, compacted and graded to the original profile. No noticeable difference in behavior was observed prior to and after trenching.

Subgrade profiles are illustrated in Figs. 5.8 to 5.11. All the 25 cm thick cross-sections were trenched after 80 passes, shown in the upper part of the figures.

Consider the 25 cm thick base course layer. Little significant deformations occurred in section 2.5 (Fig. 5.8) after 80 passes. In contrast, other three reinforced sections show more distinct deformed subgrade profile and a tear was observed in the geogrid in the left hand side wheel path (Fig. 5.10). The geotextiles developed a smoother profile than the geogrid, which exhibits a noticeable difference between the inner and outer wheel path. During trenching of the 25 cm thick geogrid reinforced section, it was observed that the subgrade soil had squeezed up through the aperture of the grid openings about 2 cm: however this was not observed in the 35 cm thick geogrid section after 500 passes where the base course aggregate, the geogrid, and the subgrade, were well interlocked at the interface.

The deformations in the 25 cm thick cross-sections generally show a fair agreement between the volumetric displacement in the wheel path and the volumetric heave on either side of the path after 80 passes. One exception is section 4.6, shown in Fig. 5.10, but that is to some extent attributed to the squeezing of the subgrade through the geogrid apertures.

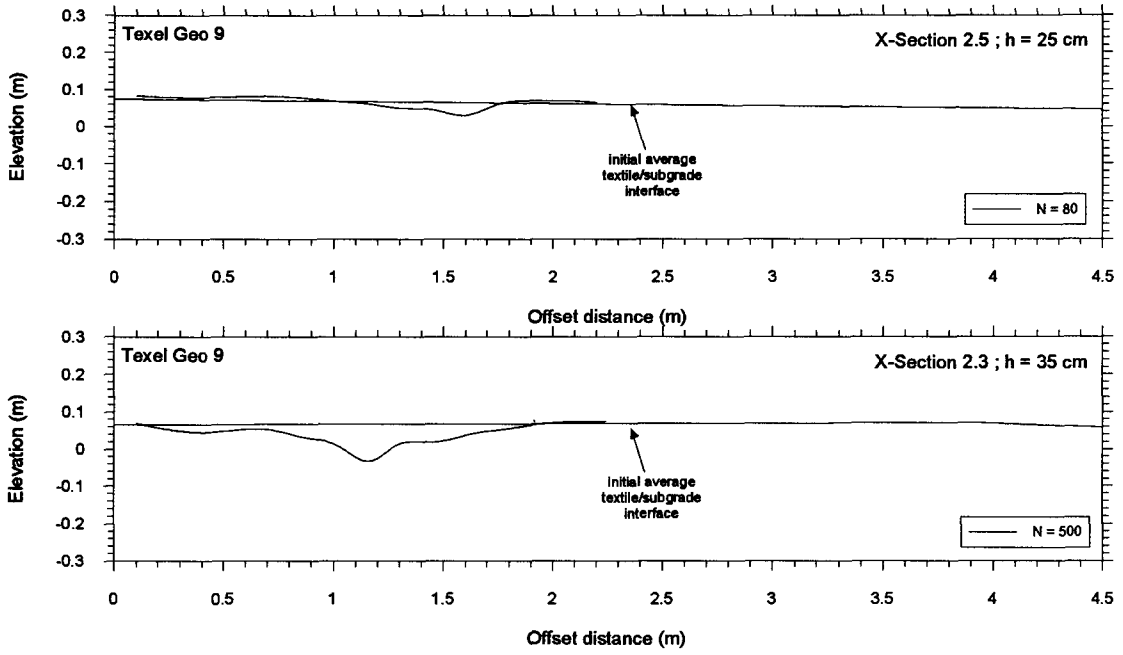

Figure 5.8 Subgrade profiles in test sections 2.5 and 2.3 - Texel Ego 9

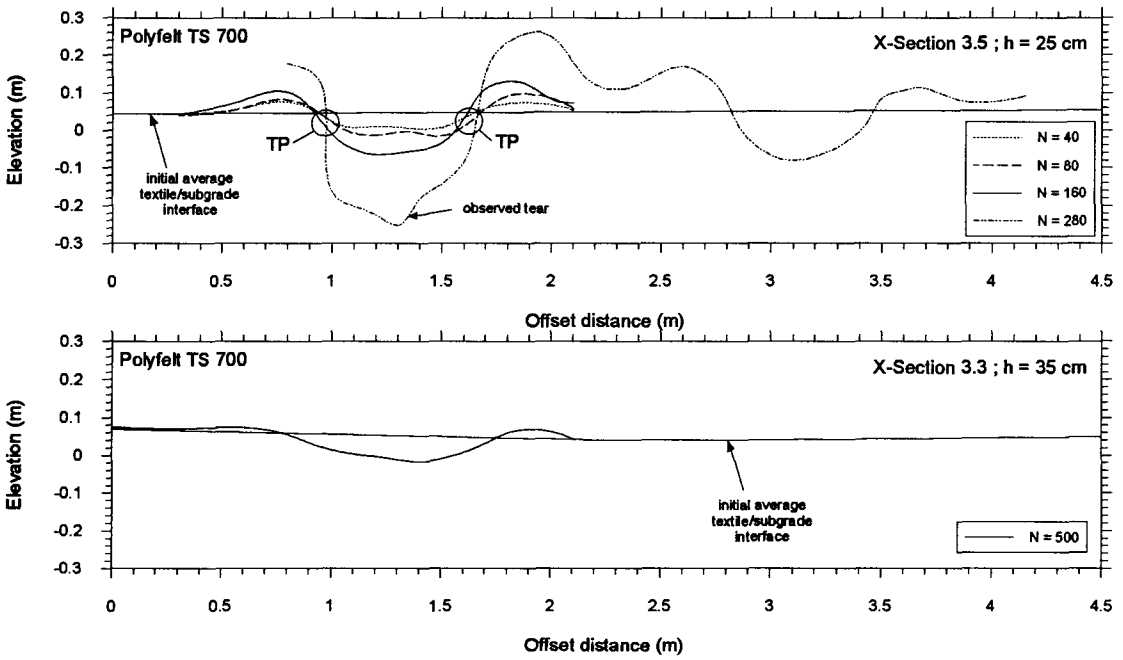

Figure 5.9 Subgrade profiles in test sections 3.5 and 3.3 - Polyfelt TS 700

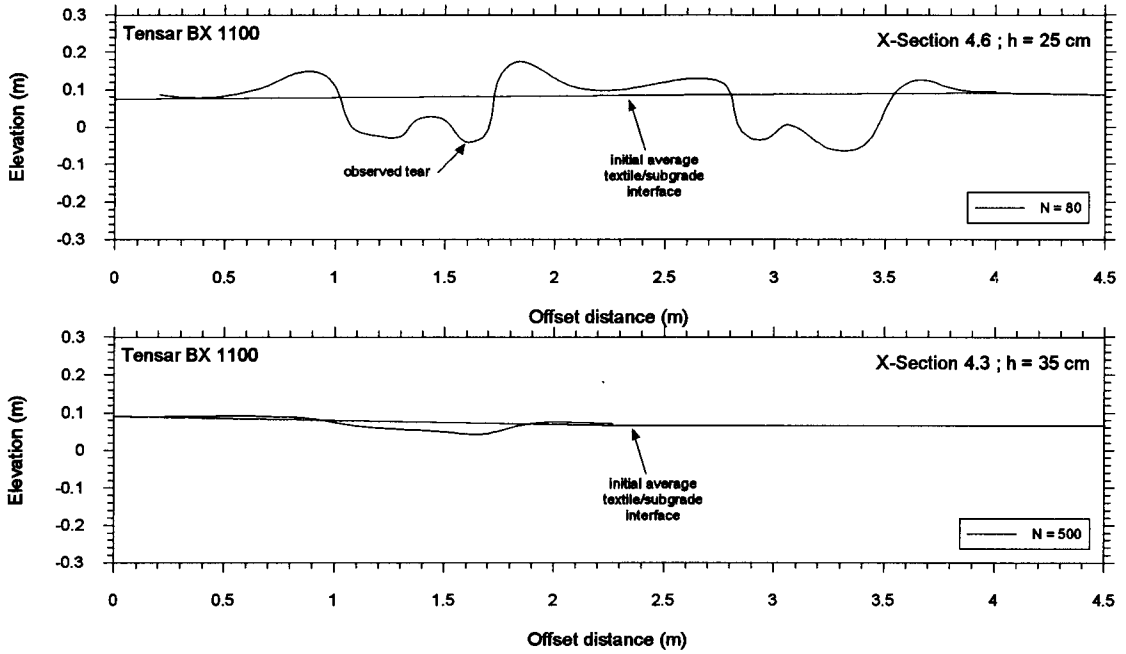

Figure 5.10 Subgrade profiles in test sections 4.6 and 4.3 - Tensar BX 1100

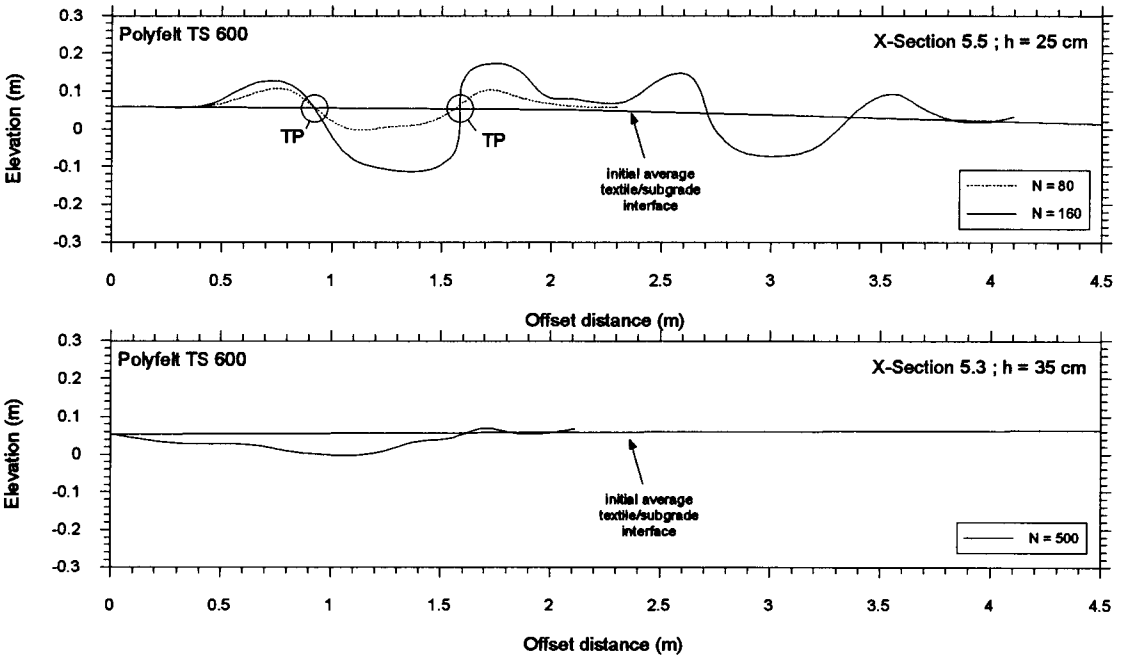

Figure 5.11 Subgrade profiles in test sections 5.5 and 5.3 - Polyfelt TS 600

Progressive observations for cross-sections 3.5 and 5.5, see Figs. 5.9 and 5.11 respectively, show a common turning point at the subgrade surface marked TP in the figures. The turning point separates rutting in the wheel path from heave outside it, and is an indication of that the load spread angle through the base course layer was increasing with increased rut depth. The symmetry of the deformed profiles is attributed to an equal anchorage resistance on either side of the turning point. It should be noted that cross-section 3.5 was repaired after 190 passes when it had reached a state of serviceability failure, however it was later excavated after 280 passes and the information included in Fig. 5.9.

The 35 cm thick cross-sections were excavated after 500 passes, but show no distinct pattern of deformation and no significant difference in relative performance is apparent.

A further evaluation of subgrade displacement can be made from the settlement plate data reported in Figs. 5.12 to 5.16. The plates were located underneath the left dual wheel path, and consequently do not necessarily indicate the maximum vertical subgrade deformation. However, the magnitudes of displacement measured from the settlement plates and from the subgrade profiles are in good agreement. One interesting common trend in the curves is that during the first ten passes there was a rapid increase in vertical displacements to about 3 cm. The system appears to stabilize after this initial settlement, and the increase of vertical displacement with number of passes is much slower. There is however a noticeable difference in behavior between the three base course thicknesses, with the exception of the very stiff Texel geotextile. There is also a difference in behavior between the test sections, at 25 cm and 35 cm thickness, where the smaller settlements of the Texel and Tensar sections (Figs. 5.13 and 5.15) are attributed to the greater stiffness of these materials. No significant difference in behavior is observed in the 50 cm thick section.

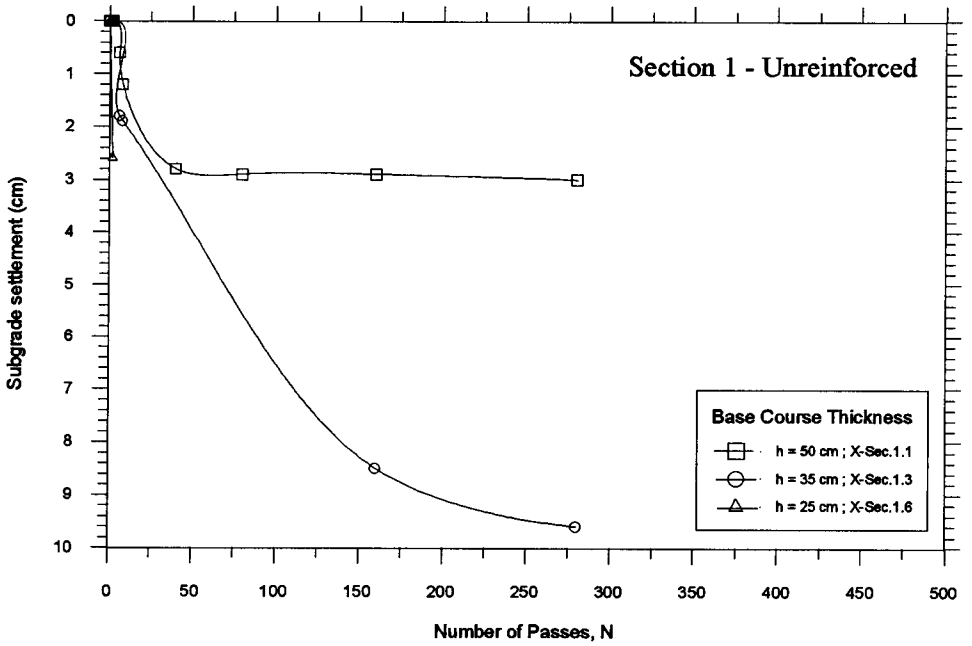

Figure 5.12 Subgrade settlement - Section 1

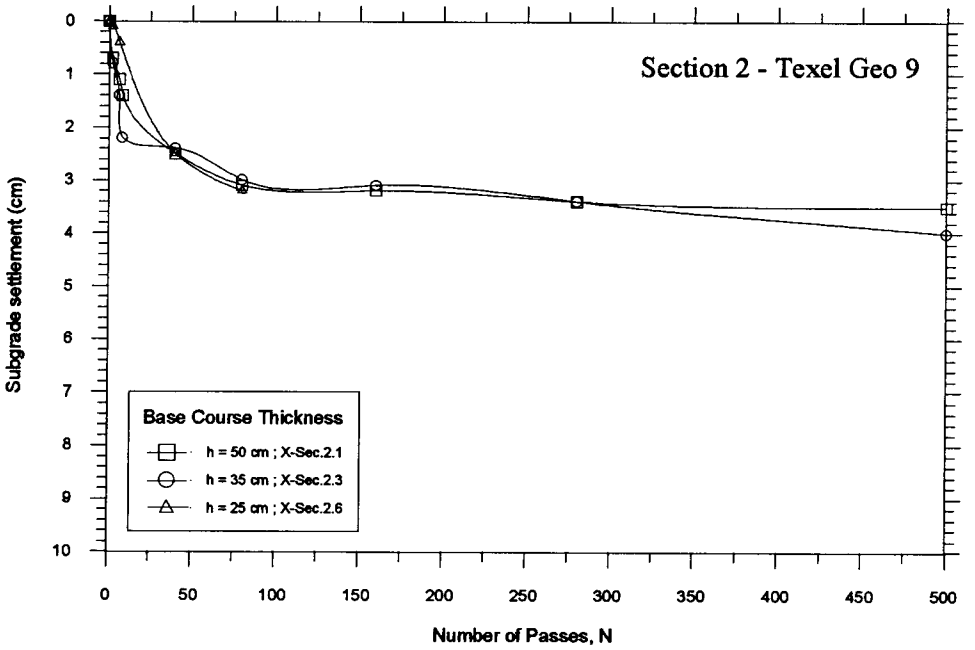

Figure 5.13 Subgrade settlement - Section 2

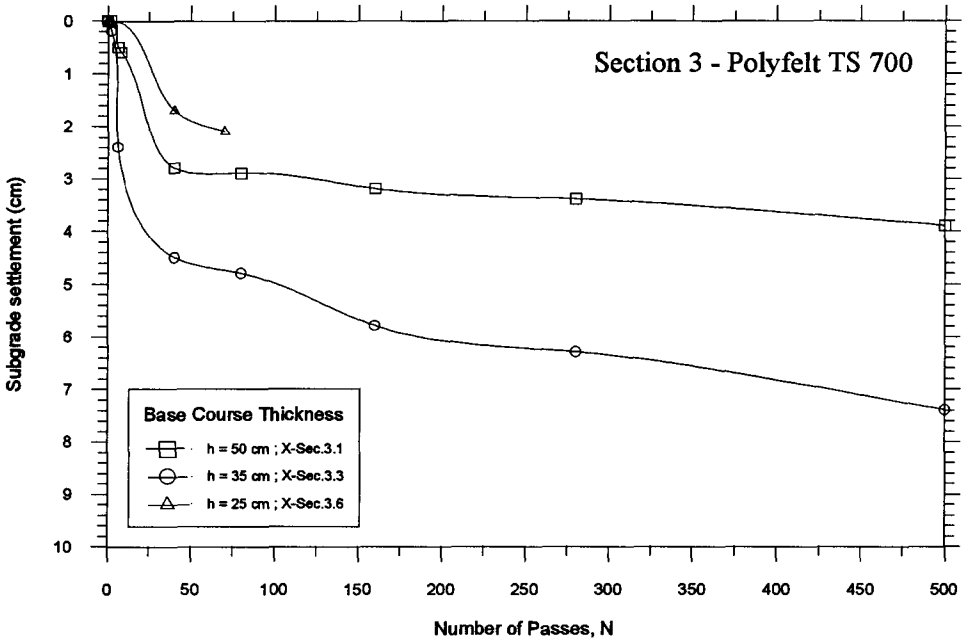

Figure 5.14 Subgrade settlement - Section 3

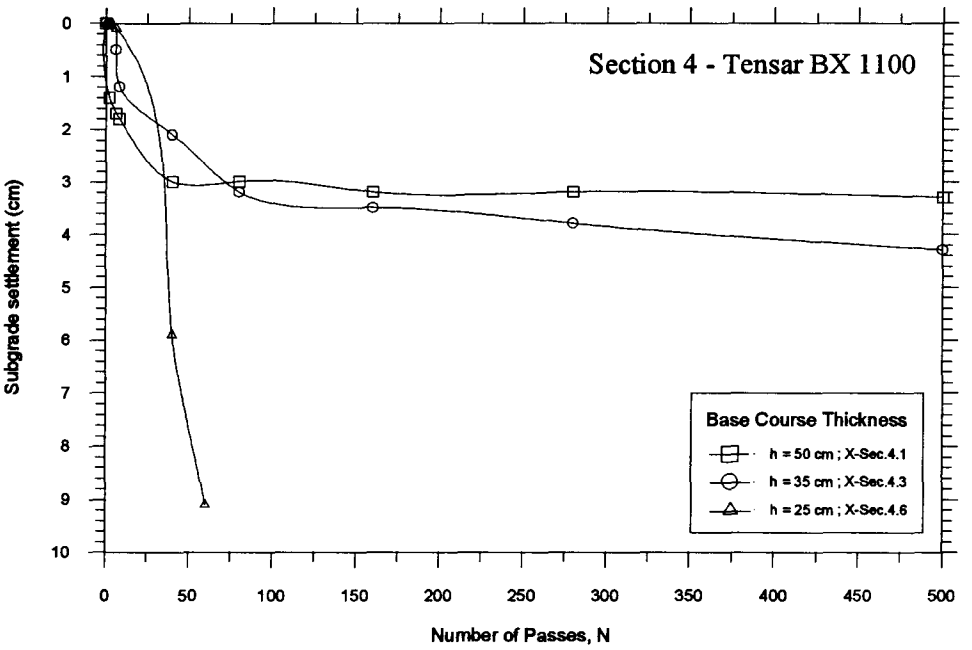

Figure 5.15 Subgrade settlement - Section 4

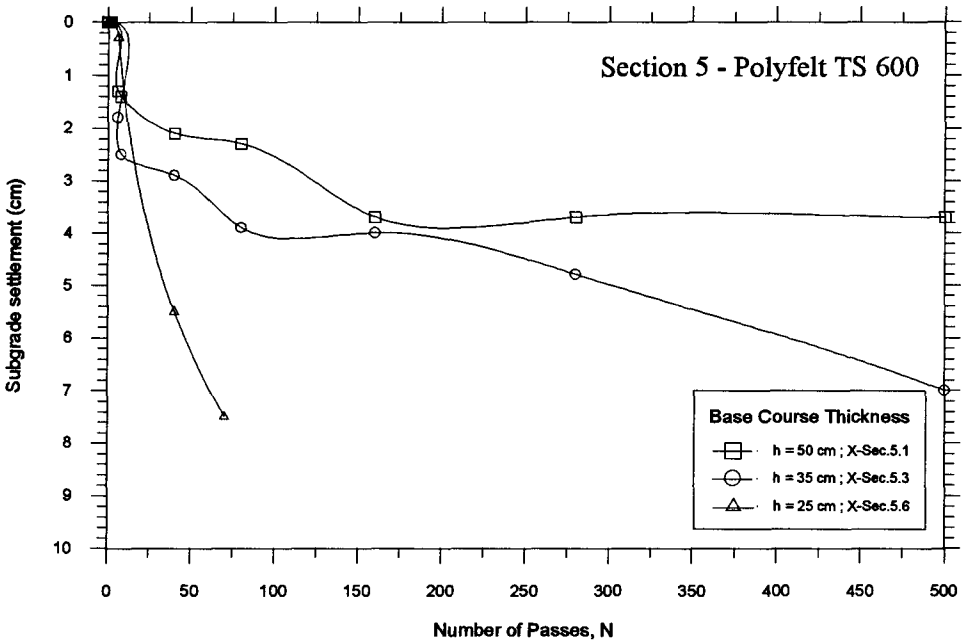

Figure 5.16 Subgrade settlement - Section 5

5.2.4 Geosynthetic Strain Measurements

Elongation of the geosynthetics was measured at the time of trenching. All of the 25 cm thick sections were measured at the location of cross-sections No.5 and additionally at cross-section No.6 in the Polyfelt test section to determine the repeatability of behavior. Measurements were also taken in the 30 cm thick Texel and Polyfelt TS 600 sections after 280 passes. Strain measurements for 35 cm thick sections were taken after 500 passes for all test sections in cross-sections No.3. The resolution of measurements is ± 0.5%

The 25 cm thick layer of section 2, Fig. 5.17, shows a distinct increase in tensile strain in the fabric with increased number of passes. However, the strain magnitude after 280 passes is not significantly larger than that after 80 passes, even though the

difference in rut depth is considerable: this section reached the serviceability failure criterion after 300 passes. No significant strains were observed in the 30 and 35 cm thick layers.

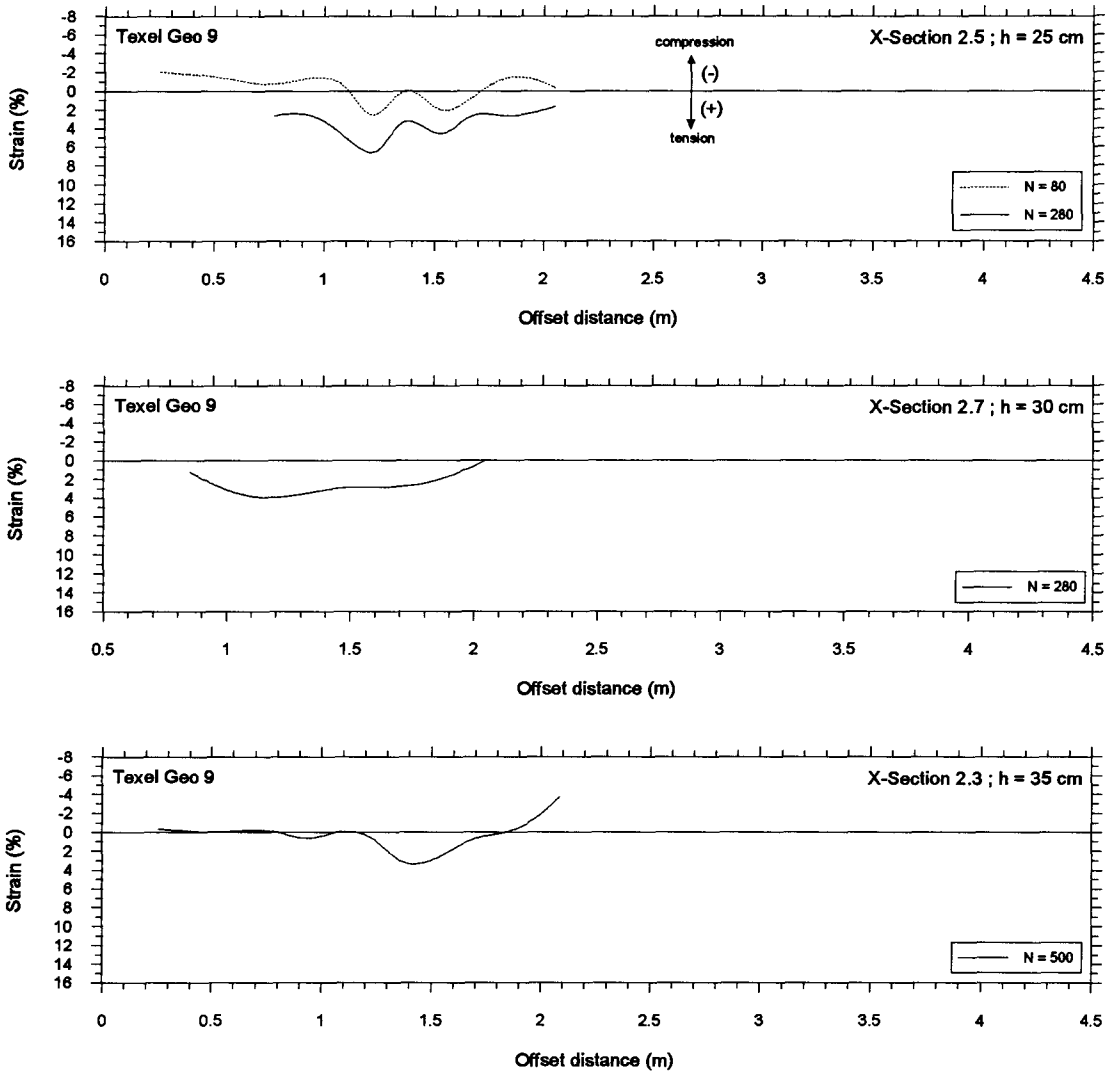

Figure 5.17 Geotextile strain measurements - Section 2

Strain measurements from the 25 cm base course thicknesses of section 3, at various numbers of passes, and from the 35 cm thick section after 500 passes, are shown in Fig. 5.18. There is a definite indication of symmetry in the 25 cm thick section, and a significant increase in tensile strain in the textile with increased number

of passes. The strain profiles show very close agreement with the observed subgrade deformation profiles discussed previously. After 500 passes on the 35 cm thick layer, a large compressive strain is recorded when no significant tensile strain is developed (Fig. 5.18): this compressive strain is attributed to folding during placement of the geotextile. Similarly no significant strain is detected in the 35 cm tick layer of section No.4 or No.5 after 500 passes, see Fig. 5.19 and 5.20.

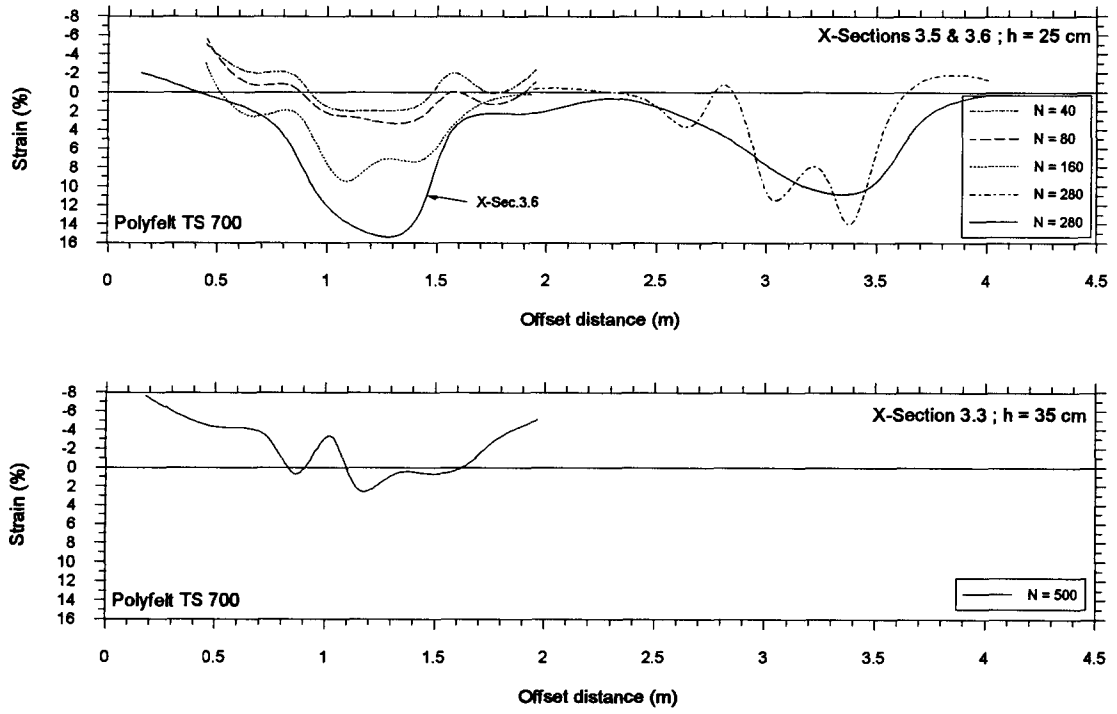

Figure 5.18 Geotextile strain measurements - Section 3

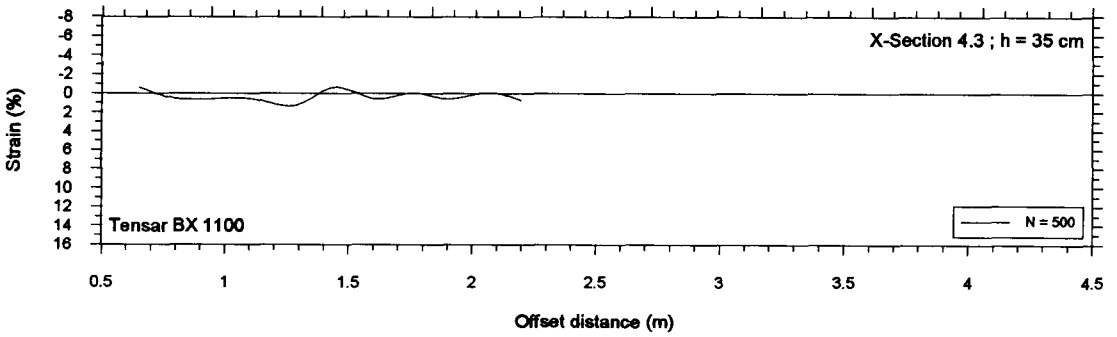

Figure 5.19 Geogrid strain measurements - Section 4

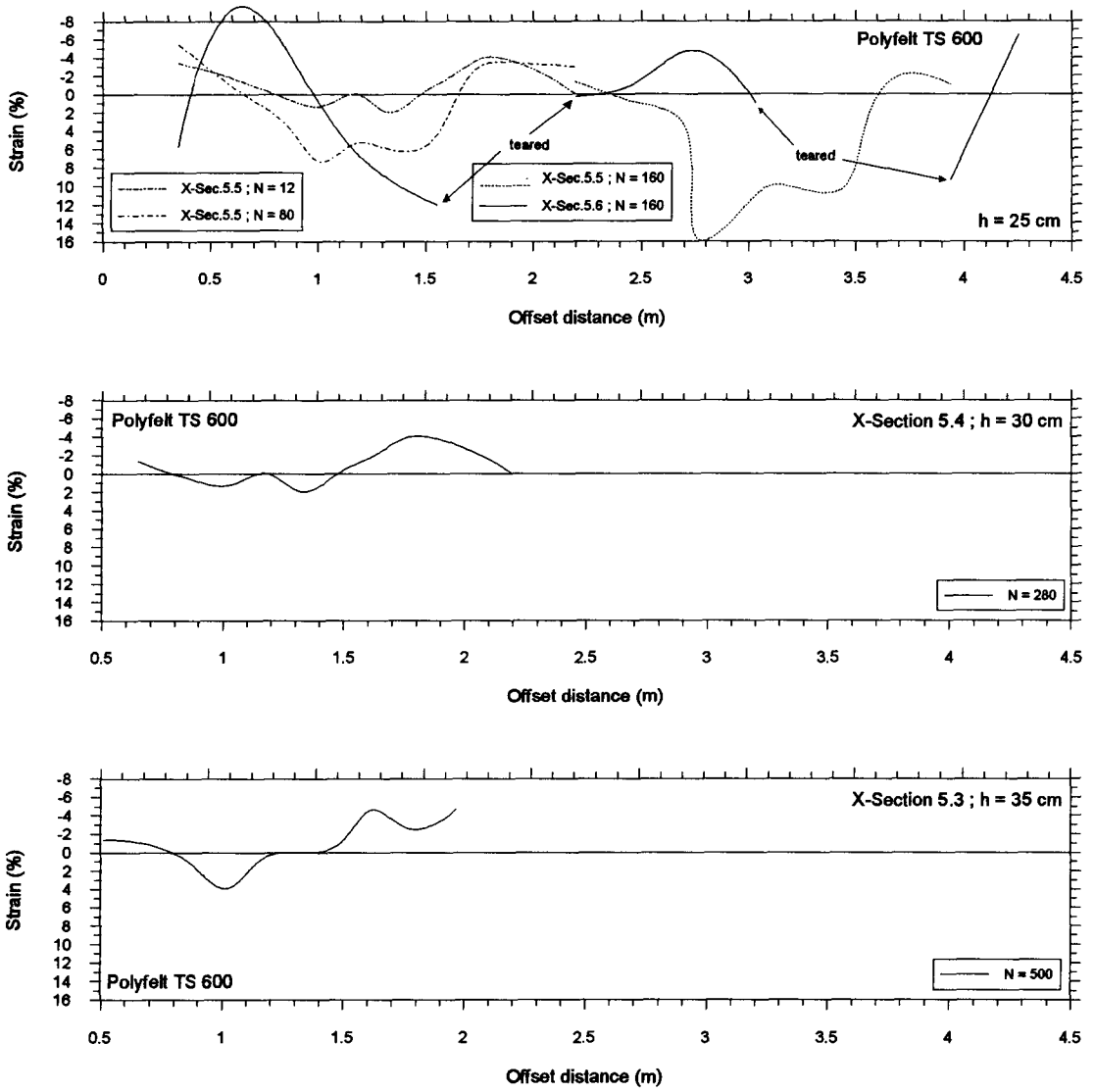

Figure 5.20 Geotextile strain measurements - Section 5

There is strong indication that the distribution of the strain underneath the loaded area in the wheel path is highly non-linear. There is also evidence of a significant difference in tensile strain between the inner and outer wheel of the two dual-wheel assemblies, even at relatively low number of vehicle passes. The pattern is most evident in the thinner sections.

A summary of the maximum tensile strain in each-cross-section is given in Table 5.1 together with calculated value of average strain in the geosynthetic underneath the loaded area.

Table 5.1 Summary of geosynthetic strain measurements

Base Course Thickness	Geosynthetic	Number of Passes, N					
		12	40	80	160	280	500
		ε (%) max (avrg.)	ε (%) max (avrg.)	ε (%) max (avrg.)	ε (%) max (avrg.)	ε (%) max (avrg.)	ε (%) max (avrg.)
h = 25 cm							
X-Sec.2.5	Texel Geo 9			2.6 (0.9)		6.6 (4.4)	
X-Sec.3.5	Polyfelt TS 700		2.0 (0.9)	3.3 (2.1)	9.5 (6.8)	13.9 (8.5)	
X.Sec.3.6	Polyfelt TS 600					15.2 (9.4)	
X-Sec.5.5	Polyfelt TS 600	2.0 (0.3)		7.4 (5.2)	16.0 (12.1)		
X-Sec.5.6	Polyfelt TS 600				12.0 (10.0)		
h = 30 cm							
X-Sec.2.7	Texel Geo 9					4.0 (3.5)	
X-Sec.5.4	Polyfelt TS 600					13.8 (10.7)	
h = 35 cm							
X-Sec.2.3	Texel Geo 9						3.3 (1.5)
X-Sec.3.3	Polyfelt TS 700						2.6 (1.0)
X-Sec.4.3	Tensar BX 1100						1.3 (0.6)
X-Sec.5.3	Polyfelt TS 600						4.0 (1.1)

There is again clear indication of increasing strain with increased number of vehicle passes. Also evident is a significant difference in the magnitude of tensile strain between the four different geosynthetics, at the base course thicknesses of 25 and 30

cm, which is attributed to the variation of stiffness of each material. The least stiff geotextile, Polyfelt TS 600, exhibits the largest strain of 16%, and the stiffest geotextile, Texel Geo 9, exhibits the smallest strains. Very small strains are observed in the 35 cm thick layer: no significant difference is observed between the three textiles, but the geogrid developed significantly less strain after the same number of passes.

Chapter 6

Interpretation of Field Data

6.1 INTRODUCTION

An interpretation of the field observations is presented here which addresses the influence of the geosynthetics, the performance of the unreinforced test section and the performance of the reinforced test sections. The intent is to verify some of the assumptions made in design methods, and compare results with the approach of Giroud and Noiray (1981).

6.2 INFLUENCE OF THE GEOSYNTHETICS

Comparison of the average measured rut depth versus number of passes in the test sections for each base course thickness (Figs. 6.1 to 6.5) indicates all of the 25 cm

thick sections are unstable, where unstable is defined as a rapidly increasing rut with increasing number of passes. However, there is significant difference in behavior between the unreinforced and the reinforced sections, particularly for the Texel Geo 9 geotextile. Examination of the number of passes at the same average rut depth, shows the Texel Geo 9 takes between 8 to 10 times more vehicle passes than the unreinforced section; the other reinforced sections take between 3 to 4 times more passes than the unreinforced section.

The varying nature of the improved response of the 25 cm thick section is attributed to a contribution from the geosynthetics which differs for each material. The Geo 9 material shows the greatest improvement, even at a very low numbers of passes. The other three geosynthetics exhibit a very similar trend up to about 50 to 75 passes, after which some difference in performance is observed. The response of the geotextiles is consistent with their tensile strength and is attributed to their stiffness. The biaxial geogrid, BX 1100, shows similar response to the TS 600 and 700 geotextiles up to about 50 passes, at which point the rut development accelerated. It is felt the separation function is of great importance when the base course thickness is relatively small. The initial performance of the geogrid is attributed to its higher stiffness and an ability to resist lateral spread of the base course aggregate by interlock. As subgrade intrusion occurs, the interlock is reduced and with it the mechanism of lateral restraint.

The 30 cm thick sections are also categorized as unstable since there is fairly rapid rut development with increasing number of passes, see Fig. 6.2. Comparison shows that the unreinforced section gives a slightly better performance than the 25 cm section, but the reinforced sections improve significantly. Although the relationship between geosynthetic stiffness and performance is less obvious, the stiffest geotextile still gives the best performance. It is felt that separation is still of some importance, but

less so than for thinner base course. This is apparent in the relative performance of the geogrid, which is better than two of the three geotextiles. Interestingly the test section with the stronger, TS 700, geotextile developed a poorer response to trafficking at less than 150 passes than the Polyfelt TS 600. It should be noted that after about 120 passes, a tear occurred in Polyfelt TS 600 fabric in the left wheel path. The tear occurred where before installation in-uniformity in the fabric thickness was observed. This explains why Polyfelt TS 600 gives a different response after 120 passes.

Figures 6.3, 6.4 and 6.5 show average rut depths with number of passes for the base course thicknesses of 35, 40 and 50 cm, respectively. All of these test sections developed a stable response characterized by a rut depth that is almost constant or slightly increasing with increasing number of passes. Although there is a significant difference in performance of the unreinforced and reinforced sections in the 35 cm thick section, there is no significant difference between the geotextile reinforced sections, and a very small improvement in the geogrid reinforced section over those with geotextiles. This behavior appears to be independent of stiffness, and therefore is attributed to a better interlock between the base course layer and the geogrid, which tends to reduce lateral displacements of the aggregate and therefore preventing subgrade intrusion.

The difference between the unreinforced and the reinforced sections reduces with increasing base course thickness, and little significant difference is observed in the 50 cm thick section, see Figs. 6.4 and 6.5. Application of linear regression to the observations suggests there would be no difference between them for a base course thickness of 60 cm at 500 passes.

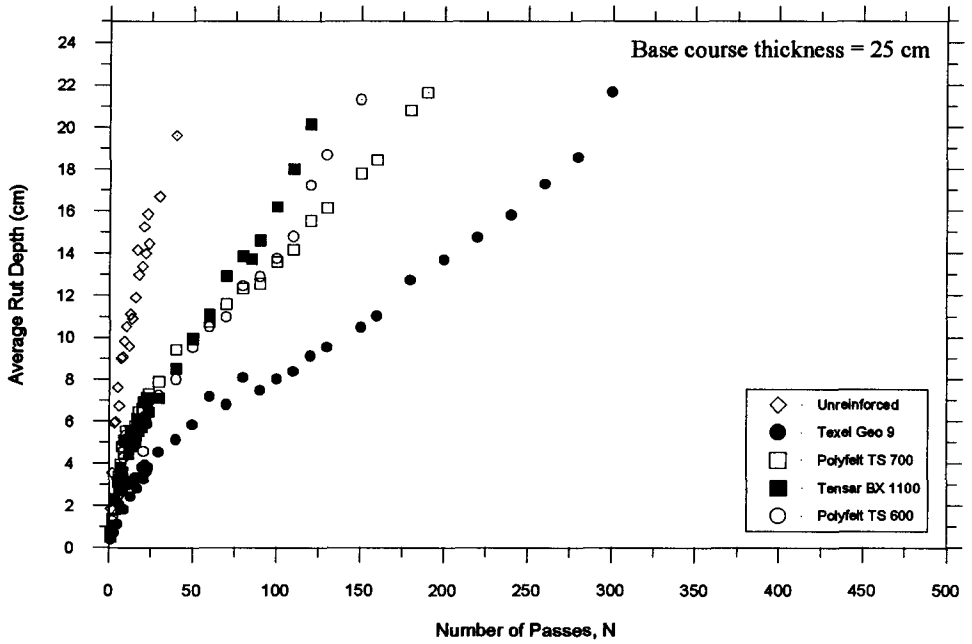

Figure 6.1 Comparison of average rut depth versus number of passes : h = 25 cm

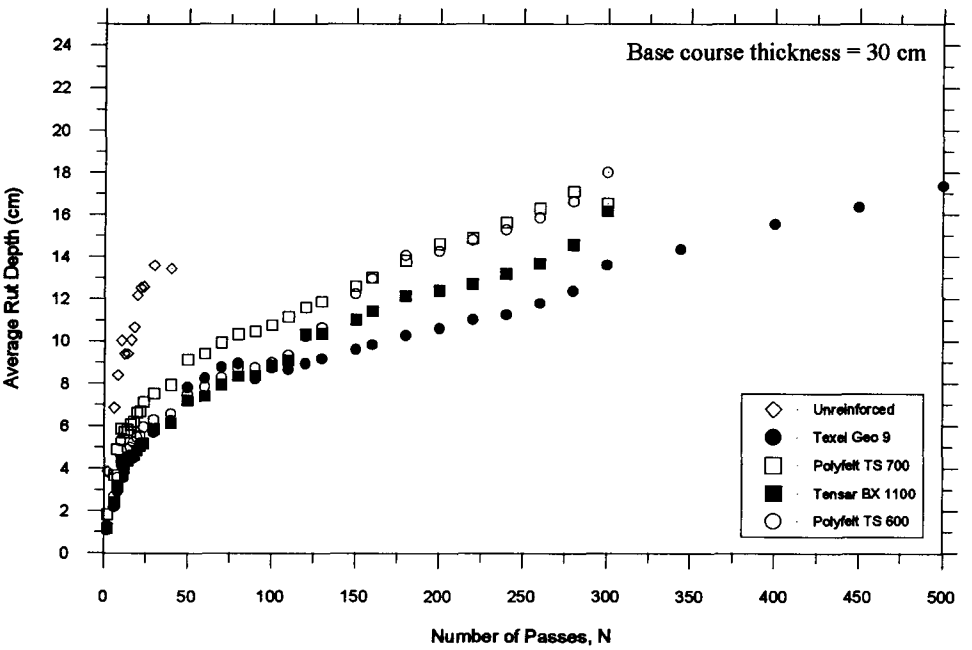

Figure 6.2 Comparison of average rut depth versus number of passes : h = 30 cm

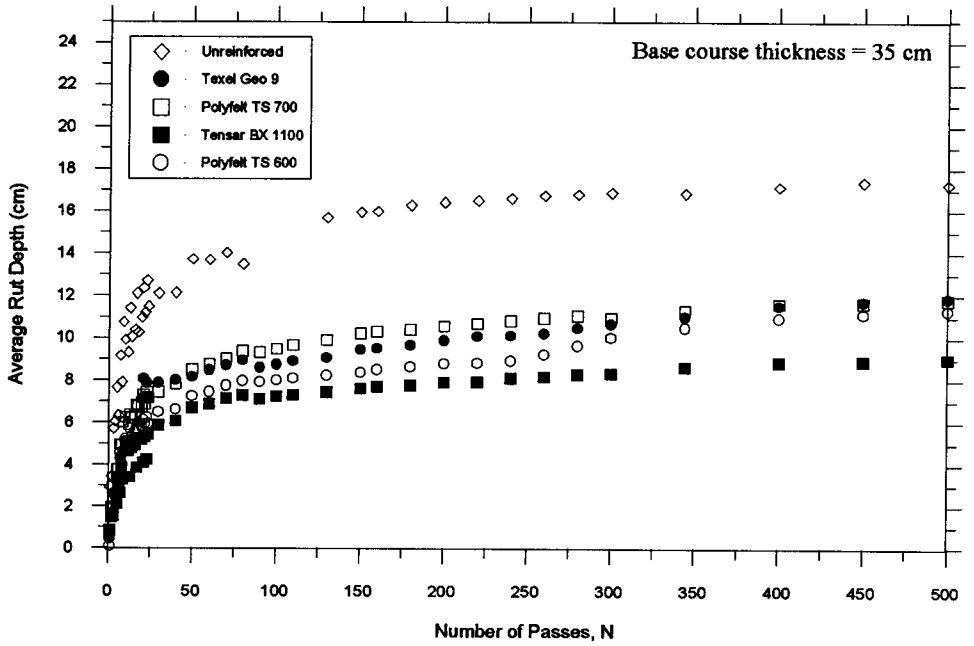

Figure 6.3 Comparison of average rut depth versus number of passes : h = 35 cm

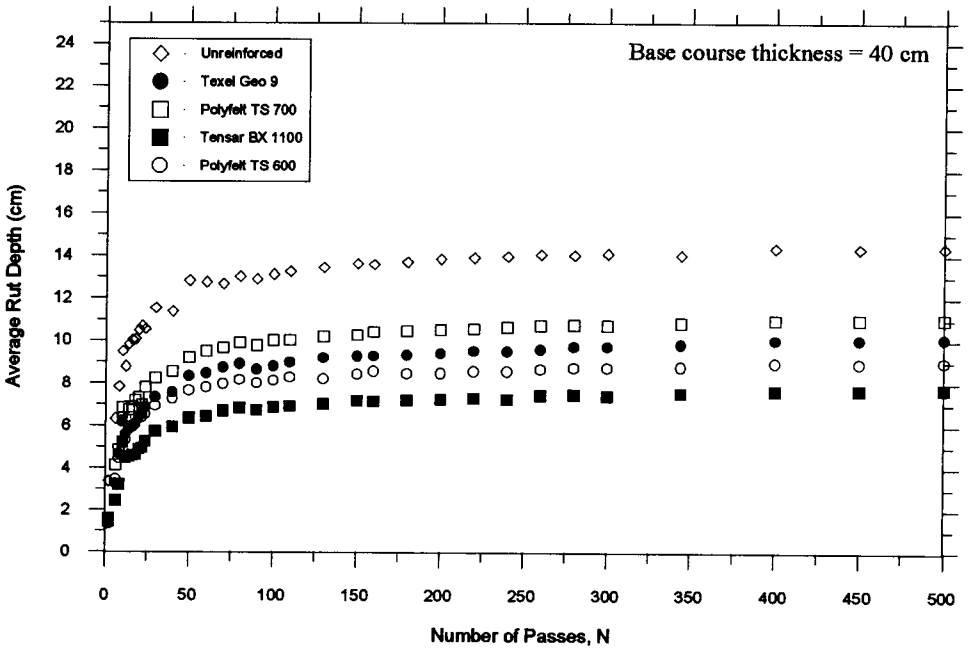

Figure 6.4 Comparison of average rut depth versus number of passes : h = 40 cm

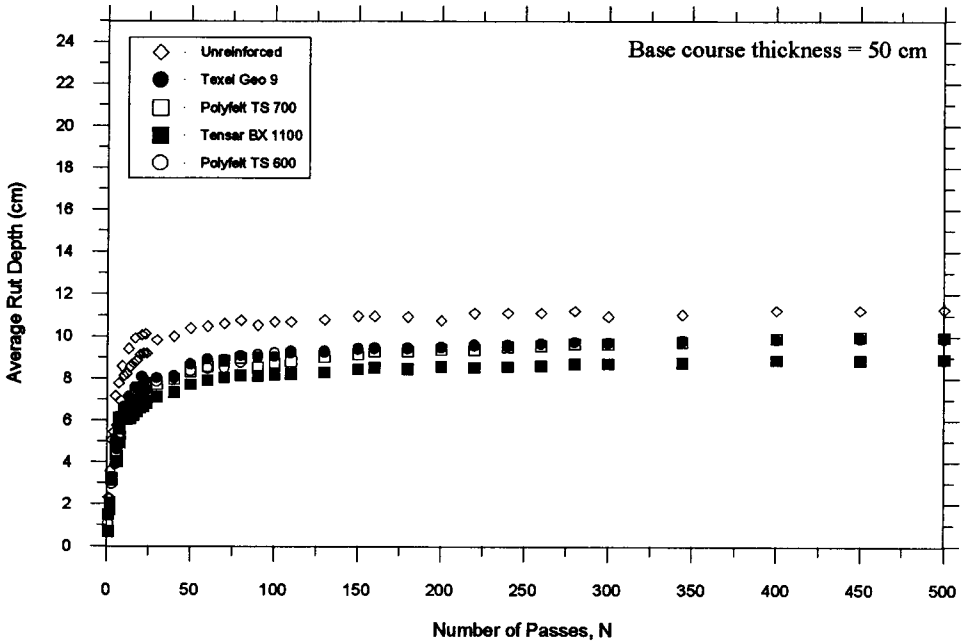

Figure 6.5 Comparison of average rut depth versus number of passes : h = 50 cm

The relationship between subgrade settlement and number of passes, Fig. 6.6, was obtained from the settlement plates (see Fig. 4.3). Since three settlement plates were installed in each section, only one measurement, and not an average, is shown in the figure.

There is a significant difference between subgrade settlements of the unreinforced and reinforced systems below the 25 cm thick section, which occurs at the onset of trafficking. The response is attributed to a tensioned-membrane effect. The reinforced sections also behave differently, with sections 4.6 and 5.6 showing a rapid settlement that is consistent with observations of surface rutting. It is concluded that, for this thin base course layer, both stiffness of the geosynthetic and adequate separation between the subgrade and base course layer are very important.

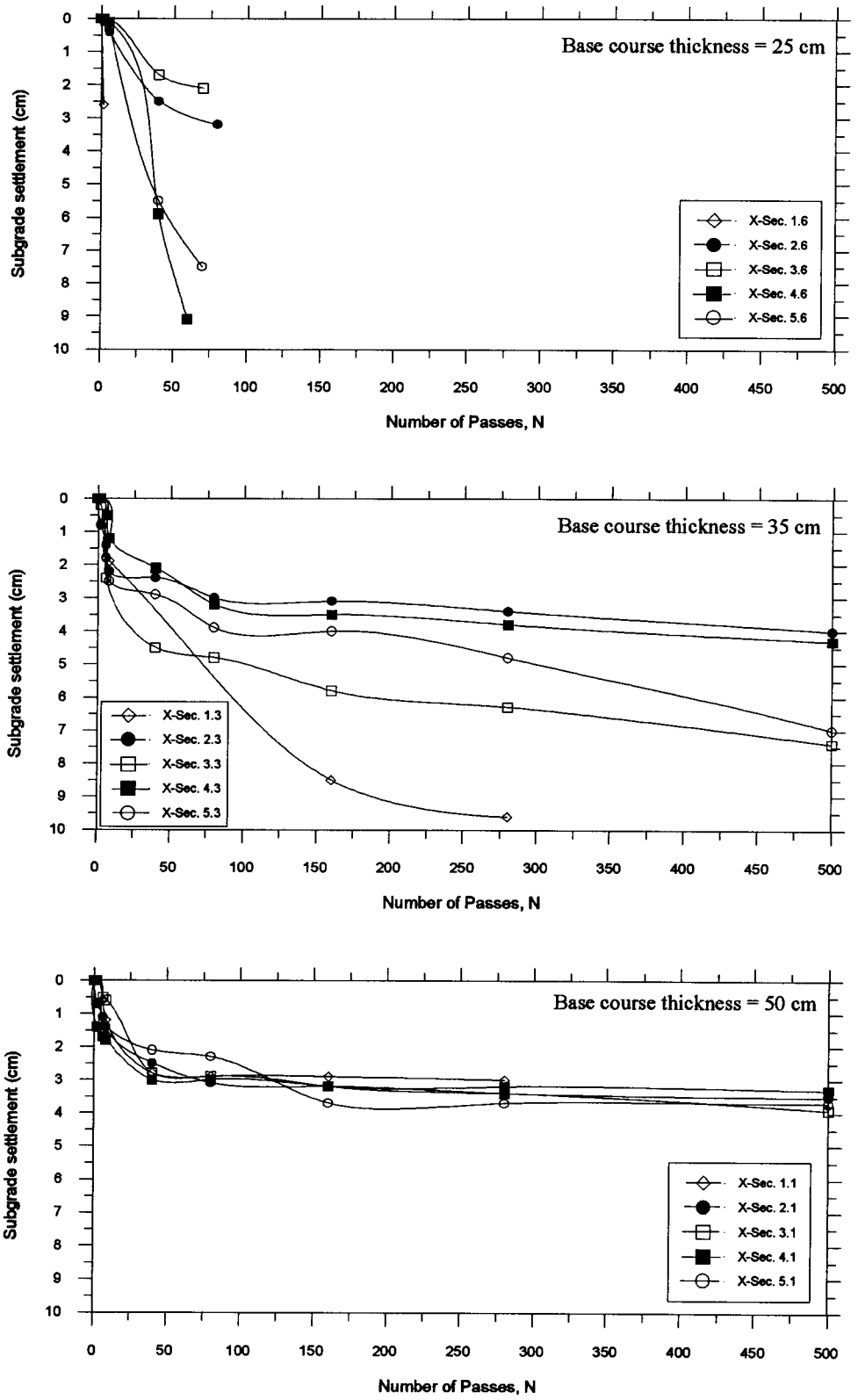

Figure 6.6 Subgrade settlement versus number of passes : h = 25, 35 & 50 cm

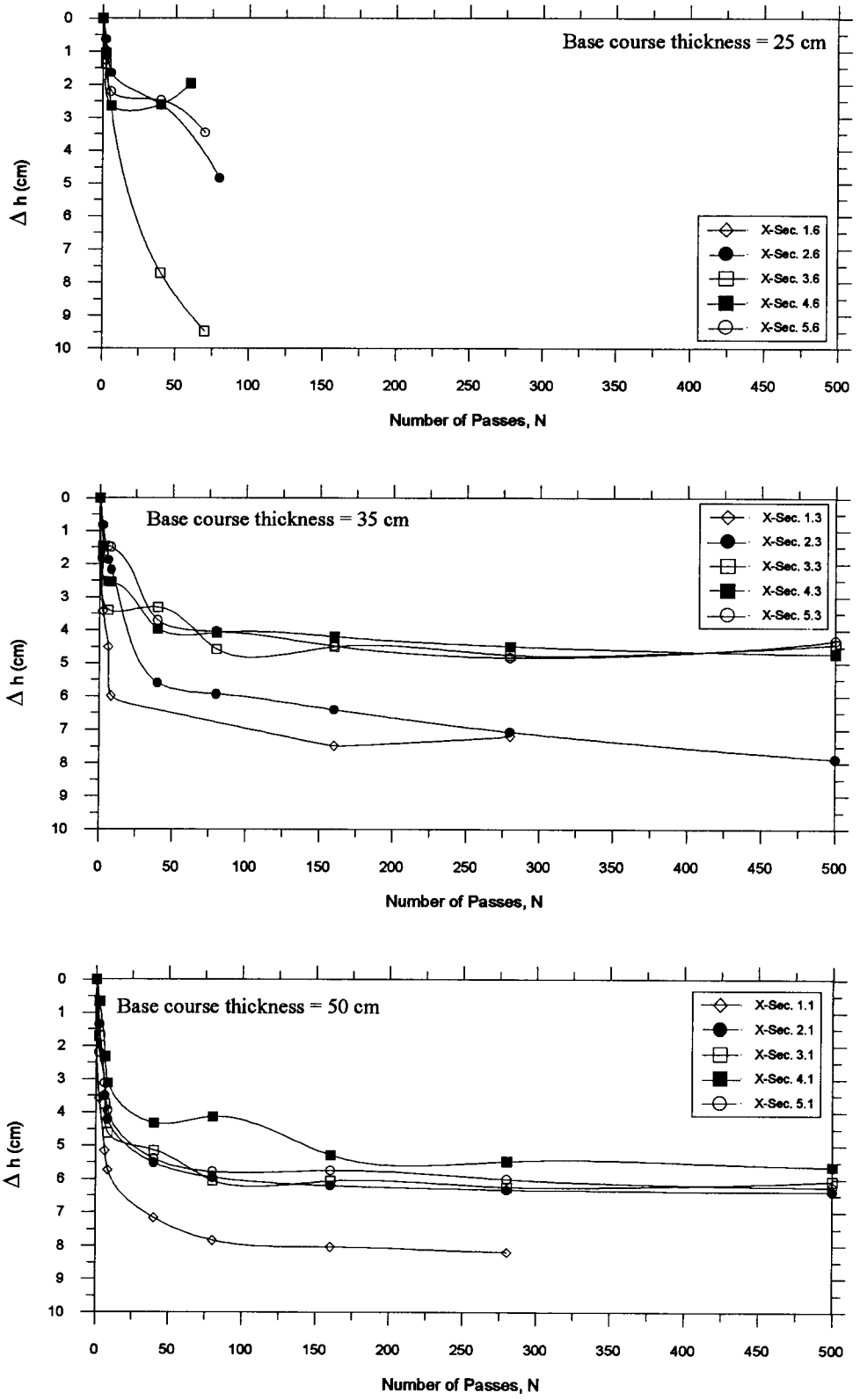

Figure 6.7 Changes in base course thickness with number of passes

Subgrade displacements below the 35 and 50 cm thick reinforced sections at the onset of trafficking are larger than those for the 25 cm thick section: The comparative response is consistent with a tensioned-membrane effect that is negligible, and a similar response in the unreinforced and reinforced systems.

The difference (Δh) between the measured rut depth and the measured subgrade settlement from the settlement plates, see Fig 6.7, is established from the same wheel path and cross section where the settlement plates are located. A horizontal line indicates the base course layer is moving with the subgrade, and no change in base course thickness occurs beneath the vehicles wheels. Hence volumetric changes in the base course layer can be quantified, assuming no lateral spread. Significant rutting occurs during the first 8 to 10 passes of trafficking, and is accompanied by about 8 % compaction (change in thickness) in the reinforced sections and between 12 and 17 % in the unreinforced section. After about 75 passes, incremental displacements of the base course and the subgrade are equal in the 35 and 50 cm thick sections. At this point, compaction of the reinforced base course layer is approximately 12 % and between 17 and 22 % in the unreinforced section. It is possible that some of this change in layer thickness is due to lateral spread of the gravel beneath the wheels, but it is likely not significant.

Unifying the observation of average rut depth, subgrade settlement and change in base course thickness versus number of passes, three general stages of response to trafficking are identified in the 35 and 50 cm sections. Firstly, there is rapid rut development with number of passes, up to 10 passes, at which point approximately 70 % of the total base course layer compaction has occurred and all the initial subgrade settlement is complete. Secondly, there is a significant increase in rut development

combined with a less significant further subgrade settlement up to around 75 passes, at which point full compaction of the base course layer is obtained. Thirdly, after 75 passes and at full compaction, vertical displacements in the base course layer and the subgrade are equal.

The relationship between rut depth and base course thickness is shown in Figs. 6.8 to 6.12. The data at few vehicle passes, say N equals 10 to 15, indicate the response of any section is independent of the base course thickness for all sections except perhaps the Geo 9 (Fig. 6.9).

A very stable response is observed in the reinforced sections when the base course thickness is larger than 40 cm. In contrast, at a base course thickness of 35 cm or less, the rut development increases with decreasing base course thickness and the system is considered to be unstable. It is however not significant, but might be categorized as a serviceability failure when the ruts are deeper than 10 cm.

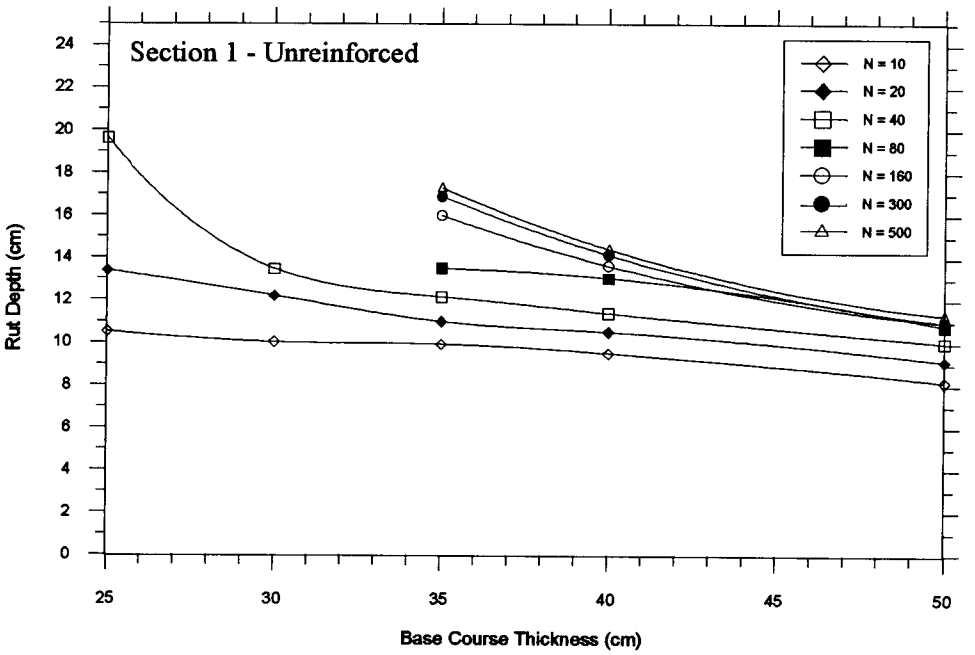

Figure 6.8 Rut depth versus base course thickness - Section 1

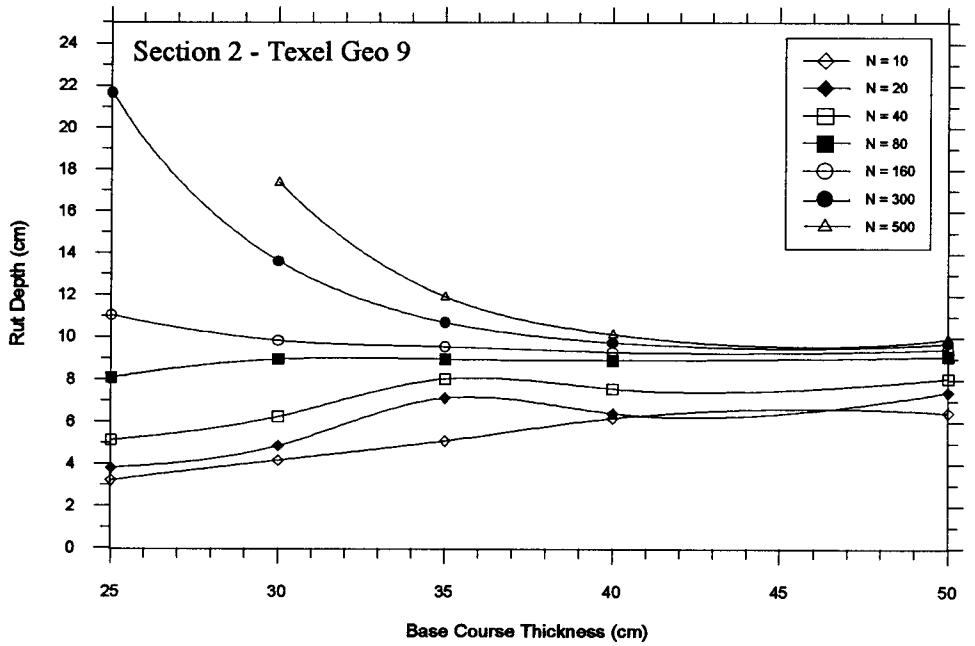

Figure 6.9 Rut depth versus base course thickness - Section 2

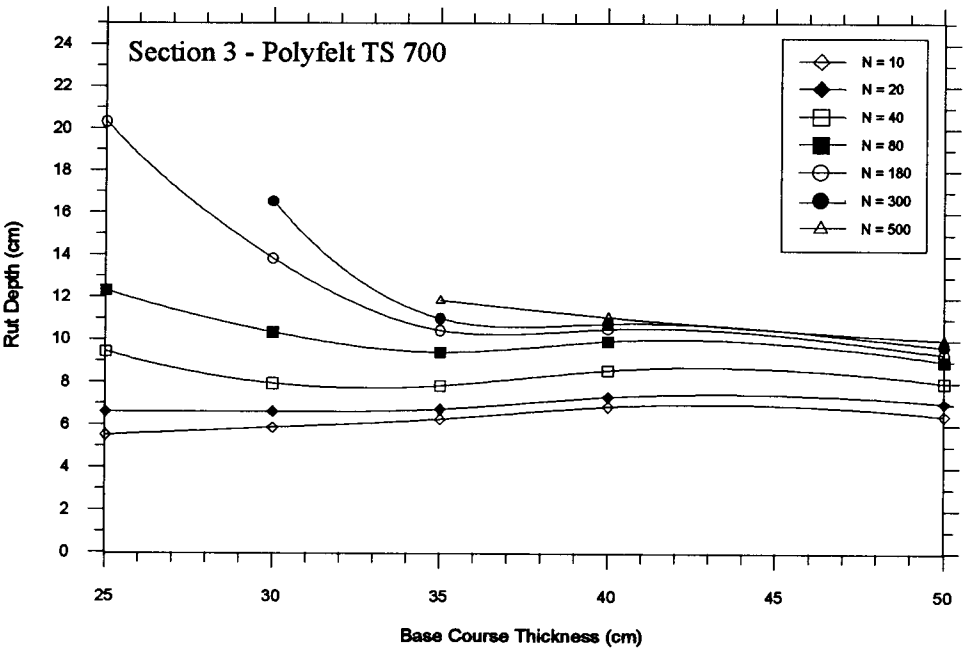

Figure 6.10 Rut depth versus base course thickness - Section 3

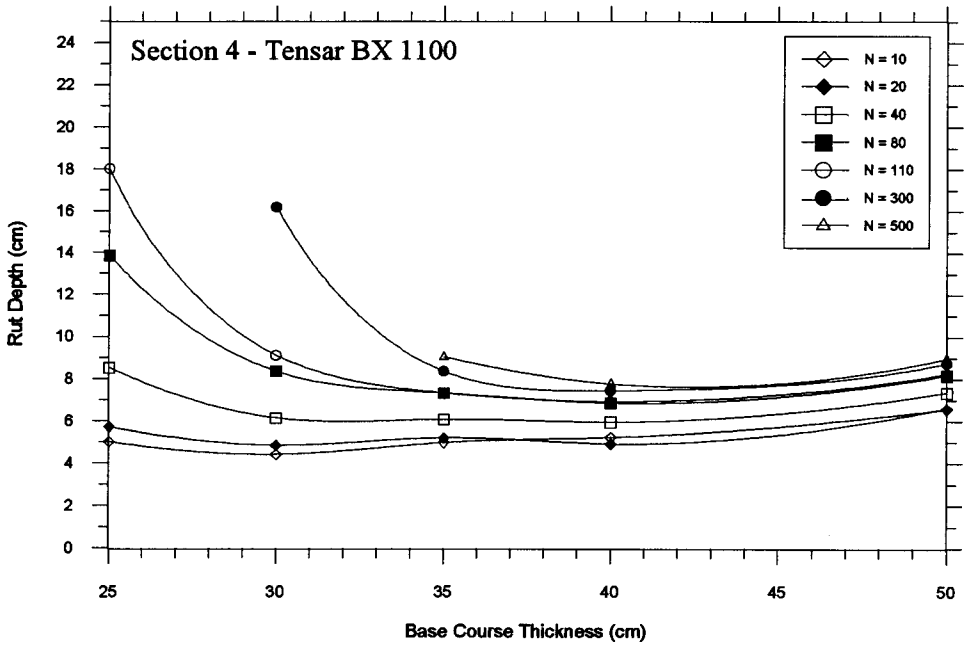

Figure 6.11 Rut depth versus base course thickness - Section 4

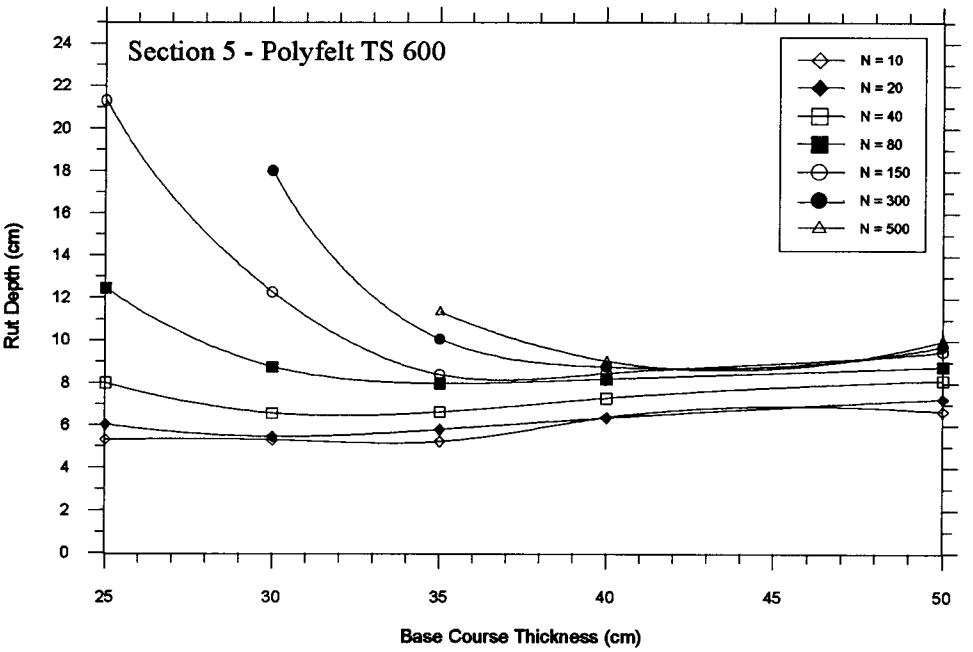

Figure 6.12 Rut depth versus base course thickness - Section 5

Very common response is observed in test sections having base course thickness greater than 35 cm. In the 35 cm thick sections, rut development is approximately at a proportional rate to doubled number of passes, whereas in the 40 and 50 cm thick sections a more stable response is observed, associated with a relatively steady state point in the 50 cm sections. As previously mentioned, no difference in rut between test sections would be anticipated for sections 60 cm or greater at 500 passes, and the steady state point would be very clear after certain number of passes, when compaction of the base course layer has taken place and the initial subgrade settlement.

It should be noted that this comparison is all related to 500 passes and if the number increases the stable response would move towards the thicker sections but a similar response as previously showed is anticipated.

6.3 UNREINFORCED PERFORMANCE

A curve that establishes the minimum design thickness of an unreinforced base course layer for different numbers of vehicle passes was proposed by Hammitt (1970), based on a full scale field trial. The equation that described the curve was then modified by Giroud and Noiray (1981) to include various axle loads and rut depths. Three sets of curves, for a standard axle load, using Giroud and Noiray's proposed equation are shown in Fig. 6.13. Three different values of undrained shear strength were used that bound the strength of the subgrade at the site of this research study, and two values of rut depth were used that bound the displacements mobilized by traffic loading in this study. The curves of base course thickness versus number of passes are very sensitive to the thickness and a small increment in base course thickness changes significantly the number of passes.

The field data from this study are plotted together with the Giroud and Noiray curves. The independence of rut depth and base course thickness is shown clearly for the case of a 5 cm rut depth and few vehicle passes (N<10) in this study. With increasing rut depth, when the dependence on the base course thickness is mobilized (at a rut depth of 15 cm), there is reasonable agreement with the empirical equation: although the magnitude is slightly different the trend is the same. It would appear the empirical equation does, however, predict more vehicle passes at a given rut depth than observed from the field trial.

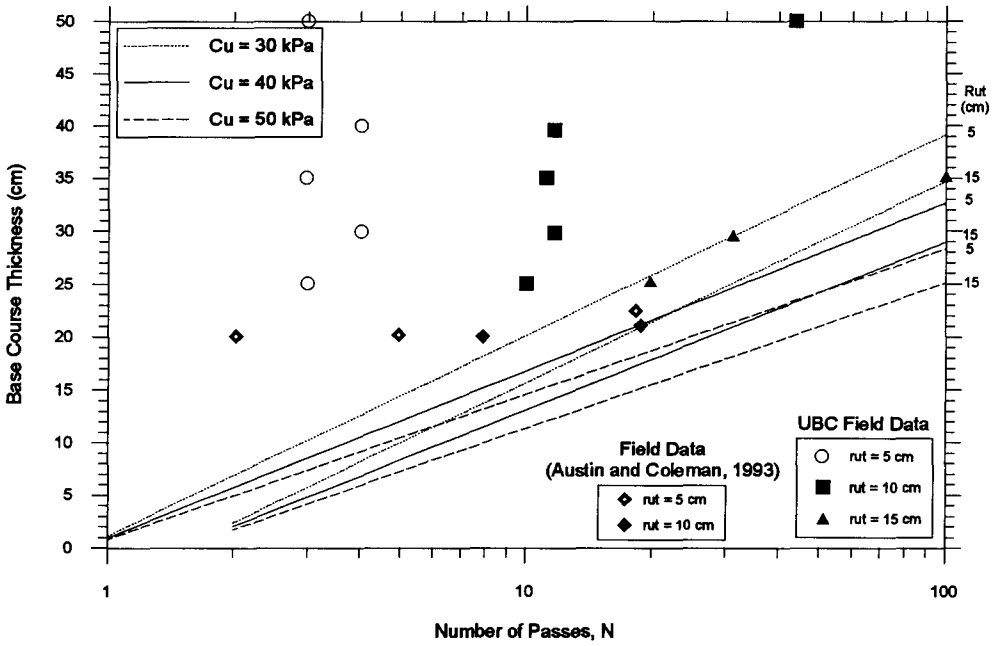

Figure 6.13 Unreinforced data comparison

However, it should be noted that the original equation proposed by Hammitt (1970) was derived by employing the method of least squares fit to data points that had considerable scatter. Furthermore, it does not consider any additional strength contribution from a base course layer with a CBR value greater than 11, e.g. a base course layer having a CBR value greater than 11 is considered to be equivalent.

While it is likely that the difference between the field data and theoretical curves is due to properties of the base course material, the compaction of the base course prior to trafficking and the derivation of the initial equation, the theoretical curves have also been extrapolated for rut depths other than those addressed by Hammitt.

Results from the field trial described by Austin and Coleman (1993) are included in Fig. 6.13. The subgrade strength was reported as a CBR of less than one, and the vehicle loading was comparable to this study. The trial comprised nine 6 m long by 6 m wide test sections, each approximately 20 cm thick; three were unreinforced, and six were reinforced with different geosynthetics. Measurements were only taken at one location within each test section. Reasonable agreement is observed with the empirical curves for more than ten passes, but the rut development in the three unreinforced control sections is very inconsistent and results indicate that base course thickness of approximately 20 cm develops a 5 cm rut after 2 to 18 passes. This is attributed to variation in both subgrade and base course strength.

6.4 REINFORCED PERFORMANCE

The performance of the reinforced sections is compared with Giroud and Noiray's design procedure, see Fig. 6.14. The input parameters used in developing this chart, following the Giroud and Noiray semi-theoretical design procedure, were based on the material properties and the loading vehicle used in the field trial: c_u = 40 kPa; P = 80.3 kN; p_c = 620 kPa; e = 1.83 m; and K = 15 kN/m. Once again it is apparent that development of the 5 cm rut is relatively independent of the base course thickness, likely as a result of initial compaction of the base course layer. For the 10 and 15 cm rut depths, the trend between base course thickness and number of passes for the field

data shows good agreement with the semi-theoretical design chart. However, the absolute magnitude of the predicted ruts is slightly different, causing the design approach to over-predict the performance of the field trial. This difference is in part attributed to the compression of the base course, which is not taken into account in the design procedure.

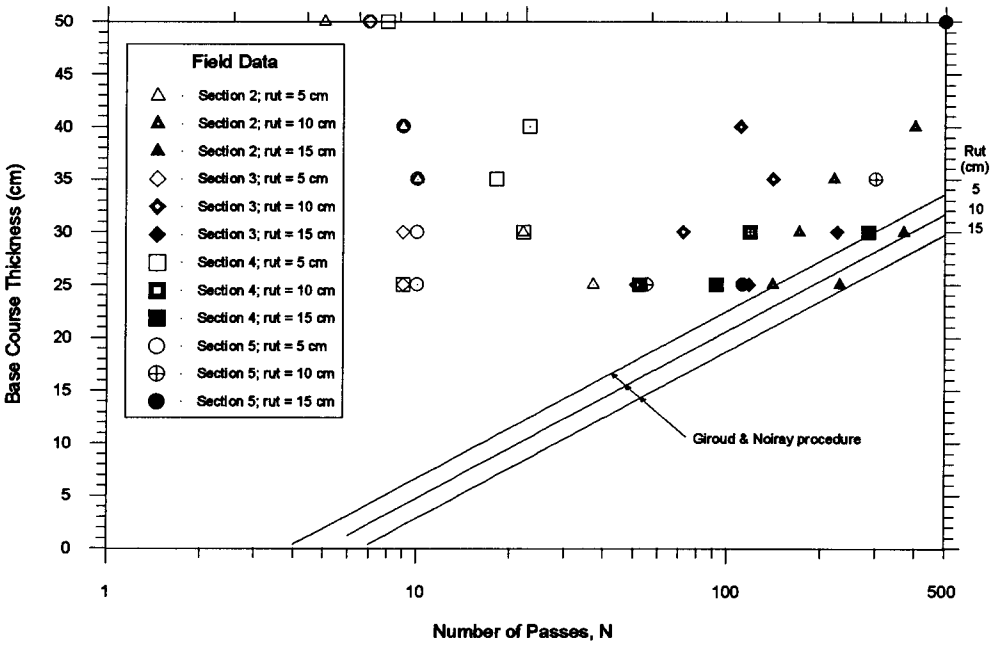

Figure 6.14 Reinforced data comparison

It is also attributed to how Giroud and Noiray treat the unreinforced sections, based on the data from Hammitt (1970), since the quasi-static analysis performed for the reinforced case does not account directly for the number of passes but takes them into account through a manipulation of the unreinforced data from Hammitt. Examination of the field data in Fig. 6.14 for the geogrid section (section 4) shows it is the only section that experience a greater increase of number of passes, with base course layer thickness, for the same rut depth compared with the Giroud and Noiray's procedure. Based on the fact that the differences in magnitude are not directly proportional for the

unreinforced and the reinforced data, and that the subgrade settlements are not directly proportional to the base course settlements, it is concluded that Giroud and Noiray's procedure is over-predicting the membrane effect on the overall performance of the reinforced sections.

6.5 LOAD DISTRIBUTION ANGLE

The load distribution angle is of importance, when designing for a minimum base course thickness employing a pyramidal load distribution, because it is used to determine the vertical stress acting on the subgrade.

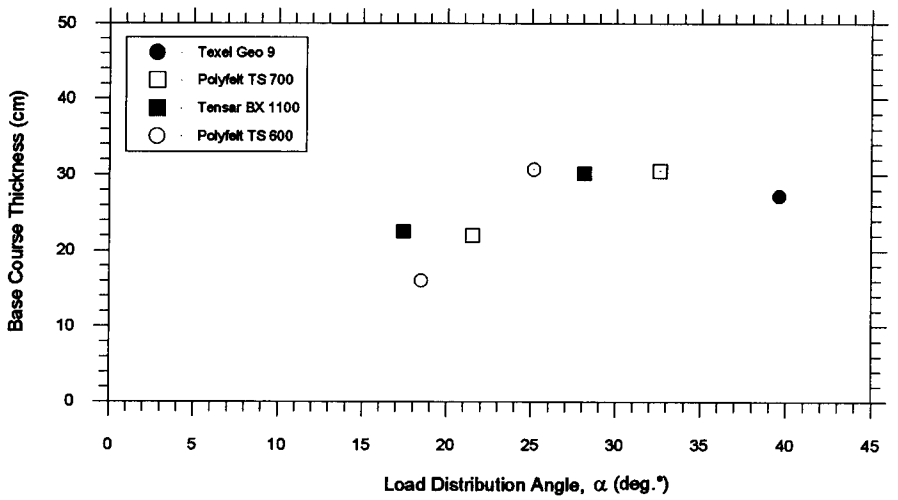

Figure 6.15 Load distribution angle versus base course thickness

Values of mobilized load distribution angle were deduced from comparison of the surface profiles (Fig. 5.2), the subgrade profiles (Figs. 5.8 to 5.11), and the change in base course thickness (Fig. 6.7), and are reported in Fig. 6.15. The load distribution

angles were determined where data of subgrade profiles were available and of a reasonable shape, and therefore only a few load distribution angles are obtained. It can be seen, Fig. 6.15, that the load distribution angle varies with depth and between test sections. The range is between 17° and 40°, which compares reasonably well with that is used in current design methods.

It is obvious that the load distribution angle, α, increases with increasing base course thickness, and based on these data points there is an indication that the variation might also be attributed to the stiffness of the geosynthetics. It would be reasonable to expect an upper bound value for α governed by characteristics of the base course material thickness. Most design methods incorporate a single value of load distribution angle, however these results indicate the behavior is more complex.

6.6 STRESSES AND BEARING CAPACITY FACTORS

Most design methods recognize that, by employing a geosynthetic in unpaved road construction over soft ground, the subgrade bearing capacity failure is moved from being one of local shear failure to general shear failure, which is an increase in bearing capacity of approximately 65%.

Estimation of vertical stresses can be calculated by several methods. Design methods usually do not consider the effects of multi-layer system and how the elastic modules ratio between the layers effect the stress distribution with depth. Haliburton and Barron (1983) did however realize this effect and concluded that by using Burmister theory (1943, 1944) of stresses and displacements in layered systems to calculate the stresses on the subgrade surface, the stresses were half the stresses that would be estimated by employing the conventional Boussinesq theory. They however

did not mention that this stress reduction based on the Burmister layered system is fairly sensitive to the modulus ratio between the layers.

To demonstrate this stress reduction effect for a two-layer system a simpler method developed by Odemark (1949) is used, which is based on Burmister's layered system theory. Two different elastic modulus ratios are shown in Fig. 6.16 to illustrate the effects of the two-layered system on stress distribution in the upper layer using a standard axle load and a tire inflation pressure of 620 kPa.

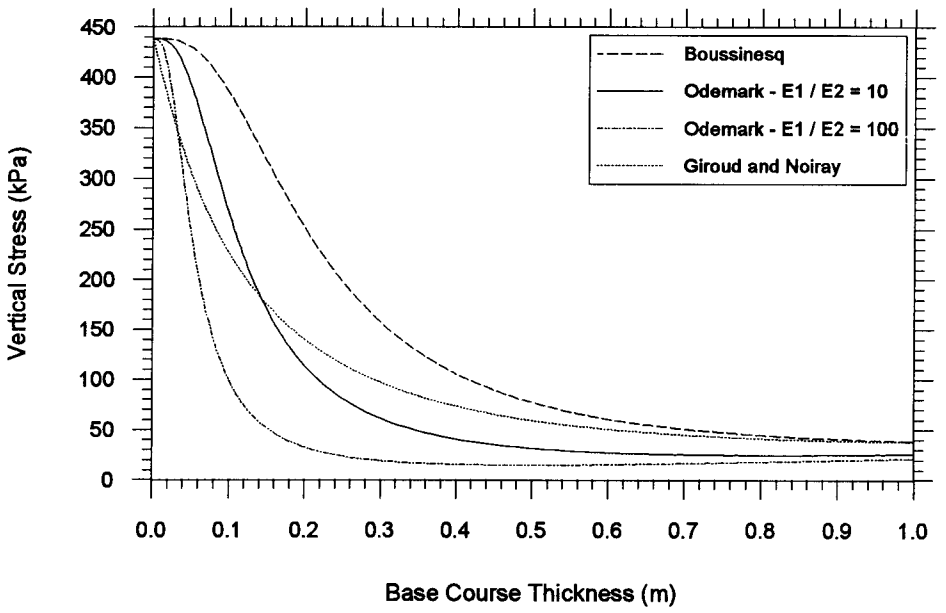

Figure 6.16 Vertical stresses on subgrade surface versus base course thickness

For comparison, the conventional Boussinesq is also shown, and the pyramidal stress reduction used in Giroud and Noiray's design procedure. It is obvious that there is significant stress reduction that takes place when two-layer system is considered, and the 50% stress reduction proposed by Haliburton and Barron (1983) seems to be in fairly good agreement with the Odemark theory, though it is dependent on the elastic modulus ratio. Vertical stresses predicted using a pyramidal stress distribution over-

predict the stresses on subgrade surface compared to the Odemark theory by 25 - 90%, depending on the base course thickness, using a modulus ratio of 10 which is the predicted ratio in the field trial.

The comparison of the unreinforced data in Fig. 6.13 indicated a good agreement at rut depths of 15 cm between the field trial data and the semi-theoretical procedure by Giroud and Noiray. The reinforced comparison indicates an over-estimation in performance which is difficult to explain assuming that the vertical stresses are overestimated. Whether this can be attributed to how the tensioned membrane effect is treated, how traffic volume is taken into account in the reinforced system, the fact that the base course material has other material properties than CBR of 11, or simply due to the reason that the ultimate bearing capacity is over estimated, is hard to tell but there is an indication that some other factors have to be considered.

The relationship between rut depth and the predicted vertical stress on the subgrade surface normalized with respect to the undrained shear strength is shown in Fig. 6.17 and Fig 6.18, for the unreinforced section and the reinforced sections respectively. The analysis was made to estimate bearing capacity factors mobilized by the unreinforced and the reinforced sections. Rut depths are plotted at certain interval of vehicle passes, and the vertical stresses calculated using the Odemark (1949) method knowing the base course thickness change for various number of passes. In the unreinforced case the bearing capacity factor, given by the normalized vertical stress, starts to increase at a value of $\sigma_z/c_u = 2.2$, which is about 70% of the bearing capacity value used in most design methods in unreinforced systems and is therefore considered to be in a fairly good agreement. The reinforced system was treated in the same manner as the unreinforced and the result are shown in Fig. 6.18. Unfortunately the changes in base course thickness for the 25 cm thick sections is only available up to 60 - 80 passes and therefore vertical stresses for passes over that number are excluded

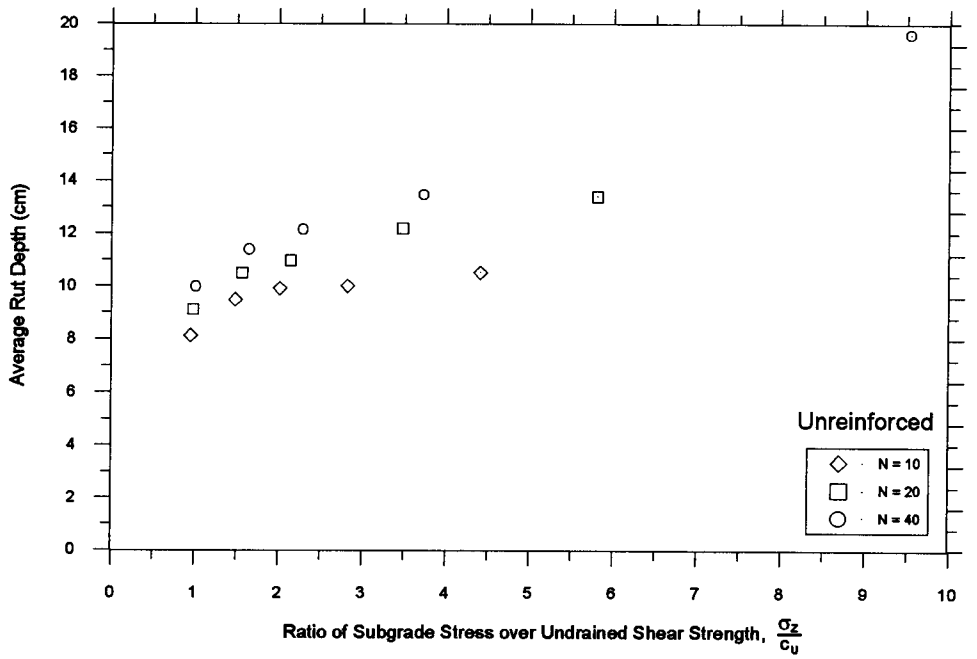

Figure 6.17 Bearing capacity factor prediction - Unreinforced Sections

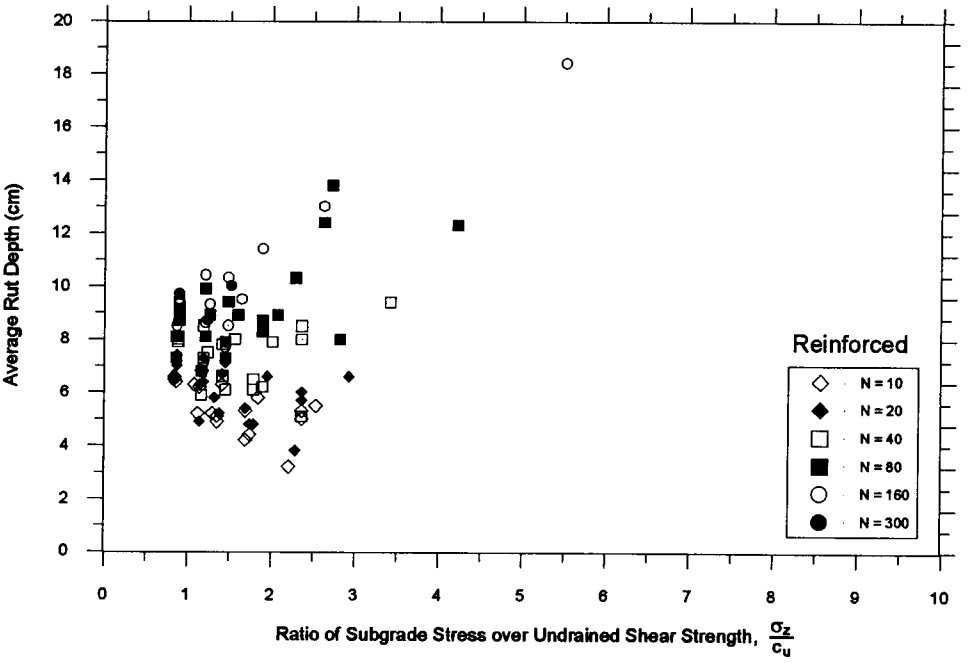

Figure 6.18 Bearing capacity factor prediction - Reinforced sections

and the highest stress level for that range of passes is between 4 and 4.5 which is still considerably less than 5.14 which is considered as being the stress level for the ultimate bearing capacity of the subgrade using theory of plasticity. The point shown in Fig. 6.18, having value of about 5.5 is extrapolated from the 25 cm thick section and is therefore not reliable. Other data points are scattered between about 0.8 and 3.5 and indicate that a ultimate bearing capacity of the subgrade was not mobilized. Therefore, it might indicate that the performance of the thinner sections is in fact attributed to something else than bearing capacity factor used in design and rather than reaching the ultimate bearing capacity the geosynthetics are torn before that stress level is mobilized resulting in a local shear failure and therefore much lower stress level than anticipated. If this is true, then outward acting shear stresses and the overall stiffness of the reinforced system are of great importance.

Chapter 7

Conclusions and Recommendations

7.1 CONCLUSIONS

The use of geosynthetics in unpaved road construction is well-recognized. However, the relative improvement of a reinforced over unreinforced system depends on structural considerations such as material properties, geometry and loading conditions. Few full scale field trials have been performed and documented which contrast the relative performance of different geosynthetics under controlled vehicle loading. Design methods differ in some respects as to their interpretation of the reinforcement action. Some basic assumptions made in the design therefore require validation through a well-controlled field trial, and observation of the response of the road system to trafficking. Some constraints of the field trial must be recognized. These results are based on one strength of subgrade. The vehicle loading is channalized, which may not always be the case in practice. Compaction of the base

course layer exerts an important influence on traffickability, and in this field trial the compaction prior to vehicle loading was likely to be less than that for regular road construction practice. It should also be recognized that this field trial is limited to 500 standard axle vehicle passes, and the relative comparison of performance for both the unreinforced section and the four reinforced sections is based on this number of passes.

An unpaved road, comprising a base course layer between 25 and 50 cm. thick over a soft subgrade of undrained shear strength approximately 40 kPa, has been used to contrast the performance of three non-woven geotextiles and a geogrid. Results from this full-scale field trial indicate a much improved performance from the reinforced sections than the unreinforced section for unpaved roads over soft ground. However the performance of each of the four different geosynthetics was similar with respect to failure, where failure is defined as an unacceptable rut depth or a serviceability failure. Compression of the base course layer was observed, which also might include some lateral spread of the gravel; the corresponding subgrade deformations were much smaller than rut measurements at the base course surface.

The performance of the unreinforced section shows reasonable agreement with the minimum design thickness proposed by Hammitt(1970) at large rut depths but not at small ruts. No significant variation of subgrade properties was observed along the test site, therefore the behavior at small rut depths is attributed to early compression of the base course layer, and the rut depth is relatively independent of base course thickness. Thereafter rut development is more dependent on base course thickness, and at this point the dependence of rut on thickness revealed a trend with increasing vehicle passes that compares well with Hammitt. However this does not occur until a rut of about 15 cm, which in many cases would be unacceptable and considered close to a serviceability failure.

The reinforced data compares quite well with theory (Giroud and Noiray, 1981), considering the trend of rut versus number of vehicle passes, but again the theory over predicts the performance. This difference is attributed in part to the initial compaction of the base course layer: in theory the base course layer is considered incompressible, and ruts at the base course surface are equal to deformations at the subgrade surface. The difference in performance between theory and the field data, is also attributed to the nature of the tensioned-membrane effect, which would be greater if the assumption of same magnitude of ruts and subgrade deformations held true. Although the tensioned-membrane effect is believed to have been significant in the 25 and 30 cm sections, in the thicker sections the membrane effect is greatly over predicted and other mechanisms are more likely to contributing to the better performance of the reinforced sections.

The field performance of the reinforced test sections suggests a particular stabilization mechanism was taking place. In the 25 and 30 cm thick sections the tensioned-membrane effect seems to be mobilized, which is specially evident in the 25 cm section where there is a clear difference in performance between the geotextiles that is related to tensile strength. Separation appears to be very important in the thinnest sections, and the geogrid does not perform so well: as base course thickness increases, the geogrid performance gets much better, which is attributed to maintenance of a good interface bond with the base course material. As base course thickness increases, the evidence of a tensioned-membrane effect is negligible at the given number of vehicle passes and moderate rut depths: stiffness and separation are the main factors contributing to the better performance of the reinforced system. In the 40 and 50 cm thick sections the geogrid consistently shows less rutting than the geotextiles. While this may be attributed to its ability to take up outward acting shear stresses on the surface of the subgrade below the vehicle wheel paths, all of the

geosynthetics behave in a similar manner. This similar performance might be a consequence of the geosynthetics exceeding a threshold stiffness for these site conditions and vehicle loading.

7.2 IMPLICATIONS FOR ENGINEERING DESIGN

The currently most widely used design method for unpaved roads over soft ground is the Giroud and Noiray (1981) procedure. Therefore it is important to recognize the observed over-prediction in performance at large numbers of vehicle passes, which increases with decreasing traffic volume. This difference is, as already stated, largely attributed to the initial base course compaction and leads to the question of whether or not the base course compaction is realistic in unpaved road design, as well as the relationship between constant base course thickness and number of vehicle passes.

Based on this field trial, it appears important to consider both stiffness of the geosynthetic and its separation ability, in design of an unpaved road over a soft subgrade for a small number of vehicle passes and a small base course thickness. It is clear that if proper separation is not provided, the stiffness alone becomes less important, i.e., a geosynthetic that provides a good seperation is a better contributor to the road system than a stiffer material which does not provide good seperation. At large numbers of passes, and a large base course thickness, separation becomes the most important stabilization factor assuming a threshold stiffness is provided.

Based on an equivalent performance, where equivalent performance is defined as the same rut depth at the same number of vehicle passes, there is potential for considerable savings in base course aggregate thickness in a reinforced system, within

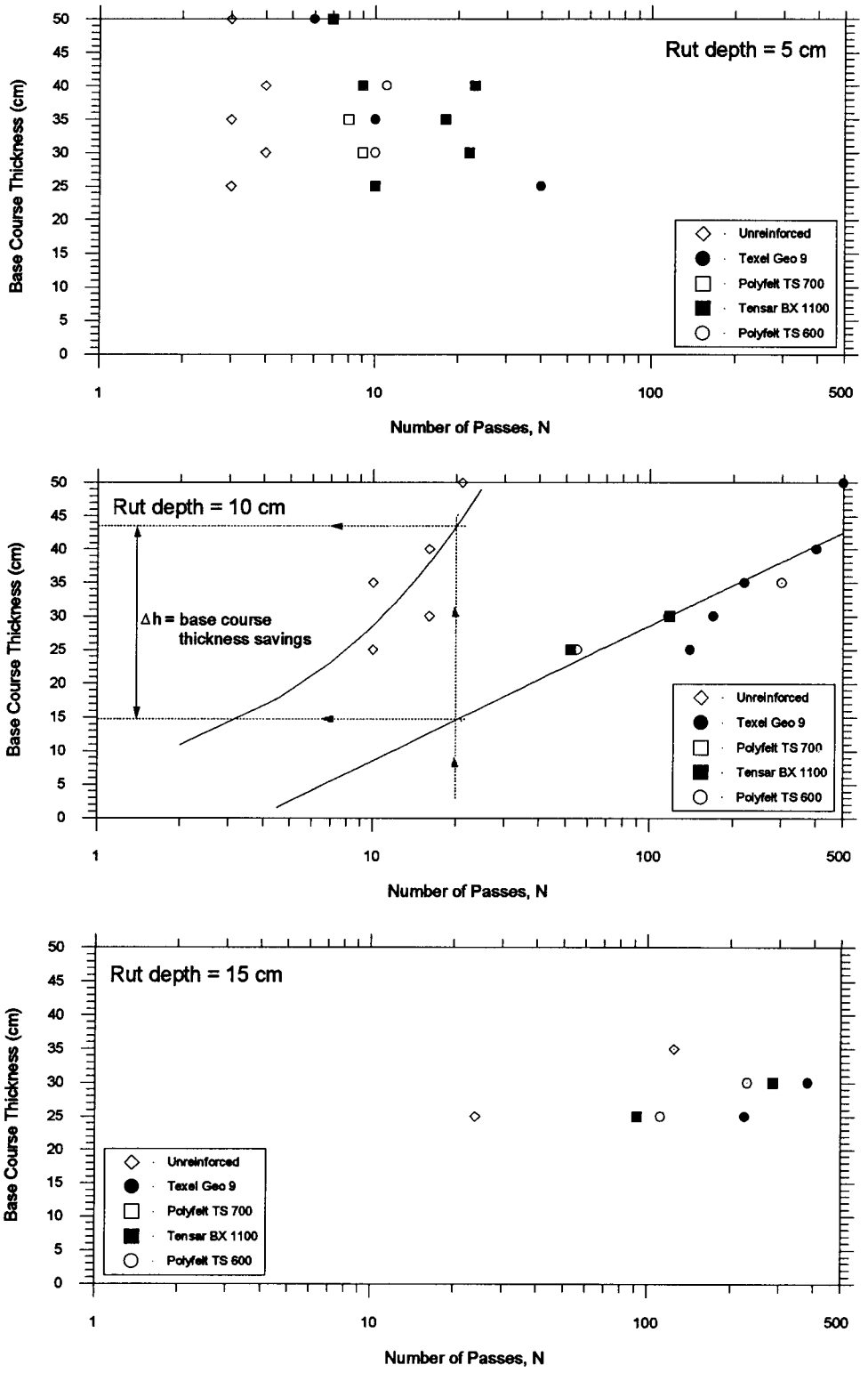

Figure 7.1 Base Course Thickness versus Number of Passes - Cost Savings Estimation

an acceptable range of rut depths. Fig. 7.1 shows the base course thickness versus number of vehicle passes for three different rut depths, for all five test sections. Savings from use of geosynthetic can be detected from the figure, for the 10 and 15 cm rut depths, whereas behavior at the 5 cm rut depth is dominated by compaction of the base course and there is no noticeable difference between the unreinforced section and the reinforced sections. Cost savings are a function of the cost of the geosynthetics and the base course gravel, and their placement, and for rut depths of 10 and 15 cm these savings can be estimated from the figure. If however the acceptable rut is less than 10 cm, Figs. 6.1 to 6.5 may be used as a guide for cases when a low number of vehicle passes will be applied, to estimate what kind of geosynthetic would be most economical to use for a given base course thickness. It can be seen that the relative improvement is essentially independent of the geosynthetic type for the rut depths of 10 and 15 cm

In order to achieve the best performance of a reinforced unpaved road the construction has to be carried out differently than for regular unpaved roads. It is important that, after the first lift of the base course aggregate placement, compaction is carried out in such manner that the geosynthetic be placed lightly in tension to better mobilize the effect of the geosynthetic. Another important factor is to start placement of the gravel and initial compaction from the edges of the road and continue to fill in and compact from the outsides towards the middle. This procedure will result in better anchorage as well as small tension in the geosynthetics is initiated.

Bibliography

Aas, G., Lacasse, S., Lunne, T., and Hoeg, K. (1986), "Use of In-Situ Tests for Foundation Design on Clay", Proceedings of the Conference on Use of In-Situ Tests in Geotechnical Engineering, ASCE Special Publication 6, pp. 1-30.

Alenowicz, J., and Dembicki, E. (1991), "Recent Laboratory Research on Unpaved Road Behavior, Geotextiles and Geomembranes, Vol.10, pp. 21-34

Armstrong, J.E. (1984), "Environmental and Engineering Applications of the Surficial Geology of the Fraser Lowland, British Columbia", Paper 83-23, Geological Survey of Canada.

Armstrong, J.E. (1956), "Surficial Geology of Vancouver Area, British Columbia", Paper 55-40, Geological Survey of Canada.

Armstrong, J.E. (1957), "Surficial Geology of New Westminster Map-Area, British Columbia", Paper 57-5, Geological Survey of Canada.

Austin, D.N., and Coleman, D.M. (1993), "A Field Evaluation of Geosynthetic-Reinforced Haul Roads Over Soft Foundation Soils", Conference Proceedings, Geosynthetics '93, Vancouver, Canada.

Bakker, J.G. (1977), "Mechanical Behavior of Membranes in Road Foundations", Proc. International Conference on the Use of Fabrics in Geotechnics, Paris, Vol.1, pp. 139-142.

Barksdale, R., Robnett, Q., and Lai, J. (1982), Proceedings, Second International Conference on Geotextiles, Las Vegas, USA, Vol. II, p375.

Bauer, A., and Preissner, H. (1986), "Studies on the Stability of a Geotextile Reinforced Two-Layer System", Proceedings, Third International Conference on Geotextiles, Vienna, Austria, pp. 1079-1084.

Becker, D.E., Crooks, J.H.A., and Been, K. (1988), "Interpretation of the Field Vane Test in Terms of In-Situ and Yield Stresses", Vane Shear Strength Testing in Soils:Field and Laboratory Studies, ASTM STP 1014, A.F. Richards, Ed., American Society for Testing and Materials, Philadelphia, pp. 71-87.

Bender, D.A., and Barenberg, E.J.(1978), "Design and Behavior of Soil-Fabric-Aggregate Systems", Transportation Research Record 671, TRB, Washington, pp. 64-75.

Bjerrum, L. (1973), "Problems of Soil Mechanics and Construction on Soft Clays", Proceedings of the 8th International Conference on Soil Mechanics and Foundation Engineering, Vol.3, pp. 111-159.

Blunden, R.H. (1973), "Urban Geology of Richmond, British Columbia", Department of Geology, University of British Columbia, Report No.15.

Blunden, R.H. (1975), "Historical Geology of the Lower Fraser River Valley", University of British Columbia, Adventures in Earth Science Series, No.3.

Bonaparte, R., and Christopher, B.R. (1987), "Design and Construction of Reinforced Embankments Over Weak Foundations", Transportation Research Record, No.1153, pp. 26-39.

Bonaparte, R., and Berg, R. (1987), "Long-Term Allowable Tension for Geosynthetic Reinforcement", Proceedings of Geosynthetics '87 Conference, New Orleans, Louisiana, USA, pp. 181-192.

Bourdeau, P.L., Miskin, K.K., and Fuller, J.M. (1990), "Behavior of Geotextile-Reinforced Soil Under Cyclic Loading", Proceedings, 4th International Conference on Geotextiles, Geomembranes and Related Products, Hague, Netherlands.

Bourdeau, P.L., Holtz, R.D., and Chapuis, J.(1988), "Effect of Anchorage and Modulus in Geotextile-Reinforced Unpaved Roads", Geotextiles and Geomembranes, Vol.7, pp. 221-230.

Bourdeau, P.L., Harr, M.E., and Holtz, R.D. (1982), "Soil-Fabric Interaction. An Analytical Model", Proceedings, Second International Conference on Geotextiles, Las Vegas, USA, Vol. II, pp. 387-391.

Brorsson, I., and Eriksson, L. (1986), "Long-Term Properties of Geotextiles and Their Function as a Separator in Road Construction", Proceedings, Third International Conference on Geotextiles, Vienna, Austria.

Burd, H.J., and Brocklehurst, C.J. (1990), "Finite Element Studies of the Mechanics of Reinforced Unpaved Roads", Proceedings, 4th International Conference on Geotextiles, Geomembranes and Related Products, Hague, Netherlands, pp. 217-221.

Burd, H.J., and Houlsby, G.T. (1989), "Numerical Modeling of Reinforced Unpaved Roads", Third Int. Symp. on Numerical Models in Geomechanics, Canada.

Burmister, D.M. (1944), "The General Theory of Stresses and Displacements in Layered Systems", Journal of Applied Physics, Vol.16, pp. 89-94, 126-127, 296-302.

Burmister, D.M. (1943), "The Theory of Stresses and Displacements in Layered Systems and Applications to the Design of Airport Runways", Highway Research Board, Proceedings of the 23rd Annual Meeting, Illinois, pp. 126-144.

Candler, R.J. (1988), "The In-Situ Measurements of the Undrained Shear Strength of Clays Using the Field Vane", Vane Shear Strength Testing in Soils:Field and Laboratory Studies, ASTM STP 1014, A.F. Richards, Ed., American Society for Testing and Materials, Philadelphia, pp. 13-45.

Christopher, B.R., and Holtz, R.D. (1985), "Geotextile Engineering Manual", published by the Federal Highway Administration, Report Number FHWA-TS-86/203, Washington, D.C., USA.

Christopher, B.R., and Holtz, R.D. (1991), "Geotextiles for Subgrade Stabilization in Permanent Roads and Highways", Proceedings of Geosynthetics '91 Conference, Atlanta, USA, pp. 701-713.

Christopher, B.R., Holtz, R.D., and Bell, D. (1986), "New Tests for Determining the In-Soil Stress-Strain Properties of Geotextiles", Proceedings, Third International Conference on Geotextiles, Vienna, Austria, pp. 683-688.

Clague, J.J., and Luternauer, J. (1982), "Late Quaternary Sedimentary Environments, Southwestern British Columbia", International Association of Sedimentologists, 11th International Congress, Hamilton.

Clague, J.J., and Luternauer, J. (1983), "Late Quaternary Geology of Southwestern British Columbia", Geological Association of Canada, Field Trip Guidebook No.10.

Craig, R.F. (1992), "Soil Mechanics", 5th Edition, Chapman & Hall, New York.

Dawson, A.R., and Little, P.H. (1990), "Reinforced Haul-Roads: Trials at Bothkennar, Scotland", Proceedings, 4th International Conference on Geotextiles, Geomembranes and Related Products, Hague, Netherlands.

De Gardiel, R., and Javor, E. (1986), "Mechanical Reinforcement of Low-Volume Roads by Geotextiles", Proceedings, Third International Conference on Geotextiles, Vienna, Austria, pp. 1021-1026.

De Groot, M., Janse, E., Maagdenburg, T.A.C., and Van den Berg, C. (1986), "Design Method and Guidelines for Geotextile Applications in Road Construction", Proceedings, Third International Conference on Geotextiles, Vienna, Austria, p741.

Delmas, Ph., Matichard, Y., Gourc, J.P., and Riondy, G. (1986), "Unsurfaced Roads Reinforced by Geotextiles-A Seven Years Experiment", Proceedings, Third International Conference on Geotextiles, Vienna, Austria, pp. 1015-1020.

Dembicki, E., and Jermolowicz, P. (1991), "Soil-Geotextile Interaction", Geotextiles and Geomembranes, Vol.10, pp. 249-268

Douglas, R.A., Bessey, R.B., and Small, R.P. (1985), "The Use of Geotextiles in Forest Road Construction", Proceedings, Second Canadian Symposium on Geotextiles and Geomembranes, Edmonton, pp. 89-96.

Douglas, R.A., and Kelly, M.A. (1986), "Geotextile Reinforced Unpaved Logging Roads: The Effect of Anchorage", Geotextiles and Geomembranes, Vol.4, pp. 93-106.

Douglas, R.A., and Valsangkar, A.J. (1992), "Unpaved Geosynthetic-Built Resource Access Roads:Stiffness Rather than Rut Depth as the Key Design Criterion, Geotextiles and Geomembranes, Vol.11, pp. 45-59.

Douglas, R.A. (1992), "Anchorage and Modulus in Geotextile-Reinforced Unpaved Roads", Geotextiles and Geomembranes, Vol.11, pp. 99-111.

Douglas, R.A. (1990), "Anchorage and Modulus in Geotextile-Reinforced Unpaved Roads", Geotextiles and Geomembranes, Vol.9, pp. 261-267.

Drucker, C.S., and Prager, W. (1952), "Soil Mechanics and Plastic Analysis or Limit Design", Quart. Appl. Math. 10, pp. 157-165.

Eisbacher, G.H. (1977), "Vancouver Geology", Geological Association of Canada, Vancouver.

El-Fermaoui, A., and Nowatzki, E. (1982), "Effect of Confining Pressure on Performance of Geotextiles in Soils", Proceedings, Second International Conference on Geotextiles, Las Vegas, USA, Vol. III, pp. 799-804.

Floss, R., Laier, H., and Bräu, G. (1990), "Dynamic Loading of Geotextile/Soil-Systems", Proceedings, 4th International Conference on Geotextiles, Geomembranes and Related Products, Hague, Netherlands, pp. 183-188.

Floss, R., and Gold, G. (1990), "Use of FEM for the Single Reinforced Two-Layer System", Proceedings, 4th International Conference on Geotextiles, Geomembranes and Related Products, Hague, Netherlands.

Giroud, J.P., and Noiray, L. (1981), "Geotextile-Reinforced Unpaved Road Design", Journal of the Geotechnical Division, ASCE, Vol.107, GT9, Sept., pp. 1233-1254.

Giroud, J.P., Ah-Line, C., and Bonaparte, R. (1984), "Design of Unpaved Roads and Trafficked Areas and Geogrids", Symposium on Polymer Grid Reinforcement in Civil Engineering, 4.1 London, 23-24 Mars, pp. 1-12.

Gourc, J.P., Perrier, H., and Riondy, G. (1983), "Unsurfaced Road on Soft Subgrade: Mechanism of Geotextile Reinforcement", Proceedings of the 8th European Conference on Soil Mechanic and Foundation Engineering, Vol.2, Helsinki, pp. 495-498.

Gourc, J.P., Matichard, Y., Perrier, H., and Delmas, P. ("1982), Bearing Capacity of a Sand Subgrade System with Geotextile", , Proceedings, Second International Conference on Geotextiles, Las Vegas, USA, Vol. II, p411.

Greig, J.W., Campanella, R.G., and Robertson P.K. (1988), "Comparison of Field Vane Results with Other In-Situ Test Results", Vane Shear Strength Testing in Soils:Field and Laboratory Studies, ASTM STP 1014, A.F. Richards, Ed., American Society for Testing and Materials, Philadelphia, pp. 247-263.

Gryczmanski, M., and Sekowski, J. (1986), "A Composite Theory Application for Analysis of Stresses in a Subsoil Reinforced by Geotextile", Proceedings, Third International Conference on Geotextiles, Vienna, Austria, pp. 181-186.

Guido, V.A., Bakkala, C.H., and Nocera, J.J. (1991), "Eccentric Plate Loading Tests on Geogrid-Reinforced Subgrades", Proceedings of Geosynthetics '91 Conference, Atlanta, USA, pp. 381-394.

Guido, V.A., Biesiadecki, G.L., and Sullivan, M.J. (1985), "Bearing Capacity of a Geotextile-Reinforced Foundation", Proceedings of the Eleventh International Conference on Soil Mechanics and Foundation Engineering, San Francisco, Vol.3, pp. 1777-1780.

Guido, V.A., Knueppel, J.D., and Sweeney, M.A. (1987), "Plate Loading Tests on Geogrid-Reinforced Earth Slabs", Proceedings of the Geosynthetics '87 Conference, New Orleans, Vol.1, pp. 216-225.

Haas, R. (1985), "Structural Behavior of Tensar Reinforced Pavements and Some Field Applications", Symposium on Polymer Grid Reinforcement in Civil Engineering, London, pp. 166-170.

Haas, R., Walls, J., and Carroll, R.G. (1989), "Geogrid Reinforcement of Granular Bases in Flexible Pavements", Transportation Research Record, No. 1188. pp. 19-27.

Haliburton, T.A., and Barron, J.V. (1983), "Optimum-Depth Method of Design for Fabric-Reinforced Unsurfaced Roads", Transpn. Res. Rec. No 916, Transportation Research Board, Washington, D.C., pp. 26-32.

Haliburton, T.A., and Fowler, J. (1980), "Design and Construction of Fabric Reinforced Roads and Embankments on Soft Foundation", Proc. 1st Canadian Symposium on Geotextiles, Montreal, pp. 138-147.

Hammit, G.M. (1970), "Thickness Requirements for Unsurfaced Roads and Airfields - Bare Base Support", Technical Report S-70-5, U.S. Army Engineers, Waterways Experiment Station, Vicksburg, Miss., July.

Harrison W.J., and Gerrard, C.M. (1972), "Elastic Theory Applied to Reinforced Earth", Journal of the Soil Mechanics and Foundations Division, Vol.98, No.SM7, pp. 1325-1345.

Hausmann, M.R. (1986), "Fabric Reinforced Unpaved Road Design Methods-Parametric Studies", Proceedings, Third International Conference on Geotextiles, Vienna, Austria, pp. 19-23.

Hausmann, M.R. (1987), "Geotextiles for Unpaved Roads-Review of Design Procedures", Geotextiles and Geomembranes 5, pp. 201-233.

Hill, R. (1963), "Elastic Properties of Reinforced Solids: Some Theoretical Principles", Journ. Mech. Phys. Solids, Vol. 11, p357.

Hirano, I., Itho, A., Itho, M., Kawahara, S., Shirasawa, M., and Shimizu, H. (1990), "Test on Traffickability of a Low Embankment on Soft Ground Reinforced with Geotextiles", Proceedings, 4th International Conference on Geotextiles, Geomembranes and Related Products, Hague, Netherlands, pp. 227-232.

Hird, C.C., and Kwok, C.M. (1990), "Parametric Studies of the Behavior of a Reinforced Embankment", Proceedings, 4th International Conference on Geotextiles, Geomembranes and Related Products, Hague, Netherlands, pp. 137-142.

Holtz, R.D., and Sivakugan. (1987), "Design Charts for Roads with Geotextiles", Geotextiles and Geomembranes, Vol.5, No.3, pp. 191-199.

Houlsby, G.T., and Jewell, R.A. (1990), "Design of Reinforced Unpaved Roads for Small Rut Depths", Proceedings, 4th International Conference on Geotextiles, Geomembranes and Related Products, Hague, Netherlands, pp. 171-176.

Houlsby, G.T., and Jewell, R.A. (1988), "Analysis of Unreinforced and Reinforced Embankments on Soft Clays by Plasticity Theory", Proceedings, 6th International Conference on Numerical Methods in Geomechanics, Innsbruck, 2, pp. 1443-1448.

Ingold, T.S., and Miller, K.S. (1986), "Short, Intermediate, and Long Term Stability of Geotextile Reinforced Embankments Over Soft Clays", Proceedings, Third International Conference on Geotextiles, Vienna, Austria, pp. 337-342.

Ingold, T.S., and Crowcroft, P. (1984), "The Notation of Geotextiles as Separators in Roads", Ground Engineering, Vol.17, No.1, January.

Jaecklin, F.P. (1986), "Design of Road Base and Geotextile by Regression Analysis from Experience Data Sources", Proceedings, Third International Conference on Geotextiles, Vienna, Austria, pp. 985-990.

Jarret, P.M. (1986), "Load Tests on Geogrid Reinforced Gravel Fills Constructed on Peat Subgrades", Proceedings, Third International Conference on Geotextiles, Vienna, Austria, pp. 87-92.

Jarrett, P.M. (1985), "Evaluation of Geogrids for Construction of Roadways Over Muskeg", Symposium on Polymer Grid Reinforcement in Civil Engineering, London, pp. 149-153.

Jarrett, P.M., Lee, R.A., and Ridell, D.V.B. (1977), "The Use of Fabrics in Road Pavements Constructed on Peat", Proc. International Conference on the Use of Fabrics in Geotechnics, Paris, Vol.1, pp. 19-22.

Jessberger, H.L. (1977), "Load-Bearing Behavior of a Gravel Subbase-Nonwoven Fabric-Soft Subgrade System", Proc. International Conference on the Use of Fabrics in Geotechnics, Paris, Vol.1, pp. 9-13.

Jewell, R.A. (1982), "A Limit Equilibrium Design Method for Reinforced Embankments on Soft Foundations", Proceedings, Second International Conference on Geotextiles, Las Vegas, USA, Vol.2, pp. 677-682.

Jewell, R.A. (1988), "The Mechanics of Reinforced Embankments on Soft Soils", Geotextiles and Geomembranes 7, pp. 237-273.

Kaniraj, S.R. (1988), "Design of Reinforced Embankments on Soft Soils", Geotechnical Engineering, Vol.19, pp. 127-142.

Kasarnovsky, V.D., Polunovsky, A.G., and Brantman, B.P. (1982), "Design of a Temporary Road Structure with the Use of Textile Membrane", Proceedings, Second International Conference on Geotextiles, Las Vegas, USA, Vol. II, p371.

Kern, C.B., and Buchanan, R.G. (1984), "Annacis Project Richmond, East-West Freeway - Interim Geotechnical Report", Ministry of Transportation and Highways, Geotechnical and Materials Branch, Victoria, B.C., Canada.

Kinney, T., and Barenberg, E. (1982), "The Strengthening Effect of Geotextiles on Soil-Geotextile-Aggregate Systems", Proceedings, Second International Conference on Geotextiles, Las Vegas, USA, Vol. II, p347.

Koerner, R.M. (1990), "Designing with Geosynthetics", 2nd Edition, Prentice Hall Publ. Co., Englewood Cliffs, NJ.

Kothari, V.K., and Das, A. (1992), "Compressional Behavior of Nonwoven Geotextiles" Geotextiles and Geomembranes, Vol.11, pp. 235-252.

Kysela, Z. (1986), "Geotextiles as a Structural Member for Load Redistribution", Proceedings, Third International Conference on Geotextiles, Vienna, Austria, pp. 239-244.

Laier, H., and Bräu, G. (1986), "The Use of Geotextiles in Road Construction Under Intensive Dynamic Loading", Proceedings, Third International Conference on Geotextiles, Vienna, Austria, pp. 995-1000.

Landva, A.O. (1980), "Vane Testing in Peat", Canadian Geotechnical Journal, Vol.17, No.1, National Research Council of Canada.

Lefebvre, G., Ladd, C.C., and Pare, J.J. (1988), "Comparison of Field Vane and Laboratory Undrained Shear Strength in Soft Sensitive Clays", Vane Shear Strength Testing in Soils:Field and Laboratory Studies, ASTM STP 1014, A.F. Richards, Ed., American Society for Testing and Materials, Philadelphia, pp. 233-246.

Ling, H.I., Wu, J.T.H., and Tatsuoka, F. (1991), "Effectiveness of In-Membrane Test in Simulating Strength and Deformation Characteristics of a Nonwoven Geotextile Under Operational Conditions", Proceedings of Geosynthetics '91 Conference, Atlanta, USA, pp. 601- 614.

Love, J.T., Burd, H.J., Milligan, G.W.E., and Houlsby, G.T. (1987), "Analytical and Model Studies of Reinforcement of a Granular Layer on a Soft Clay Subgrade", Canadian Geotechnical Journal, Vol.24, No.4, pp. 611-622.

Mahmoud, F.F., and Mashhour, M.M. (1986), "An Elastoplastic Finite Element for the Analysis of Soil-Geotextile Systems", Proceedings, Third International Conference on Geotextiles, Vienna, Austria, pp. 229-231.

McGown, A., Andrawes, K.Z., and Kabir, M.H. (1982), "Load-Extension Testing of Geotextiles Confined In-Soil", Proceedings, Second International Conference on Geotextiles, Las Vegas, USA, Vol. III, pp. 793-798.

McGown, A., Andrawes, K.Z., and Yeo, K.C. (1985), "The Load-Strain-Time Behaviour of Tensar Geogrids", Symposium on Polymer Grid Reinforcement in Civil Engineering, London, pp. 11-17.

Meyerhof, G.G. (1974), "Ultimate Bearing Capacity Of Footings on Sand Layer Overlaying Clay", Canadian Geotechnical Journal, Vol.11, No.2, pp. 223-229.

Milligan, G.W.E., Jewell, R.A., Houlsby, G.T., and Burd, H.J. (1989), "A New Approach to the Design of Unpaved Roads-Part I", Ground Engineering, Vol.22, No.3, pp. 25-29.

Milligan, G.W.E., Fannin, J., and Farrar, D.M. (1986), "Model and Full-Scale Tests of Granular Layers Reinforced with a Geogrid", Proceedings, Third International Conference on Geotextiles, Vienna, Austria, pp. 61-66.

Milligan, G.W.E., and Love, J.P. (1984), "Model Testing of Geogrids Under an Aggregate Layer on Soft Ground", Symp. on Polymer Grid Reinforcement in Civil Engineering, Paper No 4.2, London, (ICE).

Milligan, G.W.E., Jewell, R.A., Houlsby, G.T., and Burd, H.J. (1989), "A New Approach to the Design of Unpaved Roads-Part II", Ground Engineering, Vol.22, No.8, pp. 37-42.

Milligan, V., and Rochelle, P.La. (1985), "Design Methods for Embankments Over Weak Soils", Symposium on Polymer Grid Reinforcement in Civil Engineering, London, pp. 95-102.

Milligan, G.W.E., and Love, J.P. (1985) "Model Testing of Geogrids Under an Aggregate Layer on Soft Ground", Symposium on Polymer Grid Reinforcement in Civil Engineering, London, pp. 128-138.

Miura, N., Sakai, A., and Taesiri, Y. (1990), "Polymer Grid Reinforced Pavement on Soft Clay Grounds", Geotextiles and Geomembranes, Vol.9, pp. 99-123

Murray, R.T., and McGown, A. (1990), "Geotextiles in Road Construction: Summary of an OECD Report", Proceedings, 4th International Conference on Geotextiles, Geomembranes and Related Products, Hague, Netherlands.

Mylleville, B.L.J., and Rowe, R.K. (1991), "On the Design of Reinforced Embankments on Soft Brittle Clays", Proceedings of Geosynthetics '91 Conference, Atlanta, USA, pp. 395-408.

Nieuvenhuis, J.D. (1977), "Membranes and the Bearing Capacity of Road Bases", Proc. International Conference on the Use of Fabrics in Geotechnics, Paris, Vol.1, pp. 3-8.

Nishigata, T., and Yamaoka, I. (1990), "Bearing Capacity of Unpaved Road Reinforced by Geotextile", Proceedings, 4th International Conference on Geotextiles, Geomembranes and Related Products, Hague, Netherlands.

Odemark, N. (1947), "Undersökning av elasticitetsegenskaperna hos olika jordarter samt teori för beräkning av beläggningar enligt elasticitetsteorin", Statens Väginstitut, Stockholm, Sweden.

Petrik, P.M. (1977), "Development of Stresses in Reinforcement and Subgrade of a Reinforced Soil Slab", Proc. International Conference on the Use of Fabrics in Geotechnics, Paris, Vol.1, pp. 151-154.

Potter, J.F., and Currer, E.W.H. (1981), "The Effect of a Fabric Membrane on the Structural Behavior of a Granular Road Pavement", Transport and Road Research Laboratory, TRRL Laboratory Report 996.

Purushothamaraj, P., Ramiah, B.K., and Venkatakrishna Rao, K.N. (1973), "Bearing Capacity of Strip Footings in Two Layered Cohesive-friction Soils", Canadian Geotechnical Journal, Vol.11, No.32, 1974, pp. 32-45.

Ramalho-Ortiago, J.A., and Palmeia, E.M. (1982), "Geotextile Performance at an Access Road on Soft Ground near Rio de Janeiro", Proceedings, Second International Conference on Geotextiles, Las Vegas, USA, Vol. II, p353.

Raumann, G. (1982), "Geotextiles in Unpaved Roads: Design Considerations", Proceedings, Second International Conference on Geotextiles, Las Vegas, USA, Vol. II, pp. 417-422.

Resl, S., and Werner, G. (1986), "The Influence of Nonwoven Needle punched Geotextiles on the Ultimate Bearing Capacity of the Subgrade", Proceedings, Third International Conference on Geotextiles, Vienna, Austria, pp. 1009-1013.

Robnett, Q., Lai, J., and Murch, L. (1982), "Effect of Fabric Properties on the Performance and Design of Aggregate-Fabric-Soil Systems", Proceedings, Second International Conference on Geotextiles, Las Vegas, USA, Vol. II, p381.

Robnett, Q., and Lai, J.S. (1982), "Fabric-Reinforced Aggregate Roads-Overview", Transportation Research Record, No. 875. pp. 42-50.

Robnett, Q.L., Lai, J.S., Lavin, J.G., Murch, L.E., and Murrey, C.D. (1980), "Use of Geotextiles in Road Construction:An Experimental Study, Proc. 1st Canadian Symposium on Geotextiles, Montreal, pp. 113-124.

Roy, M., and Leblanc, A. (1988), "Factors Affecting the Measurements and Interpretation of the Vane Strength in Soft Sensitive Clays", Vane Shear Strength Testing in Soils:Field and Laboratory Studies, ASTM STP 1014, A.F. Richards, Ed., American Society for Testing and Materials, Philadelphia, pp. 117-128.

Ruddock. E.C., Potter, J.F., and McAvoy, A.R. (1982), "A Full-Scale Experiment on Granular and Bituminous Road Pavements Laid on Fabrics", Proceedings, Second International Conference on Geotextiles, Las Vegas, USA, Vol. II, p365.

Sawicki, A. (1983), "Plastic Limit Behavior of Reinforced Earth", Journal of the Geotechnical Engineering Division, ASCE, Vol.107, No 7, p1000.

Sellmeijer, J.B., Kenter, C.J., and Van den Berg, C. (1982), "Calculation Method for a Fabric Reinforced Road", Proc. SICG, 2, Aug., pp. 393-398.

Sellmeijer, J.B. (1990), "Design of Geotextile Reinforced Paved Roads and Parking Areas", Proceedings, 4th International Conference on Geotextiles, Geomembranes and Related Products, Hague, Netherlands.

Sellmeijer, J.B., Kenter, C.J., and Van den Berg, C. (1982), "Calculation Method for a Fabric Reinforced Road", Proceedings, Second International Conference on Geotextiles, Las Vegas, USA, Vol. II.

Silvestri, V., and Auberni, M. (1988), "Anisotropy and In-Situ Vane Tests", Vane Shear Strength Testing in Soils:Field and Laboratory Studies, ASTM STP 1014, A.F. Richards, Ed., American Society for Testing and Materials, Philadelphia, pp. 89-103.

Sorlie, A. (1977), "The Effects of Fabrics on Pavement Strength-Plate bearing Tests in the Laboratory", Proc. International Conference on the Use of Fabrics in Geotechnics, Paris, Vol.1, pp. 15-18.

Sowers, G.F., et al. (1982), "Mechanism of Geotextile-Aggregate Support in Low-Cost Roads", Proceedings, Second International Conference on Geotextiles, Las Vegas, USA, Vol. II, p341.

Steward, J., Williamson, R., and Mohney, J. (1978), "Guidelines for Use of Fabrics in Construction and Maintenance of Low-Volume Roads", USDA, Forest Service, Portland, Oregon. Also published as Report No. FHA-TS-78-205.

Steward, J., and Mohney, J. (1982), "Trial Use Results and Experience Using Geotextiles for Low-Volume Forest Roads", Proceedings, Second International Conference on Geotextiles, Las Vegas, USA, Vol. II, p335.

Steward, J.E., Williamson, R., and Mohney, J. (1983), "Guidelines for Use of Fabrics in Construction and Maintenance of Low-Volume Roads", Federal Highway Administration, Report Number FHWA-TS-78-205.

Terzaghi, K. (1943), "Theoretical Soil Mechanics", John Wiley and Sons, Inc., New York.

Terzaghi, K., and Peck, R.B. (1967), "Soil Mechanics in Engineering Practice", 2nd Edition, John Wiley and Sons, Inc., New York.

Van Zanten., Ed. (1986), "Geotextiles and Geomembranes in Civil Engineering", Wiley-Halsted.

Watari, Y., Higuchi, Y., and Aboshi, H. (1986), "Field Studies of the Behavior of Geogrids and Very Soft Ground", Proceedings, Third International Conference on Geotextiles, Vienna, Austria, pp. 187-191.

Webster, S.L., and Watkins, J.E. (1978), "Investigation of Construction Concepts for Pavements Across Soft Ground", Technical Report S-78-6, U.S. Army Engineers, Waterways Experiment Station, Vicksburg, Miss., July.

Webster, S.L., and Watkins, J.E. (1977), "Investigation of Construction Techniques for Tactical Bridge Approach Roads Across Soft Ground", Technical Report S-77-1, U.S. Army Engineers, Waterways Experiment Station, Vicksburg, Miss., February.

Wroth, C.P. (1984), Geotechnique, Vol.34, pp. 449-489.